LBL-18207
UC-91

Lawrence Berkeley Laboratory
UNIVERSITY OF CALIFORNIA

APPLIED SCIENCE DIVISION

STEAM STRIPPING OF OIL SHALE WASTEWATERS
LBL/SEEHRL Steam Stripper: Design, Operation, and Maintenance Manual

R.H. Sakaji, P. Persoff, and
C.G. Daughton

August 1984

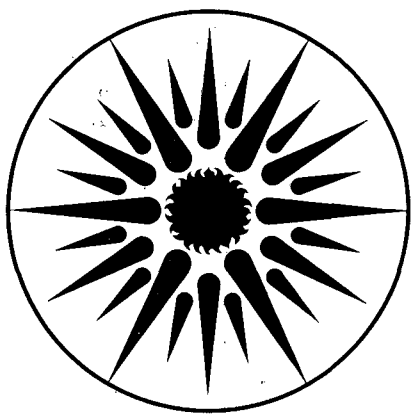

APPLIED SCIENCE
DIVISION

Prepared for the U.S. Department of Energy under Contract DE-AC03-76SF00098

STEAM STRIPPING OF OIL SHALE WASTEWATERS

LBL/SEEHRL Steam Stripper: Design, Operation, and Maintenance Manual

Richard H. Sakaji, Peter Persoff

Applied Science Division
Lawrence Berkeley Laboratory
Berkeley, California 94720

and

Christian G. Daughton

Sanitary Engineering and
Environmental Health Research Laboratory
University of California, Berkeley
Richmond, California 94804

Prepared for

U.S. Department of Energy

DOE Contract No.
DE-AC03-76SF00098

Project Manager: Ted Bartke
Laramie Project Office, Laramie, WY 82071

August 1984

LBL-18207;UCB/SEEHRL 84-3

STEAM STRIPPING OF OIL SHALE WASTEWATERS

LBL/SEEHRL Steam Stripper:
Design, Operation, and Maintenance Manual

CONTENTS

Steam Stripping of Oil Shale Wastewaters

LBL/SEEHRL Steam Stripper:
Design, Operation, and Maintenance Manual

ABSTRACT

Steam stripping is the most often proposed means of treating oil shale wastewaters for the removal of ammonia and carbon dioxide. The removal of organic carbon generally is not an objective. This manual compares current steam stripper design theory with actual operating data reported in the literature and concludes that discrepancies exist between theory and actual practice. Although this manual is by no means a complete literature review on the more detailed subject of mass transfer, references are provided so that the reader can explore the subject material more closely.

The primary intent of the manual is to give the operator a brief overview of the chemical and physical principles underlying the steam stripping process. Sufficient information is provided so that the operator can understand how the LBL/SEEHRL experimental-scale steam stripper was designed to be operated. Start-up procedures are detailed, and modifications required to improve performance are presented. Included are notes outlining periodic maintenance procedures for mechanical parts, protocols for the reduction of data, notes on the methods of chemical analysis, and the calculations used for mass balances.

ACKNOWLEDGMENTS

The LBL/SEEHRL steam stripping project is a result of the efforts of several people, without whose contributions and efforts this project would never have become a reality. The project was initiated by the efforts of Dr. J. Phyllis Fox (then at LBL) and Charles Grua (DOE). Continuing support for this program was offered by Dr. Arthur Hartstein (DOE). Initial design of the steam generation system was conceived by Dr. Badawi Tleimat (Principal Development Engineer of the Water Technology Center, UCB). Dr. Frank Pearson (Assistant Director; SEEHRL) completed the plans for fabrication of the steam stripper. Fabrication was carried out by John Potter and Stuart Foster (Senior and Assistant Mechanicians; SEEHRL). Start-up operations were initially developed with the assistance of Jeremy Cantor (Principal Research Technician; LBL).

The authors are indebted to Professor Robert E. Selleck (UCB) and to Dr. Frank Pearson for reviewing this manual and providing valuable suggestions for simplifying the sections on theory and operations; their comments and suggestions, since the inception of the project, were invaluable. We would also like to thank Qui Tran and Richard Watada (summer students; LBL) who aided in the preparation of several of the illustrations.

This work was supported by the Assistant Secretary for Fossil Energy, Office of Oil Shale, Division of Oil, Gas, and Shale Technology of the U.S. Department of Energy under Contract No. DE-AC03-76SF00098.

LIST OF TABLES

LIST OF ILLUSTRATIONS

SYMBOLS AND ABBREVIATIONS

a	surface area per unit volume
c	concentration (units of molality or molarity)
D_{AB}	diffusivity of component A in component B
f	fugacity
H	Henry's coefficient
HETP	height equivalent to a theoretical plate
HTU	height of a transfer unit
k	individual-phase mass transfer coefficient
K	overall-phase mass transfer coefficient
N	flux
o	standard state
P	total pressure
P_A	partial pressure of component A
u	chemical potential
v_x	velocity
x	mole fraction in liquid phase
y	mole fraction in gas phase

Subscripts:

A	component A
G	gas phase
L	liquid phase
1	phase 1
2	phase 2

CHAPTER 1. INTRODUCTION

Although this report is intended for use as an operation and maintenance manual for the LBL/SEEHRL large experimental-scale steam stripper, a major portion is a detailed discussion of the principles and mechanisms of steam stripping and the rationale for its proposed use in upgrading the quality of oil shale process wastewaters. Not meant as an all-inclusive review of steam stripping, this report is referenced so that the reader can gather more detailed information. The various sections of this report encompass: the theory of steam stripping, the design of the LBL/SEEHRL steam stripper, and the operation of the LBL/SEEHRL steam stripper.

The first two chapters outline the characteristics of the wastewaters that would be generated from full-scale commercial retorting processes designed for the production of the synfuel, shale oil. Chapter 3 is an overview of current steam-stripping research and its application to oil shale wastewaters; this section includes a review of problems associated with steam stripping in the petroleum industry and proposals on how these problems could be addressed in treating oil shale wastewaters. The weaknesses and strengths of current vapor-liquid equilibrium and mass-transfer models used in the design of steam strippers are reviewed in Chapter 4; a design example is included to compare predicted performance with experimental observations. Chapter 5 is a detailed description of the LBL/SEEHRL steam stripper. Chapter 6 is the operation protocol for the steam stripper. Included in this chapter is a summary of methods used for the chemical analysis of wastewaters, troubleshooting tips, and the equations used to calculate mass balances and operation efficiencies. A glossary of terms relevant to stripping theory is also provided. This operations and maintenance manual can be followed without a thorough understanding of the theoretical basis of steam stripping. The reader, therefore, can proceed directly to the section(s) of interest.

1.1 Oil Shale Wastewater Production

Shale oil is produced from the pyrolytic decomposition (retorting) of kerogen. Kerogen is a heterogeneous organic polymer that contains amine and nitrogen heterocycle substituents and sulfide cross linkages (Schmidt-Collérus and Prien 1976; Yen 1976). The elemental composition of Green River mahogany zone shale is 2.4% nitrogen and 1% sulfur (Probstein and Hicks 1982). Pyrolysis results in the release of H_2O, NH_3, H_2S, CO_2, and volatile organic species. Resulting vapor is primarily a result of: (i) mineral dehydration of the inorganic shale, (ii) combustion of kerogen, (iii) vaporization of intruding or existing groundwater (for in-situ retorts), and (iv) condensation of steam that may be used in the retorting process. These vaporized products are swept to a cooler region of the retort where a large portion of the organic and inorganic (esp. water) vapors are condensed. Intimate mixing of the water and product oil, which contains emulsifying agents such as long-chain fatty acids, in an atmosphere containing high partial pressures of CO_2, NH_3, and H_2S, produces an emulsion containing high concentrations of organic and inorganic solutes.

Process wastewaters have different origins in retorting operations (see Figure 1.1). Modified and true in-situ processes generate retort water and gas condensate. Retort water is a product of oil-water separation after the crude shale oil and water emulsion is broken. The remaining gaseous species that

fail to condense with the oil escape from the retort and are collected in a condenser. These wastewaters are called gas condensates. Surface retorting produces a "sour"[1] water; the gaseous vapors produced in the retort exit in one stream before condensation and collection.

The volumes of wastewater produced will vary among the different commercial operations. It is generally believed that a commercial-scale oil shale industry will produce about half a volume of process wastewater for every volume of shale oil (Probstein and Hicks 1982). For a 10 000 barrel-per-day oil shale plant, the wastewater production (using a conversion factor of 42 gal/barrel of oil) would be 210 000 gallons per day.

1.2 Oil Shale Wastewater Characteristics

The importance of documented origins, process histories, and proper handling/storage of wastewater samples, which until now have been obtainable only from experimental- and pilot-scale retorts, cannot be overemphasized. Experiments demonstrating treatment performance for these wastewaters may be profoundly affected by how the waters were processed and stored. Without a complete sample history, the usefulness of a wastewater sample is questionable. During storage, samples can be altered in several ways, including degassing, solute coalescence and precipitation, chemical oxidation, biological oxidation, and production of bacterial metabolites (Farrier et al. 1977). For example, Wallace et al. (1981) note that H_2S disappears rapidly during storage, presumably from oxidation. Wastewater samples used in this and other studies have been stored for long periods and, in some instances, manipulated to produce a uniform sample that could be distributed for interlaboratory comparison studies (e.g., see Daughton and Sakaji 1980).

An understanding of the limitations to the analytical methods used for characterizing these wastewaters is also important (Daughton 1984). Oil shale wastewaters, which are highly colored and contain large amounts of particulates, present a complex sample matrix that is not amenable to many of the standard, routine methods of analysis. Particulates prevent accurate sampling, color interferes with colorimetric analyses, and nonspecific assays cannot distinguish between homologous compounds (e.g., free ammonia versus aliphatic amines) (Daughton 1984). Methods have been developed and thoroughly documented, however, for several routine water-quality parameters (Daughton 1984).

Using these methods, several oil shale wastewaters have been partially characterized with respect to routine water quality parameters such as dissolved organic carbon (DOC), dissolved inorganic carbon (DIC), chemical oxygen demand (COD), hydrophilic and lipophilic organic carbon,

---

[1] The term "sour" was originally applied to crude petroleum oils that contained hydrogen sulfide. The term now applies also to a liquid containing any odoriferous substance (Probstein and Hicks 1982). The term is used here to differentiate the wastewaters produced by surface retorting from those produced by in-situ operations.

ammonia-nitrogen (NH_3-N), total nitrogen, and organic nitrogen (Daughton 1984, Appendix II). The ranges reported for parameters of interest with respect to steam stripping are: DOC (207 to 42 066 mg/L), DIC (210 to 2213 mg/L), NH_3-N (1065 to 24 689 mg/L). The range of pH values for these same waters is 8.4 to 9.4. These ranges indicate a marked variation in the character of oil shale wastewaters.

The complexity of retort wastewater composition is illustrated by the numerous classes of organic compounds that have been identified. For only one process water have the individual solutes that compose a large portion of the DOC been identified and quantitated (Leenheer, Noyes, and Stuber 1982). Using these data, Daughton and Sakaji (1984) calculated that of the total organic nitrogen present in Oxy-6 gas condensate nearly all has been accounted for by the aromatic amines, aliphatic amines, aliphatic amides, nitriles, and pyrroles. Lewis and Rawlings (1982) report that 89% of the organic carbon in this gas condensate comprises one- and two-ring aromatic carboxylic acids, amines, phenols, aliphatic carboxylic acids (5 to 9 carbon chain length), and fulvic acid. Their results show that a major portion of the total organic carbon (TOC) is hydrophobic; this conclusion was corroborated by a separate method that uses a reverse-phase fractionation procedure (Daughton 1984).

For Oxy-6 retort water, which is the most fully characterized of all retort water available to date, the identified solutes comprise a much smaller portion of the organic compounds present. This is because the separation method used for characterizing these waters is gas chromatography; most of the solutes in the gas condensate are sufficiently volatile for this method, whereas the majority of those in retort water are too polar. Raphaelian and Harrison (1981) have found some of the major organic constituents in Oxy-6 retort water to be quinolines, pyridines, aminoindoles, pyrroles, oxygenated heterocycles, phenols, fatty acids, and alkanes. Daughton and Sakaji (1984) have reported, however, that Oxy-6 retort water contains three to four times more organic nitrogen than can be accounted for by the compounds identified by Leenheer et al. (1982). Most of the organonitrogen in this retort water is higher molecular weight or extremely water soluble.

Since a major portion of the organonitrogen compounds present in Oxy-6 retort water are not volatile at the natural pH of the water, the removal of these constituents by steam stripping does not seem feasible without pH modification. In contrast, a major portion of the volatile organonitrogen compounds present in Oxy-6 gas condensate can probably be removed by steam stripping. If the goal of the treatment process is to remove specific organic solutes, then certain requirements must be met: (i) an analytical technique for quantifying the solute of interest must be used to determine removal, (ii) the stripping unit must be designed based on the organic solute that is the most difficult to remove, and (iii) the stripping process must be flexible enough in operation to account for variability in influent wastewater characteristics.

Variations in process wastewater characteristics result partially from uncontrollable and changing conditions during a given retorting operation and from differences in operation and configuration among the various retorting processes. The types of gaseous atmospheres that are used in retorting, the quality and type of raw shale, the temperature and heating mode of the retorting process, and the type of retorting process (MIS, true in-situ, and

surface retorting) all affect the composition and quantity of wastewater produced. The production of large volumes of waters whose compositions can change during a retort burn makes waste treatment methods even more difficult to apply. A wastewater treatment process, such as steam stripping, must be flexible (i.e., easily controlled and operated) to minimize the costs of operation. The process must also be able to produce an effluent of consistent quality since marked variations can perturb other downstream treatment units or affect the ultimate disposal (e.g., codisposal with spent shale).

CHAPTER 2. OIL SHALE WASTEWATER TREATMENT GOALS

2.1 Disposal Options

Commercial developers currently intend to dispose or reuse oil shale process waters (Probstein and Hicks 1982; Lewis and Rawlings 1982) according to the following options:

- discharge to ground- or surface-water
- evaporation
- land application/reclamation
- boiler feedwater
- hot spent shale quenching
- spent shale dust control/compaction (codisposal)
- cooling water

Treatment prior to reuse or disposal could reduce the problems associated with nonpoint-source air emissions, biofouling, scaling, and corrosion. Stripping oil shale wastewaters to remove dissolved gases and volatile organic compounds could minimize the uncontrolled discharge of nuisance compounds from aerated biological oxidation units, evaporation ponds, or the process of spent shale moisturizing (codisposal). If more extensive treatment than that afforded by steam stripping is required, the use of steam stripping as a pretreatment to other units could be advantageous. The removal of undesirable solutes may improve any subsequent treatment performance by decreasing requirements for chemical aids, mass loadings, and toxicant concentrations.

2.2 Treatment Options

The degree of required treatment will be dictated by environmental, occupational/health, and industrial reuse requirements. Since disposal/reuse policies have yet to be set, however, the objectives of any treatment scheme are purely hypothetical. Most likely, a series of unit operations will be needed to meet these goals (e.g., steam stripping, oil and grease removal, adsorption, biological oxidation, reverse osmosis, and chemical oxidation). The levels of treatment for the various reuse options and strategies must be set by regulatory agencies and industry so that treatment units can be designed to meet these goals without compromising health and environmental concerns. In the interim, experimental evaluation or development of treatment processes can only aim for the most extensive contaminant removals possible, while realizing that such performance may be unnecessary.

2.3 Goals of Steam Stripping

Although the goals of steam stripping for the treatment of oil shale wastewaters are not well defined, the design of steam strippers should be sufficiently flexible to treat wastewaters of wide compositional ranges while maintaining efficient operation. In general, an ideal stripper would meet the following criteria:

- remove volatile solutes
- preferentially remove organic compounds that are biorefractory
- reduce wastewater toxicity to microorganisms

- operate without reduction in removal efficiency over a wide range of conditions
- concentrate the stripped compounds in a minimal volume
- be situated in a treatment train to prevent overloading of downstream process units

The shale oil industry proposes that oil shale wastewaters be used for "co-disposal" -- cooling hot spent shale, controlling dust, and effecting compaction during spent shale disposal (Lewis and Rawlings 1982; Persoff, Hunter, and Daughton 1984). Contacting untreated wastewater with hot spent shale will effect rapid volatilization (essentially via steam distillation) of organic and inorganic solutes. Treatment of the wastewaters by stripping would substantially decrease the quantity of compounds released during codisposal and decrease the need for source-control of volatile emissions during hot spent-shale quenching. Steam stripping should be successful in removing significant quantities of volatile nuisance compounds since 80% to 90% of the DOC can be removed from Oxy-6 gas condensate by steam stripping (Lewis and Rawlings 1982).

Steam stripping can be used to equalize or reduce loading rates (organic compounds and ammonia) to those downstream treatment units that are susceptible to fluctuations in mass loading. In some cases, toxic compounds must be removed to prevent the failure of biological treatment units, or specific nutrients must be removed to induce the degradation of less favorable compounds. These objectives can be illustrated by the problems encountered in the treatment of Oxy-6 retort water. About 50% of the DOC in Oxy-6 retort water is susceptible to facile biodegradation (Jones et al. 1982). A high percentage of the refractory solutes are hypothesized to be nitrogen heterocycles. These compounds are refractory possibly because of repression of the necessary catabolic enzymes (Healy et al. 1983) by an abundance of an easily degradable nitrogen source (i.e., ammonia). Large quantities of ammonia have also been reported as toxic to biological oxidation units (Healy et al. 1983). Removal of ammonia therefore would serve to decrease the toxicity and to derepress the enzymatic systems required to cleave the heterocycle rings and abstract the nitrogen. As an example, Oxy-6 retort water contains 2800 mg/L DOC. Assume that half of this amount is biodegradable and that it can be represented by CH_2 (since it comprises mainly long chain carboxylic acids; Raphaelian and Harrison 1981). The following equation can be used for alkane degradation (given in Bailey and Ollis 1977) to determine the minimum amount of ammonia-nitrogen required for conversion of 1400 mg/L of DOC to biomass:

$$2CH_2 + 0.19\ NH_3 + 2O_2 \rightleftharpoons CH_{1.7}O_{0.5}N_{0.19} + CO_2 + 1.5\ H_2$$

The ammonia concentration must therefore be reduced below 155 mg/L before nitrogen becomes a limiting nutrient and the microorganisms are forced to abstract nitrogen from the heterocycles.

Biological treatment units are also sensitive to pH. Metcalf and Eddy (1979) state that the pH range for optimum biological growth is 6.5-7.5. Bacterial growth outside this pH range may be inhibited. The performance of other treatment units (e.g., reverse osmosis, chemical precipitation, and carbon adsorption) also depend on the pH of the feed stream. High NH_3 and HCO_3^- concentrations contribute to the total alkalinity of oil shale

wastewaters (DIC ranges from 200 to 2200 mg/L and NH_3-N ranges from 1100 to 25 000 ppm, Daughton 1984). These wastewaters also have pH values that range from 8.4-9.4 (Daughton 1984). Therefore, if the pH of the wastewaters has to be adjusted prior to treatment, a large quantity of acid will be required. If, however, the ammonia and carbonate species can be removed in a pretreatment step, the acid requirement could be decreased or eliminated.

In practice, the use of steam has several technical and economic benefits over the use of air as a stripping gas. The primary advantage of steam stripping is the elevated temperature which favors the transfer of the volatile NH_3 species (at elevated temperatures the volatility and mass transfer coefficients are increased). The combination of higher temperature and pH of oil shale wastewaters, favors the formation of dissolved ammonia gas over ammonium ion in the equilibrium reaction:

$$NH_3 + H^+ \rightleftharpoons NH_4^+$$

In contrast, stripping ammonia from water at room temperature requires a pH of 10.5 or greater to shift the equilibrium reaction to the left leading to formation of the volatile NH_3 species. Elevating the wastewater pH would normally be accomplished by the addition of a base. For oil shale wastewaters, the buffering capacity of the water would necessitate the addition of a large quantity of base to achieve the desired pH elevation. Depending on the base used, this could result in the production of a large quantity of sludge.

CHAPTER 3. STEAM STRIPPING

3.1 Introduction

Several different treatment technologies can be used to remove the dissolved forms of volatile species such as CO_2, NH_3, and H_2S. For example, ammonia can be removed from aqueous wastes by ion exchange, chemical oxidation, nitrification/denitrification, and stripping; hydrogen sulfide can be removed by chemical oxidation or stripping; carbon dioxide by chemical precipitation, ion exchange, reverse osmosis, stripping, or electrodialysis. Stripping is also applicable to the removal of certain organic solutes.

There are economic and technical limitations to the use of most treatment processes for oil shale wastewaters. For example, because of the high carbonate alkalinity, chemical treatment for CO_2 removal would produce large volumes of sludge, which would pose a separate disposal problem. The problem with sludge production would also occur with ambient-air stripping since alkali addition would be required to pretreat the wastewater to ensure efficient ammonia removal. The use of chemical oxidants may not be feasible since oxidation reactions are pH dependent; they require careful process monitoring for control, and uneconomical quantities of oxidant are required for successful treatment. A treatment process that can be used for the removal of a broad spectrum of solutes is steam stripping.

Stripping is a general term that applies to the process of removing a relatively volatile component from a liquid solution, such as wastewater. The primary objective of stripping is to effect the separation of volatile from nonvolatile components and to concentrate the volatile constituents in as small a volume as possible. The volatile solutes of the liquid are transferred to a gaseous phase. This can be accomplished in a batch operation by simply purging the liquid with a gas or in a continuous process by flowing the two phases, cocurrently or countercurrently, through a column packed with an inert material. With the continuous process, the column packing serves to promote intermixing of the two phases by increasing the area of contact (the interface). In practice, stripping is usually accomplished by distillation. In distillation, a portion of the stripped liquid is converted to vapor or gas and used as the stripping medium (Perry et al. 1963); separation is achieved by the vaporization of individual components or groups of homologous compounds. Rectification is distillation that involves condensing and returning a portion of the effluent gas stream (reflux) to the column so that the vapor stream becomes enriched when it flows countercurrent to the reflux. These separation processes usually are carried out in a column in which perforated plates (sieves) or trays are stacked on one another. This cascade of plates or trays is called a plate or sieve column. A column packed with inert material (such as ceramic saddles, Raschig rings, Berl saddles) is referred to as a packed bed.

Conceptually, the transport of solutes from one phase to another is very simple. In practice, however, the design of equipment to achieve the separation of solutes from solvent is complex. We begin the section on steam stripping by reviewing problems that the petroleum industry has had with the removal of ammonia. The section on steam stripping in the petroleum industry is followed by a discussion that focuses on "fixed" ammonia, one of the

problems that purportedly causes poor ammonia removal. These sections are followed by a review of experimental results from the steam stripping of oil shale wastewaters. These results indicate that stripper behavior is not always predictable; complex phenomena are associated with steam stripping.

3.2 Steam

When water boils, steam is produced. Before attempting to define this complex process, several terms will be defined using as an example an equilibrated, single component vapor-liquid system. We will consider a water vapor-liquid system in which the rate of condensation equals the rate of evaporation.

The Gibbs Phase Rule is a convenient formula for determining the number of properties that must be fixed to describe a system at equilibrium:

$$F = C - P + 2 \qquad (3\text{-}1)$$

where F = degrees of freedom

C = number of components

P = number of phases.

According to the Gibbs Phase Rule, a single-component system with two phases (at equilibrium) has only one degree of freedom. This means that either temperature or pressure may be varied, but once either of these intensive quantities (a physical property that is not dependent on the quantity of material present) is set, the other also becomes set. For example, if the temperature of a single-component, two-phase system at equilibrium is altered, the vapor pressure will change, and the system will reach a new equilibrium state.

Liquid boils when the vapor pressure equals the total external pressure exerted on the system. Water boils at sea level when its temperature reaches 100°C; its vapor pressure then equals 14.69 psi. The boiling effect is caused by the rise of water vapor through the liquid. When these bubbles of gaseous water reach the free surface of the liquid, they burst. The vapor immediately above the liquid surface is saturated steam and the liquid is saturated liquid. Saturated steam comprises not only gaseous water, but also entrained droplets of liquid water; it is termed wet. The presence of entrained liquid water lowers the steam quality. When steam is free of entrained liquid water, it is considered dry or of 100% quality. Since there are two phases in a wet steam system, and only one component, it has only one degree of freedom, and only one intensive characteristic (temperature or pressure) can be varied. When either temperature or pressure is fixed, all the remaining intensive characteristics are set (Holman 1974).

The temperature and pressure of a system composed of two equilibrated phases are termed the saturation temperature and saturation pressure. The term saturation vapor pressure refers to the vapor pressure of a pure liquid component when the liquid and its vapor coexist at equilibrium. When a liquid boils, the saturation vapor pressure of the liquid equals the external pressure exerted on the system; unless the system is physically confined, the

temperature of the system cannot increase further because the external pressure on the system is constant. For example, since wet steam is a two-phase system, its temperature cannot increase above saturation temperature until all the entrained liquid water is removed; this yields a single-phase system, which has two degrees of freedom. When all entrained liquid water is removed, the Gibbs Phase Rule (eq. 3-1) predicts that the system would have two degrees of freedom (since only one phase is present). The additional degree of freedom means that the gas temperature can be increased independently of the pressure. When the gas temperature is increased above what was formerly the saturation temperature, the gas is said to be superheated; a two-phase one-component system cannot be superheated.

The terms vapor and gas are often used interchangeably although each refers to a different condition. Gas is a superheated vapor, whereas the term vapor refers to a steady-state equilibrium condition where the rate of gas condensation equals the rate of evaporation at the saturation temperature and pressure (Babcock and Wilcox 1972). Dry steam, a single-phase entity, can be superheated (elevated to a temperature above the saturation temperature); it is therefore a gas. In contrast, wet steam, a two-phase one component system, cannot be superheated; it is a vapor (if small liquid particles are entrained, the term aerosol can be used to define this two-phase system). The term vapor is also defined as a gaseous substance whose temperature is below the critical point (i.e., the temperature above which liquids and gases are indistinguishable). Under isothermal conditions, below critical temperature, a vapor can be condensed to a liquid by increasing the pressure.

Superheating can be accomplished in two ways. The first involves converting entrained liquid water at saturation temperature and pressure to vapor, followed by heating to temperatures above saturation. In the second approach, superheating is induced by changing the saturation pressure. By decreasing the pressure of dry steam to below saturation, the high heat content (enthalpy) of the steam causes it to become superheated. Similarly, if the pressure drop is sufficiently great, wet steam of good quality (> 98% dry gas and 2% wet or liquid H_2O, wt/wt) becomes a superheated gas due to the high heat content of the vapor. The heat content must be sufficient to vaporize liquid water and raise the temperature of the resulting gas above saturation.

3.3 Steam Stripping in the Petroleum Industry

Steam strippers have been used, with moderate degrees of success, to remove ammonia and hydrogen sulfide from "sour" petroleum wastewaters. This use has been primarily for health and aesthetic reasons (American Petroleum Institute 1975). With the advent of PL 92-500 (The Clean Water Act), however, more emphasis has been placed on limiting the release of micronutrients such as ammonia to receiving waters. In some instances, the problem of wastewater disposal or treatment becomes more tractable when contaminants are concentrated in a side stream of reduced volume; recovery of ammonia or elemental sulfur would then become economically attractive as a resource recovery operation.

Studies by the American Petroleum Institute (API) have shown that steam strippers have not always met design specifications; significant variations have been found in stripper performance. In one instance, a stripper with twelve trays attained over 99% ammonia removal for one water, while a

twenty-tray stripper removed less than 90% from another; both were operated at about the same gas and liquid flow rates (API 1975). This indicates that serious deficiencies may exist in the criteria or data used in the design of these units, or that the analytical methodologies used to quantify performance are inadequate. The API report indicates that for many operations the treated wastewater in the effluent from strippers contains higher than predicted quantities of ammonia, and removal could not be improved by adjusting the gas or liquid flow rates.

3.4 "Fixed" Ammonia

The term "fixed" ammonia refers to ammonia that purportedly remains in the treated wastewater effluent following exhaustive stripping. The API has attempted to determine the causes of and solutions to this purported problem. One possibility is that ammonia, when present as ammonium ion, interacts with various anions to form undissociated ammonium salts. Sequestering of the ammonium ion as a salt prevents the dissociation of ammonium ion to soluble ammonia gas during reestablishment of equilibria or when the pH is increased.

The oxidation of hydrogen sulfide results in thiosulfate and other sulfur compounds that interact with cyanide to form thiocyanate, a compound that is suspected of "fixing" ammonia. Weak organic acids and sulfuric acid also may cause ammonia fixation (Bomberger and Smith 1977; API 1978). Bomberger and Smith (1977) indicate that the addition of caustic to wastewater containing "fixed" ammonia allows it to be stripped.

"Fixed" ammonia also has been attributed to problems in analytical measurements of ammonia (API 1978). The frequently used methods of distillation-titrimetry, phenate colorimetry, and selective electrode measurement do not differentiate between ammonia and volatile amines ("distillable bases") (Daughton 1984). Fixed ammonia may indeed include "distillable" bases (Bomberger and Smith 1977). If the pH is significantly elevated during caustic addition, hydrolysis of amines and urea can occur (APHA 1981; Daughton 1984); this releases organic nitrogen as ammonia.

3.5 Research on Oil Shale Wastewaters: A Literature Survey

The comparison of interlaboratory stripping data is extremely difficult since researchers frequently use different stripping gases, packed bed heights, operating temperatures, wastewaters, gas flow rates, and liquid flow rates. Most importantly, the calculation is often done on the basis of percent removal without consideration of solute or water mass balances. This is commonly done by determining the amount of ammonia remaining in the stripped effluent with no check of the amount actually removed. Successful operation of a stripper can only be ascertained by determining both removals and mass balances. Research on oil shale wastewaters indicates that the removal of ammonia can be accomplished for a majority, but not all, of these wastewaters; the operating conditions demonstrating feasibility vary among reports.

Research published on stripping oil shale wastewaters has usually involved simply determining percent removals of dissolved components. Calculations of data for water or solute mass balances are usually not presented. Without mass balance information, one must assume that condensation in or vaporization from

the packed bed is not significant and that there were no operational problems. The lack of these data forces one to make a crude comparison of stripper operations on oil shale wastewaters solely on the basis of percent or concentration removals. The literature survey in this section was conducted examining the ratio of the gas flow rate to the liquid flow rate (i.e., gas-to-liquid ratio) used, the height of the packed bed, and the percentage removal of the dissolved components (see Table 3.1).

Before proceeding with the literature review, we should briefly discuss the a major variable that determines solute removal efficiencies. This variable is the dimensionless quotient of the gas and liquid flow rates or the G/L ratio.

Use of the G/L ratio in the presentation of performance data (e.g., removal percentages) can often be misleading. Although the G/L ratio is dimensionless, it is important to keep track of the units that are used to calculate the value. Flow rates can be measured on a molar, mass, or volumetric basis. The G/L ratio calculated with molar flow rates may not necessarily equal the G/L ratio calculated on either a volumetric or mass flow basis. For example, if air is used to strip a wastewater, then the G/L ratio based on a mass flow rate would differ from the G/L ratio calculated with molar flow rates by the factor 18/29, which is the ratio of the molecular weight of water to the average molecular weight of air. If steam were used as a stripping gas, then the G/L ratio calculated on a mass basis would be equal to the G/L ratio calculated on a molar basis since the the ratio of the molecular weight of steam to water is unity. It is essential to specify both the type of stripping gas and the units of flow to calculate the G/L ratio. Unless otherwise specified, the G/L ratios used in this report will be based on molar flow rates, unless mass units are given after the listed ratio.

Murphy, Hines, and Poulson (1978) stripped a simulated oil shale wastewater, which was made by dissolving ammonium carbonate in water, with hot gas (type not specified). They found that at 93.3°C with a G/L ratio of 0.13 (kg/kg), ammonia removal was 83% using a 2.2-m packed bed. When the G/L ratio was increased to 0.19, the removal increased to 99% for the same packed-bed height.

Hines et al. (1982) used hot "gas" (gas not specified, but it was saturated with water) to strip Omega-9 wastewater at different G/L ratios. At a G/L ratio of 0.76 (kg/kg) and 93.3°C, ammonia removal was 98.6%. In contrast, when they attempted to strip water from the Laramie Energy Technology Center (LETC) 150-ton retort (run 17) at a G/L ratio of 1.74 and 93.3°C, less than 66.5% of the ammonia was removed. This study indicates that run-17 water is exceedingly difficult to strip. Furthermore, the exceedingly high G/L ratios of 0.64 and 1.74 mean that for every kg of wastewater treated, 0.64 kg or 1.74 kg of stripper gas effluent is produced.

Hines et al. (1982) also studied Oxy-6 retort water and were able to achieve a 96.3% ammonia removal at a G/L of 0.70 (kg/kg) in a 2.07-m bed. In a study on the gas condensate from the Oxy-6 retort, Pearson et al. (1980) showed that using a G/L of 0.4 (kg/kg) at 100°C, 95% of the ammonia could be removed in a 2.07-m packed bed. The G/L ratio required in this study may have resulted from wall effects, because the ratio of the column i.d. to the packing dimension was less than 8.

Mercer and Wakamiya (1980) have been able to successfully strip wastewaters from Utah retorting operations. They used a reboiler[2] with reflux that achieved a greater than 95% ammonia removal with a 0.61-m column and a boiloff rate (quantity of liquid feed converted to vapor) as low as 5% of the influent feed rate. They compared the stripping of in-situ oil shale wastewaters with that of surface wastewaters and found that wastewaters from the surface operation could only be stripped of 38% of the ammonia even though the boiloff rate was increased to 30%. Habenicht et al. (1980) had similar results with a transportable steam stripper used on the LETC 150-ton retort (September 1980). The stripper was designed to remove 99% of the ammonia at a G/L of 0.12, but only 54% of the ammonia, less than 95% of the hydrogen sulfide, and 57% of the inorganic carbon was removed during operation. The poor removals were attributed to operational problems such as poor influent distribution (e.g., channeling). Wastewaters from surface retorting operations appear to be more difficult to treat. It also appears that wastewaters from surface retorting operations contain "fixed" ammonia.

---

2 A reboiler converts a portion of the liquid influent to vapor, which is then used to strip the incoming fluid.

CHAPTER 4. STEAM STRIPPER DESIGN

4.1 Introduction

Steam stripper design relies on the availability of vapor-liquid equilibria (VLE) data and the calculation of mass-transfer coefficients. The flux of a species, A, from a given phase (solid, liquid, or gas) is the product of a driving force and a mass transfer coefficient:

$$N_A = -k\ dC/dx \qquad (4\text{-}1)$$

where N_A = flux of species A
k = mass transfer coefficient
dC/dx = driving force

Mass transfer of species A between phases is driven by nonequilibrium conditions, which are provided by the difference between the concentration present and the concentration that would occur if the system were at equilibrium. Therefore, VLE data (i.e., the composition of gas and liquid phases at equilibrium) are required for rational steam stripper design.

As cited earlier, the API survey on the performance of petroleum industry sour water strippers (API 1975) indicated a wide variation in performance. Performance calculations, using the VLE model of van Krevelen, Hoftjizer, and Huntjens (1949) combined with standard design procedures, predicted concentrations of ammonia and hydrogen sulfide in stripper reflux streams two to four times greater than were measured in full- and laboratory-scale operations. These data indicate the potential for overtreatment and overdesign; such inefficient operation would result in wasted resources and uneconomical operation.

4.2 Mass-Balance Equations

A simple technique used by scientists and engineers to evaluate, model, and design treatment systems uses the Law of Conservation of Mass. Taking the time to perform this simple technique, often referred to as a mass balance, allows the scientist or engineer to validate data collected during experimentation or operation. In addition, mass balance equations are used in conjunction with heat balance equations for the design of separation equipment, such as ammonia strippers.

The mass balance equation can be explained by grammatically describing each of its terms. For an arbitrary volume, of constant size, the mass balance for a solute, A, entering or leaving this volume is:

mass of A accumulated in volume	=	mass of A fed	−	mass of A leaving	+	mass of A generated	−	mass of A consumed	(4-2)

Equation 4-2 will be translated into a mathematical expression by using the following example.

Consider a packed tower where two immiscible fluid phases (e.g., liquid and gas) are contacted by flowing countercurrent to each other. The incoming liquid contains a large quantity of a volatile solute, A, which is transferred from the liquid to the gas phase. Figure 4.1a illustrates this hypothetical example using the following variable names: L, molar liquid flow rate per unit area; G, molar gas flow rate per unit area; x, mole fraction of A in the liquid phase; and y, mole fraction of A in the gas phase. The streams entering or leaving the bottom of the packed tower are subscripted 0, and the streams entering or leaving the top of the packed tower are subscripted 1.

Using this example, eq. 4-2 can be translated into a mathematical expression, by taking a differential element of height, dz, at section A-A of Figure 4.1a. The flow of fluids through the differential element are illustrated in Figure 4.1b. To further simplify this illustration, examine the gas-liquid interface within the borders of this element (see Figure 4.2). Several steps are required for a molecule of A to pass from the liquid phase to the gas phase. First the molecule must move from the bulk solution toward the liquid-phase boundary layer that precedes the interface. The molecule must then traverse the boundary layer to the actual interface. The molecule then crosses the interface into the gas-phase boundary layer and crosses the gas-phase boundary layer into the bulk gas phase. Using a form of eq. 4-1, two equations that describe the flux of material through each of the individual phases up to the interface can be written as:

$$N_A = k_l(x_i - x_\infty) \qquad \text{(liquid phase)} \qquad (4\text{-}3)$$

$$N_A = k_g(y_\infty - y_i) \qquad \text{(gas phase)} \qquad (4\text{-}4)$$

where N_A = molar flux; molar flow rate per unit area (mole/m^2-sec)

k_l = individual liquid-phase mass transfer coefficient (mole/m^2-sec)

k_g = individual gas-phase mass transfer coefficient (mole/m^2-sec)

x_i = mole fraction of A at the liquid-phase interface

x_∞ = mole fraction of A in the liquid-phase bulk

y_i = mole fraction of A at the gas-phase interface

y_∞ = mole fraction of A in the gas-phase bulk

The differential element contains a differential quantity of interfacial area through which the molecules can travel. This differential interface is expressed as:

$$dA_i = aA_x dz \qquad (4\text{-}5)$$

where dA_i = differential interfacial area

a = interfacial area per unit volume of packed bed

A_x = crossectional area of the packed bed

dz = differential height of packed bed

Equations 4-3 to 4-5 can be used to write a mass balance expression. This expression will be a differential equation for overall mass balance.

Three assumptions will simplify the translation of eq. 4-2 into a mathematical expression. First, assume that the operation is at steady-state, which means that mass does not accumulate in the differential element. Second, solute A is not generated in the differential element, and third, solute A is not consumed in the differential element. These assumptions mean that the term on the left side of eq. 4-2 is zero and that the last two terms on the right side of eq. 4-2 are also zero. The mass balance equation then simplifies to the expression that equates the mass fed into the element with the mass leaving the element. Assume that the molar flow rates of the fluid streams do not change through the entire tower for the overall process as illustrated in Figure 4.1a. The expression for the overall mass balance is:

$$0 = (Lx_1 + Gy_0) - (Lx_0 + Gy_1)$$

(moles of A entering the reactor) (moles of A exiting the reactor)

which upon rearrangement becomes:

$$L(x_1 - x_0) = G(y_1 - y_0)$$

$$\text{or } L/G = (y_1 - y_0)/(x_1 - x_0) \qquad (4\text{-}6)$$

The mass balance equation for the differential element of crossectional area (A_x) can be written:

$$-N_A dA_i = A_x d(Gy) = A_x d(Lx) \qquad (4\text{-}7)$$

Again, assuming that the mass flow rates of the gas and liquid do not change appreciably through the packed bed, the values of L and G will be constant and eq. 4-7 can be written:

$$-N_A dA_i = A_x G dy = A_x L dx \qquad (4\text{-}8)$$

Integrating the right two terms of eq. 4-8 for any point within the tower gives the expression:

$$G(y_0 - y_1) = L(x_0 - x_1)$$

which, upon rearrangement, is identical to eq. 4-6. The overall mass balance expressed as eq. 4-8 can only be applied when the mass flow rates of the liquid and gas streams are constant over the entire length of the tower. This occurs only when the quantity of material transferred between phases is very small.

The differential mass balance is obtained by substituting eqs. 4-3 or 4-4, and 4-5 into the left term of eq. 4-8 to give to following two equations:

$$k_y(y_i - y_\infty)aA_x dz = A_x d(Gy) \qquad \text{gas phase}$$

$$k_x(x_i - x_\infty)aA_x dz = A_x d(Lx) \qquad \text{liquid phase} \qquad (4\text{-}9)$$

Integration of either equation, after separation of variables, will give the height of the packed bed required to achieve a specified degree of separation. To calculate the required packed bed height, however, the concentration of A at the interface must be known. One method of solving these equations is to assume that the interfacial concentration of A in the liquid phase is in equilibrium with the interfacial concentration of A in the gas phase. Neither interfacial concentration is easy to measure, however. Before proceeding with the solution to eq. 4-9, a short discussion on the equilibrium relationship between two phases is in order.

4.3 Vapor-Liquid Equilibrium

Accurate VLE data can be used to ensure efficient and economical process design and operation; furthermore, the development of models is desirable so that VLE behavior can be predicted over a wide range of conditions, minimizing the amount of real data that need be collected. VLE data are commonly plotted as an equilibrium isotherm over a range of compositions. It is common, however, to find that operating conditions within a stripping tower vary not only as a function of composition, but also as a function of temperature. Therefore, VLE data must be able to predict vapor and liquid phase compositions over a range of operating conditions. An equilibrium curve is a collection of points that contains all possible pairs of compositions (x,y) in the vapor and liquid phases for a given temperature. This curve predicts all possible compositions for a given equilibrium stage of a reactor.

In general, models are mathematical statements used to predict behavior and provide insight to the interpretation of physical phenomena. A successful model would accurately predict VLE data over a wide range of conditions. Mathematical solution of the numerous simultaneous equations used to model molecular interactions, chemical equilibria, and phase equilibria are more tractable with the use of high-speed computers. Knowledge of the available VLE models and their shortcomings can aid the engineer in selecting the most appropriate model on which to base design.

To design a VLE model, several mathematical relationships that involve chemical and phase equilibria must be satisfied. Since equilibrium can be defined as that state from which there is no tendency to spontaneously depart (Prausnitz 1969), system values are independent of time and history. These models are mathematical relationships that attempt to model nonideal system behavior by including terms that account for molecular interactions which, in part, are able to predict nonideal behavior of molecules.

4.3.1 Fugacity and phase equilibrium.

Phase equilibrium, for a component (A) partitioned between two phases, is attained when the chemical potential of A is equal in both phases. Gibbs used the abstract thermodynamic term chemical potential to describe the equilibrium relationship. The term fugacity is used to translate the abstract and nonmeasurable concept of chemical potential to a more physically meaningful parameter. Mathematically, fugacity is the product of a fugacity coefficient and ideal partial pressure of the gas. Fugacity therefore provides the translation from the ideal concept of partial pressure to the nonideal or corrected partial pressure. Fugacity (f) of a component is the partial

pressure of that component in a gaseous mixture assuming all components of the mixture to be ideal. At equilibrium, the fugacity of a component is equal in both phases (Prausnitz 1969).

Fugacity coefficients are calculated by using expressions for configurational properties (electrostatic, inductive, dispersive, and chemical forces) to account for molecular interactions leading to gas behavior that deviates from the ideal gas equation of state. Equations of state are mathematical statements (e.g., virial equation) that predict the behavior of gases. These equations are functions of the terms used to model the configurational properties. The virial equation gives the compressibility factor as a power series in pressure or reciprocal volume.

$$z = Pv/nRT = 1 + B/v + C/v^2 + D/v^3 + \ldots.$$

where B, C, and D = virial coefficients
z = compressibility factor
P = pressure
v = volume of gas
n = number of moles of gas
R = universal gas constant
T = temperature

Each of the coefficients in the expansion terms are related to the configurational properties. Since the coefficients are a function of the interactions that occur between molecules in a pure gas or gaseous mixture, the equation of state can be used to predict behavior over a range of different states. For example, the second virial coefficient (B) is a function of two-molecule interactions, and the third virial coefficient (C) is a function of three-molecule interactions. Substituting the equation of state into the correct thermodynamic relationship and integrating over the proper range results in an expression for the fugacity coefficient.

$$\ln \phi = (2/v) \sum_j y_j B_{ij} + (3/2v^2) \sum_j \sum_k y_j y_k C_{ijk} - \ln z_{mix}$$

where ϕ = fugacity coefficient
v = specific volume of the gas
B,C = virial coefficients
y_j = mole fraction of species j in the gas phase
z_{mix} = compressibility factor of the mixture
i,j,k = gaseous species present in the mixture.

The fugacity can then be calculated as the product of the fugacity coefficient, the mole fraction of the species in the gas phase, and the total pressure of the system.

4.3.2 Activity, chemical equilibrium, and phase equilibrium.

Equations of chemical equilibria express conservation of mass, charge balance (electroneutrality), and association-dissociation reactions (see Table 4.1). The concepts of mass conservation and electroneutrality are

self-explanatory. Equilibrium constants (K_{eq}) are more complex, since they govern the degree to which association-dissociation reactions occur. For the reaction:

$$aA + bB \rightleftharpoons cC + dD$$

K_{eq} is expressed by the equation:

$$K_{eq} = [(C)^c(D)^d]/[(A)^a(B)^b]$$

where A, B, C, D = activities of respective species

a, b, c, d = stoichiometric coefficients of the respective species

Mathematically, the definition of activity is the ratio of the fugacity at the state of interest to that measured at some standard state. If a constant temperature is maintained between the state of interest and the standard state, the change in chemical potential between the two states is given by the equation:

$$u - u^o = RT \ln(f/f^o)$$

where u = chemical potential

R = universal gas constant

T = temperature

f = fugacity

^{o} = standard state

The relationship between chemical potential and fugacity is used as a conceptual aid to visualize the transition from abstract thermodynamics to a real physical measurement.

The ratio f/f^o is the activity, and it shows how "active" a substance is, since it is a measure of the difference in chemical potential between the state of interest and the standard state. For solutions, the standard state is usually taken as the infinitely dilute solution. Activity is also expressed as the product of the actual concentration and the activity coefficient. In an infinitely dilute solution, the activity coefficient is unity by definition, and the activity is equal to the actual concentration. A solution departs from infinitely dilute solution behavior when the solution is of high ionic strength or when the concentration of analyte is no longer dilute.

As the concentration of ions in solution increases, the electrostatic interaction between ions increases, and the activity of a single ion decreases. This interaction results in an activity value that differs from the analytical concentration. For nonionizing molecules, forces such as the van der Waals force will decrease or increase the activity of solutes. Activity coefficients are calculated by empirical correlations such as the Debye-Hückel or extended Debye-Hückel formulas (for ions) and from thermodynamic functions such as the excess Gibbs free energy (for nonionizing solutes).

Activity coefficients for electrolytes are calculated by using equations that are functions of ionic strength (e.g., the extended Debye-Hückel equation):

$$\log Y_{\pm} = -AZ^2(I)^{0.5}/[1 + Ba(I)^{0.5}] \qquad (4\text{-}10)$$

where $Y_{\pm}$ = activity coefficient of ion

$A = 1.82 \times 10^6 (eT)^{-1.5}$

Z = charge of the ion

I = ionic strength = $0.5 \sum_i C_i Z_i^2$

$B = 50.3(eT)^{-0.5}$

a = adjustable parameter corresponding to ion size

e = dielectric constant of the medium

T = absolute temperature

C = analytical concentration of ion i

The ionic strength of a solution measures the intensity of the electric field in solution. Mathematically, ionic strength is a function of the analytical concentration of ions in solution. Electrostatic interactions are important not only in the calculation of activity coefficients, but also because they affect the solubility of compounds.

Empirical correlations or an appropriate excess thermodynamic function (e.g., excess Gibbs free energy) can account for the concentration effect in the activity coefficient calculation for nonionizing solutes (nonelectrolytes). Activity coefficients calculated from excess thermodynamic functions are accurate because they account for molecular interactions. These calculations, however, increase the complexity and time required to solve the equations of equilibrium. There are several excess thermodynamic functions. To explain the concept of an excess function, the Gibbs free energy will be used as an example. When two solutions are mixed, the Gibbs free energy of the mixture is equal to the sum of the Gibbs free energy of each ideal solution plus an additional term labeled the excess Gibbs free energy for the nonideal solution behavior. The excess Gibbs free energy can be mathematically modeled (e.g., two-suffix Margules equation). The activity coefficient is a direct function of the excess Gibbs free energy.

Equilibrium constants (K_{eq}) indicate the degree to which a weak electrolyte ionizes or interacts with other solutes at a given temperature. An equilibrium constant represents the condition at which the rate of the forward reaction equals the rate of the back reaction. For oil shale wastewaters, the matrix of solutes is extremely complex, and the reactions listed in Table 4.1 are only representative.

The theoretical degree of ionization, for a given solute, can be determined by using the respective equilibrium constants and analytical measurements of the compound(s) of interest (with the appropriate activity coefficients). Equilibrium constants for these reactions (25°C), are readily available. These constants can be extrapolated from 25 to 100°C for constant pressure systems by

the van't Hoff equation (Holman 1974):

$$\ln (K_2/K_1) = (\Delta H^o/R)(1/T_1 - 1/T_2)$$

where R = universal gas constant, 1.987 cal/mol-deg

K = equilibrium constant

subscript 1,2 = going from state of interest (25°C) to a new state (100°C)

Δ = change in

H^o = enthalpy of the reaction, kcal/mol

T = absolute temperature

Equilibrium constants from this extrapolation are summarized in Table 4.1 along with a few experimentally determined values. As the temperature of the system increases, there is a decrease in the pK (i.e., -log K_{eq}) values. For example, as the temperature of the system increases, the formation of dissolved ammonia gas is favored; the pK of the reaction $NH_4^+ \rightleftharpoons NH_3 + H^+$ decreases from 9.24 to 7.42; at 25°C, 50% of the total ammonia-nitrogen is in the NH_3 form at pH 9.24 versus 50% of the total ammonia-nitrogen being in the NH_3 form at pH 7.42 at 100°C. As the dissociation of ammonium ion proceeds, protons are released into the alkaline medium and react with anions such as hydroxide, hydrosulfide, sulfide, carbonate, and bicarbonate. The equilibrium reactions for these species is thereby shifted to the dissolved-gas forms, which can also be stripped. Increasing the temperature favors the formation of ammonia gas over ammonium ion and concomitantly lowers the pH and facilitates the stripping of acid gases.

4.3.3 Gas solubility.

The solubility of gas in liquid is governed by two laws. The first (Raoult's Law) states that the solubility of a component (A), as measured by its mole fraction, is the ratio of the partial pressure of A in the gaseous mixture at the state of interest to the vapor pressure of pure A at the state of interest. This only holds when the solution is nearly pure A. The second (Henry's Law) states that the solubility of the gas is proportional to the partial pressure. This relation only holds for dilute solutions and is expressed as:

$$Hx = p = yP \qquad (4\text{-}11)$$

or

$$y = (H/P)x = mx$$

where H = Henry's Law Constant

y = mole fraction of A in the gas phase

x = mole fraction of A in the liquid phase

p = partial pressure of A in the gas phase

P = total pressure

m = (H/P)

The nonideal gas-phase behavior of the solute is not accounted for in Henry's Law. The essential assumption underlying this law is that the activity coefficient of the solute is constant and not a function of the liquid-phase concentration. When the activity coefficient is not constant, an appropriate equation (e.g., two-suffix Margules) must be used. Substituting this equation into a correct form of Henry's Law yields equations such as the Krichevsky-Ilinskaya equation (see: Prausnitz 1969). Furthermore, Henry's Law applies only if the concentration of the soluble gas (i.e., NH_3) is considered; ionization and dissociation products, calculated from chemical equilibrium equations, must be subtracted from total ammoniac-nitrogen concentrations before Henry's Law is valid. Generally, Henry's Law is applicable if the total system pressure is less than 5 atm and the mole fraction of solute in the liquid phase is less than 3%.

Ions present in solution also affect the solubility of neutral organic molecules and gases. Solutions of high ionic strength are known to decrease the solubility of gases. Furthermore, the specific ions present also affect the solubility. For example, van Krevelen and Hoftjizer (1948) found that carbon dioxide is more soluble in a potassium bicarbonate-carbonate solution than in a sodium bicarbonate-carbonate solution. For neutral organic molecules, increasing ionic strength decreases their solubilities. This phenomena, "salting out," is caused by the dissolved ions attracting and holding water molecules, thus preventing them from interacting with the neutral organic molecules.

4.3.4 Effect of ionic strength on activity coefficients and gas solubility: an example.

The following illustrates the calculation of an activity coefficient and solubility for ammonia. The major ions in Oxy-6 retort water and their concentrations (ppm) are: sodium (4000), sulfate (960), chloride (535), bicarbonate and carbonate (measured cumulatively as DIC, 985) and ammoniac-nitrogen (1100). Ionic strength is calculated assuming a pH of 9.3 and temperature of 25°C so that the DIC would exist primarily as bicarbonate, and 50% of ammoniac-nitrogen would be present as ammonium ion. The ionic strength of this water is calculated from the subequation of eq. 4-10 and is 0.1 M. The activity coefficient for ammonia was calculated from the extended Debye-Hückel equation (eq. 4-10) using B = 0.33 for water at 25°C, and A = 0.5 for water at 25°C, and assuming $a = 3 \times 10^{-8}$ cm (Stumm and Morgan 1970). The calculated activity coefficient for ammonium ion is 0.76.

Henry's coefficient is affected by waters of high ionic strength. Using the tables and charts in Danckwerts (1970), the influence of ions on the solubility of ammonia at 25°C can be calculated. To simplify the calculation, we will assume that if the ionic strength of Oxy-6 retort water were primarily determined by sodium and chloride ions, the affect on Henry's coefficient could be calculated from the equation:

$$\log_{10}(H_o/H_A) = hI \qquad (4\text{-}12)$$

where $h = h_+ + h_- + h_g$ = solubility factor (h_+, h_-, h_g are solubility factor contributions by negative, positive, and gaseous molecules) (Danckwerts 1970)

H_o = Henry's coefficient for the solute in the candidate solution

H_A = Henry's coefficient for the solute in water

I = ionic strength

The ratio of H_o to H_A would be 1.023, meaning that Henry's coefficient for the solute in the candidate solution would be larger. The solubility of ammonia therefore would be decreased in a solution with significant ionic strength.

4.3.5 Azeotrope formation.

Azeotrope formation is a possibility that should be considered in situations where ammonia is difficult to strip. An azeotrope is a solution that contains at least two components and whose liquid and vapor phases contain equivalent mole fractions of solute and whose vapor pressure curve exhibits a minimum or maximum. Azeotrope formation prevents solute separation. Azeotrope formation has been examined using the simple binary system of NH_3 and water (van Aken, Drexhage, and de Swaan Arons 1975). Their research concludes that increased ionization at high dilution results in the formation of an azeotrope.

Azeotrope formation occurs when component behavior departs from Raoult's Law and the relative volatility of the mixture is unity. The relative volatility (or separation factor) for a binary solution is the ratio of vapor pressures for both pure components; it is a measure of how easily the components will separate (unity means no separation). In an azeotropic system, separation of volatile components can be achieved only when the azeotrope is broken. This can be done with the addition of electrolytes, which change the activities of the solutes. The addition of nonelectrolytes can also change the activity coefficients by affecting Henry's coefficient since the physical solubility of the component is affected by the types of solutes present in the solutions. Similarly, molecular interactions and equilibrium constants are affected by the addition of nonelectrolytes, because of a change in the fugacity caused by molecular interactions between solutes. The activity of ionizing species is also affected by the addition of nonelectrolytes, because the activity coefficient is inversely proportional to the dielectric constant of the medium. These points illustrate that there are several ways in which the components of an azeotrope can be separated.

4.3.6 Available VLE models.

The first VLE model used for design of sour water strippers was constructed by van Krevelen et al. (1949). Although this model (for a weak electrolyte system of ammonia, hydrogen sulfide, and carbon dioxide) is accurate for temperatures up to 60°C, it assumes that a single-parameter empirical equation is sufficient to correct activity coefficients for ionic strength and that the hydrogen sulfide and carbon dioxide exist only as ionized species. The model

is unable to account for decreased ammonia volatility at low ammonia concentrations, and it is applicable only to ammonia-rich systems over a limited range of ammonia-to-carbon dioxide ratios.

The next two models were published concurrently, but were developed with different assumptions. The API (1978) Sour Water Equilibrium Program (SWEQ) extended the VLE model ranges: temperature (20 to 140°C), pressure (50 psia), and concentration (1 ppm to 30% wt/wt). This model uses an empirical, concentration-dependent formula to calculate Henry's coefficient and assumes that Raoult's Law holds for water. The model cannot account for nonideal gas phase behavior and adjusts the equilibrium constants for ionic strength by using an empirical equation. Errors in the models of van Krevelen et al. (1949) and API (1978) may be attributed to the extension of empirical equations beyond their applicable range.

The second model (Edwards, Newman, and Prausnitz 1975) for volatile weak electrolytes covers the temperature range of 0 to 100°C. They assumed the activity coefficient of water to be unity and that solute concentrations below two molal did not require the use of three-body interaction terms. The required binary-interaction parameters were obtained by reducing existing data or using appropriate empirical correlations. Their model is limited by the accuracy of extrapolations used to calculate equilibrium constants and Henry's coefficient. They also extended the Debye-Hückel equation for activity coefficient calculation beyond its range of applicability (to 0.5 molal ionic strength). Edwards et al. (1978) extended the model of Edwards et al. (1975) to 170°C, 6 molal ionic strength, and solute concentration of 10 to 20 molal using the correlation of Pitzer (1973) and Pitzer and Kim (1974) for activity coefficient calculations; however, this model is still limited by the accuracy of the extrapolation used to calculate equilibrium constants and Henry's coefficient.

The model of Beutier and Renon (1978) used the thermodynamic framework of Edwards et al. (1975) and ternary interaction parameters to improve the data fit. The use of ternary parameters improves the data fit, but is questionable because little is known about the accuracy of the binary parameter data from which the ternary parameters were derived. The model is limited to temperatures below 100°C and is unable to represent experimental data at high molalities of undissociated ammonia. At low concentrations, the models of both Edwards et al. (1975) and Beutier and Renon (1978) agree well; when the solute concentration increases, however, Beutier and Renon (1978) note that the model of Edwards et al. (1975) gives a poorer data fit.

The model of Edwards et al. (1975) was improved by the work of Pawlikowski, Newman, and Prausnitz (1982). Improved binary interaction parameters were entered into a computer program, TIDES, (Pawlikowski, Newman, and Prausnitz 1983) and used to calculate the liquid phase molalities of ammonia and hydrogen sulfide with better accuracy.

4.3.7 Model accuracy.

When used in stripping calculations, the SWEQ model (API 1978) predicts 30% higher steam requirements for a reflux tower than those predicted by the model of van Krevelen et al. (API 1975); for a nonrefluxed tower, the steam

requirement calculated from the SWEQ model is 20% higher. The accuracy of the models, however, has yet to be verified by operation and evaluation of an actual stripper. If these values are accurate, they indicate that reported poor stripper performance may be attributed to operation using suboptimal levels of stripping gas. Increased gas requirements, however, will increase the cost of operating a steam stripper. This illustrates the need for accurate VLE models on which to base design.

Calculations done in the API study (1978), using the VLE model of van Krevelen et al. (1949), show that if the fixed ammonia is subtracted from the feed concentration prior to design calculations and added to the predicted effluent stream concentration, this model can be used for design. Tray efficiencies for full- and laboratory-scale operations were calculated to be 65% and up to 100%, respectively. Calculations done in the API study also showed that the predicted concentration of ammonia and hydrogen sulfide in the reflux condensate was two to four times greater than actually measured in full- and laboratory-scale operations, further illustrating the need for accurate VLE models.

The accuracy of the VLE models described in section 4.3.6 are compared in Table 4.2. Summarized experimental and calculated results show that the model used by Pawlikowski et al. (1983) best represents available VLE data. Their data comparison was limited to a ternary system of NH_3-H_2S-H_2O at a single temperature. The model, however, represents the VLE data for NH_3 and H_2S with the lowest average percent error in the difference between the calculated and experimental values. After further testing on real wastewaters and on systems containing carbon dioxide, this model should receive serious consideration for use in designing sour-water stripping systems.

4.4 Mass Transfer Theory

The preceding discussion focused on the chemical relationships that govern the stripping of dissolved gases from liquids. This section will discuss the theory of mass transfer and show how VLE data are used in the design of strippers (by continuing with the discussion of eq. 4-9 from the end of section 4.2). Although empirical correlations between mass transfer coefficients and hydrodynamic flow conditions are available, the design of industrial strippers relies heavily on performance data from existing units.

4.4.1 Introduction to solute transport.

Mass transfer rates are important to the stripping process since they (i) determine the degree of equilibration that occurs in a given stage, (ii) govern the separation obtained in continuous contacting equipment, and (iii) define the separation obtained in rate-governed processes (King 1980). Mass transfer can occur by several processes including molecular diffusion, convection, and turbulent mixing. The derivation of mass transport equations has been thoroughly outlined in several texts (Bennett and Myers 1974; Bird, Stewart, and Lightfoot 1960; King 1980; Leva 1953). This section is only a brief summary of transport phenomena and its application to stripper design.

4.4.2 Mass transfer coefficients.

The flux of material from one phase to another, N_A, is proportional to a concentration gradient and is expressed as:

$$N_A = k\,(C^* - C) \qquad (4\text{-}13)$$

where N_A = molar flux of component A (g-mol/cm^2-s)

k = constant of proportionality or mass transfer coefficient (cm/s)

C^* = concentration of A in equilibrium with the bulk-phase concentration of A (g-mol/cm^3)

C = bulk-phase concentration of A

The calculation of the mass transfer coefficient must account for the physical flow conditions (axial dispersion, radial dispersion, eddy diffusion, molecular diffusion, etc.). Thibodeaux (1979) derives an expression similar to equation 4.9 by using the general transport equation in the y-direction for a binary system:

$$N_A = x(N_A + N_B) - C(D_{AB}^{\,l} + D_{AB}^{\,t})\,\partial x/\partial y \qquad (4\text{-}14)$$

where N_B = molar flux of B

x = mole fraction of A

C = molar concentration (g-mol/cm^3)

$D_{AB}^{\,l}$ = diffusivity of A in B under laminar flow conditions (cm^2/s)

$D_{AB}^{\,t}$ = diffusivity of A in B under turbulent flow conditions (cm^2/s)

y = plane perpendicular to the flux

This equation can be replaced by the more general expression:

$$N_A = x(N_A + N_B) + \alpha\Delta x/\Delta y$$

where $\alpha = (D_{AB}^{\,l} + D_{AB}^{\,t})C$

x = mole fraction of component A.

In this equation, the sum of the diffusion terms has been replaced by a mass transfer coefficient, since the individual diffusivities are hard to determine. Although the mass transfer coefficient is also dependent on the rate of mass transfer, the equation can be simplified. If the first term on the right side of the equation (bulk flow term) is small compared to the diffusional term, then the mass transfer coefficient is independent of the rate of mass transfer. This approximation holds when the mole fraction of A is less than or equal to 0.05. The molar flux term resulting from the bulk motion of fluid can then be set equal to zero. This simplification results in the expression:

$$N_A = \alpha\Delta x/\Delta y = k\Delta x$$

where the term, Δx, represents the difference between the equilibrium mole fraction and the bulk fluid mole fraction of equation 4.9 and $\alpha/\Delta y = k$, the mass transfer coefficient.

4.4.2.1 Empirical correlations. Mass transfer coefficients can then be calculated by using dimensional analysis as outlined in Bennett and Myers (1974). In a complicated system such as a packed-bed tower, it is not possible to treat the system with rigid theoretical development. Dimensional analysis gives the general form of a relationship that links flow conditions with molecular diffusion to calculate the mass transfer coefficient. The general form of the equation is:

$$Sh = a\, Re^{b}\, Sc^{c} \qquad (4\text{-}15)$$

where Sh = Sherwood number = kx/D_{AB}
Re = Reynolds number = xu_x/v
Sc = Schmidt number = v/D_{AB}
x = distance from leading edge of flat surface
v = kinematic viscosity
u_x = velocity of the bulk phase
a,b,c = empirical coefficients

A numerical solution (Levenspiel, Weinstein, and Li 1956) to eq. 4-15 can be used to obtain values for the empirical coefficients by multiple linear regression. The technique requires that one dependent variable be a linear function of any number of independent variables.

Onda, Takeuchi, and Okumoto (1968) fitted liquid- and gas-phase mass transfer data to the following dimensionless correlations:

$$k_G RT/aD = C_1 (G/au)^{0.7} (v/D)^{0.333} (aD)^{-2.0} \qquad \text{(gas phase)} \qquad (4\text{-}16)$$

$$k_L (1/vg)^{0.333} = 0.0051 (L/a_w u)^{0.66} (v/D)^{-0.5} (ad_p)^{0.4} \qquad \text{(liquid phase)} \qquad (4\text{-}17)$$

where R = universal gas constant
T = temperature
a = surface area per unit volume
D = diffusivity
C_1 = packing coefficient
u = viscosity
v = kinematic viscosity
g = gravitational constant

a_w = wetted surface area per unit volume

d_p = packing particle diameter

From these analogies, the mass transfer coefficients for a single-phase system can be calculated and used in the transport equations. These analogies indicate that the mass transfer coefficients are affected by viscosity, density, diffusivity, and packing characteristics. The design of most separation units, however, is more complicated since the transport of solute occurs across a phase boundary. Each of the eqs. in 4-9 are general equations that are relevant only to transport in a single phase, such as for the transport of a species from the bulk solution to a phase boundary.

4.4.2.2 Models. Transport models proposed by Nernst (stagnant layer), Higbie (penetration theory), and Danckwerts (surface renewal theory) have shown that the mass transfer coefficient is proportional to diffusivity. The stagnant layer model predicts that the mass transfer coefficient is directly proportional to the diffusivity. The penetration and surface-renewal models predict that mass transfer coefficients are proportional to the diffusivity to the 0.5 power. Actual laboratory data show that the exponent on the Schmidt number is between 0.33 and 0.66, indicating that the models of Higbie and Danckwerts are close but not exact. Scriven (1968; 1969a,b) suggests that the correct model is one in which a variety of nearly laminar flows, on a small scale, carry the solute toward or away from the gas-liquid interface. All these models indicate that mass transfer theory and reality are not too far apart, but there is still some discrepancy on model applicability and usage.

4.3.2.3 Mass transfer at a phase boundary. The previous equations have only considered mass transfer in a single phase. To further explain why equilibrium conditions are so important, we will more closely examine eqs. 4-3 and 4-4. As previously discussed in section 4.2, these equations relate the difference between interfacial and bulk concentrations of A in the liquid and gas phases to the flux of A. Interfacial compositions at phase boundaries, however, are difficult to accurately quantify. The flux of A can be related to the product of an overall mass transfer coefficient times the difference between the bulk phase mole fraction and the equilibrium mole fraction. The equilibrium mole fraction (in the liquid phase) is the concentration at equilibrium with the bulk composition of the gas phase, as dictated by Henry's Law (eq. 4-11).

The equations of mass transfer, based on overall mass transfer coefficients, are then defined:

$$N_A = K_x (x^* - x) \qquad \text{liquid phase} \qquad (4\text{-}18)$$

$$N_A = K_y (y^* - y) \qquad \text{gas phase} \qquad (4\text{-}19)$$

where K_x = overall liquid-phase mass transfer coefficient based on liquid-phase concentration

K_y = overall gas-phase mass transfer coefficient based on gas-phase concentration

x^* = equilibrium mole fraction in liquid phase

y^* = equilibrium mole fraction in gas phase

If we assume that equilibrium between the gas and liquid phases follows Henry's law and that equilibrium conditions exist at the gas-liquid interface, then we know from eq. 4-11 that $y = xH/P$. We can then rewrite eq. 4-3 for the liquid phase by replacing x_i with y_i/m where $m = H/P$. The resulting equation is multiplied through by m/k_x to obtain:

$$y_i - mx = N_A m/k_l \qquad (4\text{-}20)$$

Eqs. 4-4 and 4-20 can be added to give:

$$y - mx = N_A\,(1/k_g + m/k_l) \qquad (4\text{-}21)$$

where mx is the mole function of solute at equilibrium with a liquid of mole fraction x (i.e., y^*). Eq. 4-19 is divided through by K_y to give:

$$N_A/K_y = y^* - y \qquad (4\text{-}22)$$

Comparing Eqs. 4-21 and 4-22 shows that

$$1/K_y = (1/k_g) + (m/k_l) \qquad (4\text{-}23)$$

Similarly, $1/K_x = (1/mk_g) + (1/k_l) = 1/mK_y$ (4-24)

These equations show that if H (Henry's constant) is relatively large (i.e., A is relatively insoluble or volatile), and if m/k_l in equation 4.21 is greater than $1/k_g$, then K_x is approximately equal to k_l, meaning mass transfer in the system is controlled by resistance to mass transfer in the liquid phase. If m is small (i.e., A is relatively soluble or nonvolatile) and if m/k_l is small, then K_y is approximately equal to k_g, and mass transfer is controlled by the resistance in the gas phase. There is a direct analogy between the form of mass transfer coefficients in equations 4-23 and 4-24 and the calculation of resistance for a series of resistors, i.e., the inverse of mass transfer coefficients can be viewed as a resistance to mass transfer.

The additivity of individual phase mass-transfer coefficients, expressed by eqs. 4-23 and 4-24 can be very deceptive. For this relationship to hold, several conditions must be met (King 1964):

- Henry's Law constant must be constant, or the slope of the equilibrium curve at the properly defined value of x must be employed.

- Only k_l and k_g are the significant resistances to mass transfer; there is no resistance to mass transfer at the interface. This means that the interfacial concentrations in the gas and liquid phases are at equilibrium.

- Hydrodynamic conditions under which resistances are added are identical to the conditions under which the individual phase mass-transfer coefficients were determined.

- The individual phase mass-transfer coefficients must not interact; the value of each mass transfer coefficient is independent of the other.

The assumption that one phase controls mass transfer has been successfully used when CO_2 or NH_3 is absorbed or desorbed (gas-phase controlled) or in the case of vaporization in which there is no liquid-phase resistance.

The example we have used up to this point is a simple model. When a compound such as ammonia is stripped from a wastewater, another step is required in its transport between phases (section 4-2). This additional step involves the dissociation of protonated ammonium ion to dissolved ammonia gas. If the rate of diffusion to the interface is limiting, the overall rate of transport may not be affected by chemical reactions or bulk-phase flows. A high rate of mass transfer, caused by a chemical reaction, is an example of a process that is limited by the rate of diffusion. Only when the rate of reaction is significantly slower than the rate of diffusion will the reaction rate control the rate of mass transfer.

The rates of mass transfer can be significantly affected by the sample matrix, because the interface between the gas and liquid phases can be perturbed to promote solute transport (Brian, Vivian, and Mayr 1971). Sternling and Scriven (1959) note eight factors that promote interfacial turbulence and affect the convective transport of solute between phases at the interface between phases: (1) solute transfer out of a phase of higher viscosity, (2) solute transport out of a phase in which its diffusivity is lower, (3) a large difference in kinematic viscosity and diffusivity between the two phases, (4) the presence of a steep concentration gradient near the interface, (5) a change in the solute concentration which affects the interfacial tension, (6) low viscosities and diffusivities in the two phases, (7) the absence of surface active agents, and (8) large interfacial area relative to volume of the phases.

Most mass transfer models and discussions assume that the use of two mass transfer coefficients is sufficient to describe the transfer of mass between phases. There is actually a third resistance to mass-transfer that should be added to equations 4-23 and 4-24 -- the resistance to mass transfer caused by the presence of surface-active materials. Until now, in this discussion, we assumed that mass transfer across a phase boundary did not affect the overall process of mass transfer. Researchers (e.g., Bailey and Ollis 1977) have found that surface-active agents in two-phase systems change the flow and circulation patterns within droplets. In gas-liquid contacting equipment, froth and spray characteristics reflect changes in the relative surface tension. The addition of surfactants decreases the efficiency of a separation process by reducing the liquid-phase mass transfer coefficient (Sherwood, Pigford, and Wilke 1975). To understand now surfactants affect the process of mass transfer, the initiation of internal circulation and roll cells in a two-phase system will be briefly discussed.

Roll cells are a result of interfacial turbulence (see Fig. 4.4). As mass transfers between phases, localized concentration variations occur due to nonuniform mass transfer across the interface. This results in random variations of interfacial tension (Sherwood et al. 1975). An instability is caused by the random variations in interfacial tensions. In turn, these random

variations depend on the rate of change of interfacial tension or surface pressure with solute concentration and result in the formation of ripples and roll cells. As the roll cell forms, circulation between the interfacial surface and the bulk fluid (Marangoni Phenomena) results in convective transport of the solute. The formation of roll cells promotes the transfer of mass between phases.

Circulation (e.g., within a water droplet) can also be caused by the transfer of momentum as two fluids flow past each other. In gas-liquid contacting equipment, circulation within a droplet of water is caused by the transfer of momentum between phases.

While a discussion of thermodynamics is beyond the scope of this manual, a brief discussion of surface-active agents is important. Surface active agents (surfactants), in a gas-liquid system, migrate to the interface to decrease the intermolecular forces on the surfactant molecule. Since surfactants are amphipathic (i.e., have lipophilic and hydrophilic moieties), the repulsive force usually developed between the liquid water molecules and the lipophilic end of the surfactant are minimized when the surfactant is at the gas-liquid interface; the lipophilic end orients toward the gas phase, where the intermolecular distance between the solvent molecules and solute (surfactant) is increased (Fig. 4.5). Concentration of amphipathic molecules (e.g., fatty acids or aliphatic amines) at an interface may inhibit the formation of roll cells and thereby decrease the rate of mass transfer. Several organic solutes in oil shale wastewaters are amphipathic. Those present at high concentrations include alkylated pyridines and fatty acids (Raphaelian and Harrison 1981). When the surfactants collect at the phase boundary, the liquid droplet becomes "rigid," and the resistance to mass transfer across the interface increases.

4.4.2.4 Packed-bed height. A stripping column or separation unit must be of sufficient height to achieve the desired separation. The height of a stripping column can be determined by using the equations that we have developed up to this point. For our example, we will assume that there is no significant resistance to mass transfer at the interface. We can substitute eq. 4-18 (for mass transfer based on overall mass transfer coefficient) for $k_x(x_i - x_\infty)$ and eq. 4-5 into eq. 4-9 and integrate over the length of the packed bed:

$$(L/K_x a) \int [1/(x^* - x)]dx = z$$

The height of the packed bed is the product of a constant and an integral. The value of the integral is dimensionless and the constant is in units of length. The constant is known as the height of transfer unit (HTU) and is based on the liquid-phase overall mass-transfer coefficient. A single transfer unit is the height required to achieve a change in composition that is numerically equal to the average driving force in the section. The value of the integral is known as the number of transfer units (NTU) based on the liquid-phase overall mass-transfer coefficient. Mathematically expressed these statements take the following forms:

$$HTU_{OL} = L/K_x a$$

and

$$NTU_{OL} = \int 1/(x^* - x)dx \qquad (4\text{-}25)$$

where the subscript OL on the HTU equation indicates that the overall mass-transfer coefficient has been calculated assuming that the main resistance to mass-transfer is in the liquid phase and and the OL subscript on the NTU equation indicates the number of transfer units has been calculated using the liquid phase concentrations.

The product of the HTU_{OL} and the NTU_{OL} is the height of the packed bed required to achieve a given degree of removal. Three analogous equations for HTU and NTU can be derived for individual phase mass-transfer coefficients (subscripted G and L for gas and liquid phases respectively) and the gas-phase overall (OG) mass-transfer coefficient. These equations are:

$$HTU_L = G/k_l a;\ HTU_G = L/k_g a;\ HTU_{OG} = G/K_y a;$$

$$NTU_L = \int (1/(x_i - x))dx;\ NTU_G = \int (1/(y - y_i))dy;\ NTU_{OG} = \int (1/(y - y^*))dy.$$

We can derive one more working equation using the HTU equations derived above. If we multiply eq. 4-23 by (1/a) and substitute the HTU definitions into the equation we get:

$$HTU_{OG} = HTU_G + (mG/L)HTU_L \qquad (4\text{-}26)$$

This equation introduces the relationship mG/L which is also known as the stripping factor, S, and shows that the HTU based on an overall mass-transfer coefficient is dependent on Henry's Law Constant as well as on the gas and liquid flow rates.

The stripping factor is important because the value of this ratio determines the degree of separation that can occur when two phases are contacted. When temperature and pressure are specified, making m constant, the value of S will be determined solely by the G/L ratio. When $S < 1$, solute stripping is limited by the equilibrium that can be attained between the two contacted phases (Bennett and Myers 1974; Perry, Chilton, and Kirkpatrick 1963). As the G/L decreases, the equilibrium and operating lines cross, meaning that only a limited degree of stripping can occur, even in an infinitely high column. When $S > 1$, the degree of stripping is limited only by the column height.

If S is large, eq. 4-26 reduces to $HTU_{OG} = S(HTU_L)$, and HTU_L or HTU_{OG} can be used to determine the height of a transfer unit. The fact that S is large also means that resistance to mass transfer is in the liquid phase. Another way of commonly stating this is to say that the mass transfer process is liquid-phase controlled. In contrast, when S is small, $HTU_{OG} = HTU_G$, and the transfer process is gas phase controlled. The estimates of HTU_G and HTU_L are shown in Table 4.3. In our example, HTU_G and HTU_L are the same order of magnitude and $S(HTU_L)$ is slightly larger than HTU_G meaning the resistance to mass transfer in neither phase is dominant or controlling. In this example, the HTU_{OG} must be calculated from liquid and gas phase resistances.

Equation 4-25 must now be integrated to determine the NTU_{OG} required to achieve the desired degree of separation. The individual phase mass-transfer coefficients, HTU_L or HTU_G, must be used to rigorously calculate the height of the packed bed required for the contacting of concentrated solutions. This calculation requires computation of the interfacial concentration followed by a numerical integration of eq. 4-25 to determine the NTU. For a dilute solution (L, G, and m are constant), a numerical answer can be computed by using the logarithmic mean driving force equations:

$$NTU_{OG} = (y_0 - y_1)/(y - y^*)_{lm}$$

or

$$NTU_{OL} = (x_0 - x_1)/(x - x^*)_{lm}.$$

where

$$(y - y^*)_{lm} = [(y - y^*)_0 - (y - y^*)_1]/\ln[(y - y^*)_0/(y - y^*)_1]$$

$$(x^* - x)_{lm} = [(x^* - x)_0 - (x^* - x)_1]/\ln[(x^* - x)_0/(x^* - x)_1]$$

Alternatively, the equations of Colburn (1939) can be used. These equations are:

$$NTU_{OG} = \ln [(1 - S)((y_0 - mx_1)/(y_1 - mx_1)) + S]/(1 - S) \qquad (4\text{-}27)$$

$$NTU_{OL} = \ln[(1 - 1/S)((x_0 - y_1/m)/(x_1 - y_1/m) + 1/S]/(1 - 1/S)$$

The use of the NTU and HTU equations will become more apparent when we discuss the design example in section 4.4.3, but we can see from Colburn's equations and from eq. 4-26 that S is important in determining the height of the packed bed. Before continuing we will digress to discuss the packing characteristics that influence the value of the mass transfer coefficient.

4.4.2.5 Hydrodynamic considerations. Most packed-bed reactors have been mathematically approximated as plug flow reactors. Flow elements are assumed to travel in a discrete piston or plug through the reactor (i.e., particles that enter the reactor leave the reactor in the same order). Particles remain in the reactor for a period equal to the theoretical detention time. There are several other characteristics of a plug-flow reactor. These include: (i) no velocity gradient (see Fig. 4.6) within the differential element or plug, (ii) no backmixing of solutes, and (iii) no concentration gradient within the differential element or plug. This type of flow is approached with the flow of a single phase through a bed of "small" particles (Gunn 1968) such as in packed chromatographic columns. This assumption ignores both molecular diffusion on a micro scale and the development of a velocity profile, both of which contribute to axial dispersion and deviation from plug flow, conditions that are unavoidable in practice. In addition, the flow patterns within each phase and the solute diffusivities combine to affect the individual-phase mass-transfer coefficients.

At the other extreme is complete mixing such as in a complete-stirred-tank reactor (CSTR). Particles entering the tank leave in proportion to their statistical population; as the particles enter the tank they are immediately dispersed. Flow through a series of CSTRs, however, can approach plug-flow. Towers that are made of trays or plates are frequently modeled as a series of CSTRs with each tray or plate being treated as an equilibrium stage (the gas and liquid phases leaving a plate or stage are in equilibrium), and each plate or tray is considered a reactor.

Stripping towers packed with saddles exhibit some deviation from plug-flow. This deviation is caused by a radial velocity gradient, molecular diffusion, and backmixing. The drag from the counter-flowing streams causes local flow elements to reverse direction, and since fluid elements move forward at differing local velocities, a longitudinal velocity gradient is formed. Deviation from ideality must be expressed mathematically so that the design equations and models can accurately predict solute transport in turbulent- and laminar-flow conditions (Mecklenburgh and Hartland 1975) and to allow extrapolation from pilot-scale to large-scale operation.

Mass transfer in a turbulent system is essentially a mixing process caused by the blending and mixing of eddies. Turbulence is characterized by a rapid and irregular fluctuation of velocity about the time-mean velocity at a given point; particles no longer travel in discrete streamlines. In turbulent flow, eddies roll and mix with each other; a fast eddy moving adjacent to a slow stream, can intermix and transport momentum to the slower stream. Eddies constantly form, intermix, fragment, disappear, and reform; these processes are not well understood.

Turbulent motion is described in terms of intensity, which is related to the magnitude of the velocity fluctuations. Eddy size is statistically measured by models such as Taylor, Eulerian, and Lagrangian, and by Prandtl mixing length. These models and their mathematical derivations are outlined in Sherwood et al. (1975).

Analytical problems exist with using these models to describe flow patterns in mass transfer processes. In turbulent flow, the flow field is inadequately specified, and molecular diffusion takes place within and between the eddies. Molecular diffusion and eddy diffusion occur simultaneously, and a rigorous treatment is not usually possible since convective transport results in part from the mixing and dispersion that occurs in the reactor. Mixing and dispersion have been reviewed and summarized in Levenspiel and Bischoff (1963). Models to solve the coupled equations that describe the transport phenomena are reviewed in Scriven (1969a, b).

Other examples of physical phenomena that influence convective mass transfer and cause deviations from plug flow models include end effects, channeling or longitudinal mixing, drag motion, and radial mixing. Drag motion, for example, involves the localized flow reversal of counterflowing streams caused by frictional resistance to flow and surface phenomena at the gas-liquid interface. These effects can decrease or increase individual-phase mass-transfer coefficients causing up to 25% variation in a given mass transfer coefficient (Sherwood et al. 1975).

Departures from plug flow are especially pronounced when (i) conditions are set for a large solute separation factor (e.g., 99.9%), (ii) a low HTU is achieved, (iii) large eddies or circulation patterns develop in the continuous phase due to the lack of flow restrictions, or (iv) gas or liquid flow rates are extremely high. "End effects" are caused by mass transfer that occurs at the ends of a packed bed where the liquid is introduced by spraying (inlet) or where the liquid drips off the packing onto a bed support (outlet). Treybal (1980) suggests correcting for end effects by operating the column over a range of bed heights at constant gas and water flow rates and extrapolating the coefficients back to a bed height of zero. Presumably, end effects for a given column are constant and do not change as a function of column height. This means that end effects will have a more pronounced effect on mass transfer coefficients derived from shorter columns.

Channeling (i.e., uneven flow through a bed) can be caused by packing material of nonuniform size, poor distribution of packing material in the column, or an uneven dispersion of liquid over the packed bed. The effects of channeling are reduced when the ratio of packing size to column inside diameter (D_p/D_c) is at most 1:8 (Treybal 1980; Perry 1963, Chapter 18, p. 32), but a minimum ratio of 1:15 is recommended. Gunn (1968) states that variations in fluid velocity and dispersion coefficients can be neglected when the D_p/D_c ratio is less than 1:12.

In a stripping tower, a continuous phase (i.e., gas) flows countercurrent to a discontinuous phase (i.e., liquid). The gas is driven up through the packed bed by a pressure drop between the gas inlet and the top of the packed bed. If either the gas flow rate or the liquid flow rate is increased relative to the other, deleterious conditions can develop. These are known as loading and flooding, respectively (Treybal 1980). Under normal conditions with a set gas flow rate, the pressure drop increases when the liquid flow rate is increased. This results primarily because of the reduced free cross-sectional area available for the flow of gas.

If the liquid flow rate is held constant and the gas flow is increased, the condition known as loading ensues; the pressure drop through the packed bed then increases rapidly with only small increases in the gas flow rate. The characteristics of the mass transfer coefficient may change radically at the loading point. If the gas flow rate is continually increased, a point is reached where an abrupt change in the operating conditions occurs. A layer of liquid may form at the top of the column, or liquid may fill the tower starting at the bottom; the system goes from a gas-continuous/liquid-dispersed system to a gas-dispersed/liquid-continuous system (also known as "inversion"). In addition, slugs of foam may rise rapidly upward through the packing; entrainment of the liquid by the effluent gas increases rapidly. All of these conditions are accompanied by a rapid drop in gas pressure which signals flooding.

Most columns are designed to be operated up to 50% of the flooding conditions (defined by the hydrodynamic flow characteristics). Flooding calculations are based on the physical properties of the flowing fluids and the packing material. Use of these calculations to determine gas and liquid flow rates will be demonstrated in section 4.4.4. An understanding of the physical

limitations of steam stripper operation allows for the separation of the physical problems of mass transfer from those associated with the chemistry of a multicomponent system.

The rate at which mass is transferred is normally calculated by multiplying the mass transfer coefficient by the interfacial area through which mass transfer occurs (eq. 4-9). Determining this value is an extremely difficult task since the interfacial area is not simply the surface area per unit volume of the packing material. The interfacial area varies because the wetted surface forms, drips, and reforms causing the surface to expand and contract (Bennett and Myers 1974).

Flooding a tower with water before adding the packing material allows the packing to settle in a random orientation. The physical shape of the packing material is designed so that no two pieces can intermesh or interlock in such a manner that large portions of surface area become covered and rendered ineffective. Shulman et al. (1955) state that the wetted area increases as the packing size decreases. This does not necessarily mean, however, that the effective area for mass transfer increases. The effective area for mass transfer can not be correlated to the wetted area or packing density (surface area per unit volume) by any simple correlation; it also appears to be independent of the gas flow rate. The maximum effective surface area for Intalox saddles occurs with 1" saddles, and the effective surface area for larger and smaller saddles decreases. The smaller saddles have a larger static holdup (pockets of water) giving stagnant wetted areas. Larger packing exhibits fewer points of contact resulting in less static holdup, and research has shown that the effective area of larger packing is closer to the wetted area.

Liquid holdup may play a role in the mass transfer process. The total liquid holdup is the sum of two components; the static holdup, which is liquid that does not drain from the column, and the operating holdup, which is the difference between the total holdup and the static holdup. Operating holdup is independent of the packing characteristics; it is dependent on gas flow rate. Static holdup may play an important but unknown role in the mass transfer process. Shulman et al. (1955) state that the static holdup is important in vaporization processes, but not in desorption or absorption processes. Unlike operational holdup, static holdup is independent of the gas and liquid flow rates; it depends on the characteristics of the packing material.

Packing material serves to promote the development of a large surface area between the gas and liquid phases. Packed beds provide for larger liquid-gas interfacial contact areas and less of a pressure drop than tray systems; with trays, gas must pass through standing water on each tray. Packing material suitable for use in a stripping tower must allow for desirable fluid-flow characteristics. It must maximize both void space and interfacial area. The packing material also must have sufficient structural strength so that chipping or cracking does not occur during installation, and it must be chemically and thermally inert so that it does not react with the wastewater or melt.

4.4.3 Use of equations in design.

The design of a steam stripping column is based on VLE models and a certain degree of empiricism. The following narrative will outline the steps taken in determining the height of the LBL/SEEHRL steam stripper. This example illustrates some of the problems associated with using existing empirical correlations for design.

Consider a binary vapor-liquid system in which one component is transferred between phases. The Gibbs phase rule predicts that there are two degrees of freedom; this system, however, has four variables: temperature, pressure, vapor-phase mole fraction of component, and liquid-phase mole fraction of component. Therefore, if the temperature and mole fraction in the liquid phase are fixed, the mole fraction of component in the gas phase is determined. Consider a range of mole fractions in the liquid phase at a given temperature; each liquid-phase mole fraction will have a corresponding gas-phase mole fraction. When plotted as x-y coordinates, the data comprise a line called the equilibrium line (VLE diagram). For a stage process, if the concentrations leaving each stage are in equilibrium with the influent concentrations, then the equilibrium curve represents all concentrations in the reactor. If the coordinates (x_0, y_0) and (x_1, y_1) from eq. 4-6 are plotted with the equilibrium curve, the line joining the two coordinates has a slope of L/G and is known as the operating line (Fig. 4.3).

4.4.4 Design example.

The practical design of steam strippers currently relies heavily on actual performance data or VLE models such as van Krevelen's (cited in API 1975). The API design manual follows the method of Beychok (1967). Van Krevelen's model relies on a series of charts to calculate the partial pressures of the volatile compounds for each stage and the effluent concentration for that stage. Alternatively, the method outlined in Bennett and Myers (1974) can be used. Empirical correlations between HTU data and liquid and gas flow rates are used in conjunction with mass balances to determine the height of the packed bed. Since these correlations have not been worked out for 1/4-in. Intalox saddles, the LBL/SEEHRL steam stripper was designed using mass transfer coefficients from different models and experimental data available in the literature.

Before beginning the design example, we should note that several assumptions were made to make the calculations easier. The wastewater would not contain H_2S and the column would be isothermally and adiabatically operated at 110°C. The objective of the stripper would be to achieve 99% removal of ammonia. All values of the physical constants used in this example are summarized in Table 4.4.

We can begin the design problem by calculating Henry's Law constant using either the API (1978) equation or the equation of Edwards et al. (1978). Since the operating pressure is known, the G/L ratio can be calculated by assuming a value for the stripping factor between 1.25 and 2.0. Henry's coefficient can be calculated from the equation given by API (1978):

$$\ln(H) = 178.339 - 15517.91/T - 25.6767\ln(T) + 0.019660(T) + (131.4/T - 0.1682)(N) + 0.06(2C + S)$$

where T = temperature, ^{o}R

N = free ammonia concentration, (g-mol/kg of solution)

C = total unionized CO_2 in solution, (g-mol/kg of solution)

S = total undissociated H_2S in solution, (g-mol/kg of solution)

H = Henry's Coefficient, (psia/g-mol/kg of solution)

If we assume that the CO_2 and NH_3 are present in their undissociated forms, then Henry's Law constant can be calculated for each of the wastewaters. As discussed previously, Henry's Law constant should not depend on the quantity of undissociated material present in the wastewater. Table 4.5 is a summary of the values calculated by the API equation. Alternatively, Henry's Law constant could also be calculated from the equation given by Edwards et al. (1978):

$$\ln H = D_1 + D_2/T + D_3 \ln T + D_4 T$$

where H = Henry's law constant

D = coefficients given in Edwards et al. (1978)

T = temperature

The values for H from this correlation are also listed in Table 4.5. The difference between the average Henry's Law constant calculated from the API correlation and that from the equation of Edwards et al. is 4.2%. For our design example we will use a value of 18.3 for Henry's Law constant. With this value, we can calculate the G/L ratio for stripping factors of 1.25 and 2.0; the G/L ratio for each stripping factor was 0.0997 and 0.1596, respectively. The calculated G/L ratio can now be used to determine the gas flow rate at flooding from graphs given in Leva (1953) or Bennett and Myers (1974). For a 2-in. i.d. column packed with 1/4-in. Intalox saddles, the gas flow rate at flooding would be 407 lb/f^2h (S = 1.25) or 478 lb/f^2h (S = 2.0). The actual gas flow rate would be determined by using a fraction of these values (known as a percent of flooding) to ensure that flooding and loading conditions do not occur in the packed bed. The liquid loading rate is then calculated as the quotient of the gas flow rate and the G/L ratio.

Once the gas and liquid flow rates can be determined, the height of the packed bed can be calculated. The NTU, based on the overall gas-phase mass-transfer coefficient, is calculated from eq. 4-27. The NTU values for 99% ammonia removal are given in Table 4.6 for an S = 1.25. Since the height of the packed bed is the product of the number of transfer units and the height of a transfer unit, we must now evaluate the terms of eq. 4-26 to determine the height of a transfer unit based on the overall gas-phase mass-transfer coefficient.

Since the stripping factor in eq. 4-26 is known or selected, only HTU_L and HTU_G must be determined from empirical formulas such as:

$HTU_G = 1.01 \ (G^{0.31}/L^{0.33})$ (Sherwood and Holloway 1940)

$$HTU_L = (1/0.021)(u_L^2/p^2_L g)^{0.33}(L/a_t u_L)^{0.51}(u_L/p_L D_L)^{0.50} \quad \text{(Perry 1973)}$$

Alternatively, the empirical correlations of Onda et al. (eqs. 4-16 and 4-17) can be used to calculate the individual-phase mass-transfer coefficients from which the HTU values can be calculated (e.g., $HTU_G = G/k_G aP$ and $HTU_L = L/k_L a$).

The equations for HTU are independent of concentration, but dependent on gas and liquid flow rates for a given packing material and will not vary significantly among the different wastewaters for given gas and liquid flow rates. The most significant variation occurs between the HTU values calculated by the different correlations. The NTU equations are strongly dependent on concentration and will vary among the different wastewaters as shown by the values listed in Table 4.6. The range of heights that results from the multiplication of the HTU and NTU values from these calculations is presented in Table 4.7. There is a wide discrepancy in the height of the column required for 99% ammonia removal for a given wastewater. This discrepancy is a result of the equations used to calculate HTU_{OG}.

Pearson et al. (1980) found that a G/L (kg/kg) ratio of 0.47 was required to remove 93% of the ammonia from Oxy-6 gas condensate; this G/L ratio is four times greater than that predicted by these design calculations. The height of the packed bed predicted by these design calculations is longer than the bed (1.83 m) used by Pearson et al. (1980). The discrepancy between experimental data and the predicted performance data may be explained, in part, by the difference in operating conditions. The shorter column was insufficient to allow the desired separation. The difference in operating temperatures should have actually aided in the removal of ammonia. At the 122°C temperature used in the study by Pearson et al. (1980), Henry's Law coefficient would reduce the required G/L ratio; this would mean that the gas requirements should have been lower than the value that was actually used. Alternatively, this means that the G/L ratio which was used should have made ammonia stripping easier at the higher temperature, unless the physical operating conditions had hampered removals. There is insufficient data to evaluate whether poor operation could be attributed to chemical interactions or problems in operation.

Temperature may also play an important role in the stripping process. In the previous discussions, operation of the stripper was assumed to be both isothermal and adiabatic, a highly idealized situation. In practice, a temperature gradient may develop in the stripping column. Since Henry's Law coefficient is a function of temperature, the assumption that it is constant may not be valid. For example, using the equation for Henry's Law constant for ammonia (Edwards et al. 1978), the constant decreases by 13% going from 100°C to 95°C. This decrease means that the gas becomes more soluble at the lower temperature. The increase in solubility also means that a longer packed bed would be required to effect a given degree of separation if isothermal conditions are not maintained. The gas stripping process in general is an endothermic process. The heat of stripping (i.e., the heat required to remove a solute from an aqueous phase) along with its concentration dependence is given in Table 4.8 for ammonia and carbon dioxide. Since the stripping of these gases is an endothermic process, a decreasing temperature gradient may develop in the column. Therefore, temperature effects may not be negligible when examining experimental data.

The phase equilibrium data used in the design calculations may not be sufficient for the design and operation of stripping equipment, and the use of actual operational data may be inadequate because of variations in the wastewater solute matrix. Empirical correlations for determining Henry's Law coefficient may not account for the variations in molecular interaction that occur on the molecular level. As the solutions become less ideal with the addition of numerous solutes, the calculation of interaction parameters for the construction of phase equilibrium diagrams may not be accurate. If the laboratory columns in the preceding experiments had been designed for the low G/L ratios calculated by standard design procedures, the packed beds may have been too short to achieve the desired removals. The higher gas flow rates required to meet the design removal efficiencies may have resulted in loaded or flooded columns; the packed columns may not have been able to withstand the increased loading. These problems can lead to overdesign, resulting in excessive operational costs, or to underdesign, resulting in equipment that is unable to cope with severe changes in operating conditions. Habenicht's (1980) experience may indicate that classical design procedures as outlined in Beychok (1967) and Bennett and Myers (1974) may be limited by the chemical equilibria data that are available. Lack of good phase-equilibrium data may limit the ability of the stripper and operator to deal with changes in the character of the wastewater stream as changes in the retorting process occur.

Demonstrations in steam stripping have clearly shown the process to be capable of achieving significant removals of ammonia. The efficiency of the process, however, is questionable. The variability in performance data strongly suggests that actual design and operation of these units may still be in the "black box" stage. The problems surrounding the efficient design and operation of these units remains to be clearly elucidated.

4.5 Summary

Although steam stripping is a well studied process, the interactions of physical and chemical variables often complicate its study and require that simplifying assumptions be used (e.g., neglecting the resistance to mass transfer caused by surfactants at the interfacial boundary) so that the stripping process can be more conveniently modelled mathematically. Without simplifying assumptions in the development of mathematical models, steam stripper design would rely primarily on empirical correlations to predict mass transfer coefficients. Mass transfer coefficients and VLE values have been predicted using both mathematical models and empirical correlations with various degrees of success. The performance of these strippers, however, has not always been predictable. Poor stripper performance and variability in stripper operation may reflect various deficiencies.

- process inflexibility (e.g., the inability to treat a wastewater stream of varying composition)
- inability to identify, separate, and classify problems according to physical or chemical origin
- lack of knowledge in predicting vapor-liquid partitioning of solutes

- oversimplified models that may only be applicable to specific wastewaters
- use of chemical methods of analysis for quantifying stripper performance that are prone to interferences (not solute specific)

In spite of these shortcomings, a properly designed steam stripper should be able to consistently produce an effluent of acceptable quality for the numerous discharge or reuse options, including:

- discharge to ground- or surface-waters
- discharge to a downstream treatment unit
- evaporation
- application to land (irrigation or spraying)
- use for boiler or cooling tower makeup water
- use in codisposal of spent shale

As a pretreatment for other processes, steam stripping can decrease the loading by removing biorefractory compounds, reducing microbial toxicity, or alleviating enzyme repression. The process should be readily adaptable to a wide range of operating conditions to accomodate varying influent quality. These goals must be achieved by concentrating the stripped compounds in a minimal volume of condensed overheads. Published literature indicates that current design procedures may not be sufficient to ensure that a steam stripper could consistently operate with oil shale wastewaters and produce an effluent of acceptable quality to meet all of these goals.

While this manual was not meant as an all-inclusive review of steam stripping, its primary goal was to provide a background on stripping for the steam stripper operator. To this end, the first two chapters discussed the origin and characteristics of oil shale wastewaters, indicating their variability in water quality. This was followed by a synopsis of the problems associated with stripping wastewaters and more specifically a review on the stripping of oil shale wastewaters. The final section provided a review of vapor-liquid equilibrium with a review of some of the models used for predicting vapor-liquid equilibrium, mass transfer models (with a section on the formulas used to determine mass transfer coefficients), and design procedures used to determine the height of a stripping column. An example of determining packed-bed column height was included in the final section; column heights for the 99% removal of ammonia from different oil shale wastewaters was calculated.

The LBL/SEEHRL steam stripper is being used to demonstrate the use of steam stripping for the treatment of oil shale wastewaters and to examine the effect of physical variables on treatment performance. To achieve these goals, the final two chapters in this manual contain the operating instructions for this stripper. These chapters contain the step-by-step startup, operation, and shutdown procedures for the unit. Also included are a troubleshooting guide and data reduction guide. Before proceding with experimental work, the operator is advised to carefully read and review all the operating procedures.

CHAPTER 5. EQUIPMENT

The discussion in Chapters 1 through 4 focused on the chemical theory of equilibrium and steam stripping with their application to design. Design usually focuses on the stripping column, but in practice the column requires a support system to prepare the gas and liquid streams entering the column, to condense and collect the streams leaving the column, to pump fluids through the system, and to control the overall system operation. This chapter describes the design and construction of the LBL/SEEHRL steam stripper system in detail. Chapter 6 presents detailed operating instructions.

5.1 Introduction

The LBL/SEEHRL steam stripper is shown schematically in Figure 5.1. Each unit is given a two-letter abbreviation (in parentheses) that will be used for future reference. All valves are numbered according to the unit they are associated with (e.g., valve SG-1 vents the steam generator). For positive identification of all valves, see photographs in Appendix B.

Gas and liquid flow countercurrent to each other through the packed-bed column (PB). The gas phase is steam. In the LBL/SEEHRL steam stripper system, ambient-temperature ASTM Type III water is converted to steam and superheated (dried) before entering the column. Steam leaving the column contains the stripped compounds and is collected in an overheads condenser (OC). The stripped gases may or may not dissolve in the condensed overheads depending upon their solubility; low-molecular-weight organic compounds may also condense as an immiscible liquid phase.

The liquid entering the stripping column (e.g., untreated retort water) is first raised to the temperature of the column by passage through a feed preheater (FP). The preheated feed enters the top of the column and flows downward by gravity, countercurrent to steam which flows upward. Inert packing material (Intalox ceramic saddles) promotes interphase mass transfer by ensuring that the liquid and gas phases contact each other with a large interfacial area which is constantly renewed by the formation and reformation of water drops. When the retort water reaches the bottom of the column, much of its volatile solute content has been transferred to the gas phase (stripped). The stripped water leaving the bottom of the column is collected in the bottoms collector (BC).

This system is designed to operate under isothermal conditions (i.e., gas and liquid temperatures equal and uniform throughout the column). This ensures that there is no evaporation of liquid feed or condensation of steam in the column. Under these conditions, mass transfer between the phases would result only from diffusion-driven processes described in Section 4.3, and not from evaporation or condensation of water.

5.2 Structural Support

All the vessels of the steam stripper system are mounted on the front face of a Unistrut cage. The cage is 20 ft tall and 10 ft X 5 ft 9-3/4 in. in plan (Fig. 5.2). The six main vertical members (indicated by heavy lines in Fig. 5.2) are P1001 Unistrut, double 1-5/8 X 1-5/8-in. 12-gauge channels.

All other structural members are P1000 Unistrut, single 1-5/8 X 1-5/8-in. 12-gauge channels (see Appendix A). The entire structure is anchored to a concrete slab by 6 Unistrut post bases (P2037A) and is also secured by guy wires to the structure of the SEEHRL pilot plant building.

There are two decks, constructed of 2-in. X 12-in. rough redwood, at elevations of 6 ft 9 in. and 13 ft 6 in. above the floor. Access to the landings is by vertical ladders built into the cage. The ladder to the upper deck is enclosed in a safety cage and has a safety harness.

5.3 Materials of Construction

All major vessels of the steam stripper system (Fig. 5.1) (except the steam drier (SD), which was installed as a prefabricated unit, and the stripping column, which was assembled from Pyrex beaded glass tubing) were fabricated from 8-in. schedule 40, type 316L stainless steel pipe. The exact i.d. and o.d. are 7.981 and 8.625 in., respectively. The closed ends of the vessels were fabricated by welding a slip-on flange to the open ends of the pipe and bolting on a blind flange. The stripping column consists of two 8-ft lengths of 2-in. o.d. beaded Pyrex tubing, packed with 1/4-in. Intalox ceramic saddles.

All vessel penetrations were made by drilling and tapping through the blind flanges, except those for sight glasses and for valves BC-1 and -2, which were drilled and tapped through the cylindrical pipe wall. All connections from vessels to lines are through Swagelok 1/2-in male pipe-to-tube adaptors. The flanges were drilled and tapped 1/2-in. NPT, and the connection was sealed with X-pando pipe joint compound (X-pando Corp., Long Island City, NY).

All lines connecting vessels are 1/2-in. o.d. stainless steel tubing, wall thickness 0.065 in., except the line from the feed preheater to the stripping column, which is 1/8-in. o.d. stainless steel tubing. Tubing connections are made with 316 stainless steel Swagelok or Gyrolok compression fittings. The Pyrex stripping column and overheads condenser are connected by 2-in. schedule 40 stainless steel pipe fittings; this larger size connection has been used to accommodate temperature sensing equipment. As shown in Figure 5.1, crosses are connected above the stripping column, above the overheads condenser, and below the stripping column. Sight glasses are 1/2-in. o.d. beaded Pyrex tubing, connected with Swagelok compression fittings with Teflon ferrules.

All vessels and piping are covered with fiberglass insulation. The insulation thickness is 1 in. on the steam generator (SG) and 2 in. on all other vessels and piping.

5.3.1 Valves.

All valves are 1/2-in. stainless steel gate valves (Jenkins Bros.; see Appendix A) with Teflon packing, unless otherwise specified. Valves PB-5 and PB-7 are 316 stainless steel globe valves with graphite-asbestos packing (Dragon, model 10P057). Valves OC-7 and OC-8 are also 316 stainless steel globe valves with graphite-asbestos packing (Dragon, model 10M057), and valve PB-6 is a 316 stainless 2-inch ball valve with Teflon packing (Apollo, no.

87-108-01). For positive identification of all valves, see photographs in Appendix B.

5.4 Vessels

5.4.1 Steam generator (SG).

The steam generator consists of a vertical stainless steel pipe 8 ft long by 8 in. i.d. The outside of the steam generator is covered with 1-in. fiberglass insulation. The ends are bolted stainless steel flanges.

The top end-flange is drilled and tapped to accept a water recirculation line (inlet), a manual bleed-off valve (SG-3), a pressure relief valve (set for 60 psig), and a resistance temperature detector (RTD). The bottom end-flange is drilled and tapped to accept an immersion heater (see 5.4.1.1) and a water recirculation line (outlet).

The bottom section of the steam generator acts as a reservoir for water that is to be converted to steam. The level and volume of water in this reservoir are indicated by a calibrated sight glass. Water in the reservoir is heated but does not boil because it is under a pressure greater than the saturation pressure. A "flash-evaporator pump" (see 5.4.1.2) circulates heated water through the recirculation line from the bottom of the reservoir to a spray head at the top of the steam generator; as water emerges from the spray, its pressure is reduced, and it flashes to steam (rapidly evaporates).

At the start of a run, the steam generator reservoir must be filled with enough ASTM Type III water to produce steam for the duration of the run. This water is produced by running tap water through a Millipore RO-20 reverse osmosis treatment system. For the method of filling the steam generator, see the start-up directions in section 6.5, step 8.

5.4.1.1 Immersion heater. Heat for raising steam is supplied by a 6-kW Calrod immersion heater, model MP 4508 (General Electric Co., Schenectady, NY). The catalog description of the immersion heater is included in Appendix A. A proportional controller supplies 460V electric power in response to the temperature sensed by RTD-21. For operation of the RTDs and proportional controllers see 5.9 and 6.2.1. The immersion heater is threaded through the bottom end-flange (2-1/2 in. NPT), and the heating element extends 12-1/16 in. into the steam generator.

5.4.1.2 Flash evaporator pump. The flash evaporator pump circulates water from the bottom of the steam generator to a stainless steel spray head inside the top of the steam generator. This pump is an Eastern model D11, type 105, 1/4 HP centrifugal pump manufactured by LFE Fluid Control Division. Nameplate information, catalog description, and maintenance instructions are included in Appendix A. The flash evaporator pump is controlled by an on-off switch on the control panel (see 5.7)

5.4.2 Steam drier (SD).

Steam leaving the steam generator is saturated; it is in equilibrium with liquid water and therefore its temperature is the boiling point of water at the pressure in the steam generator. After leaving the steam generator, it

may lose some energy in transit to the packed-bed stripping column. This could cause some of the steam to condense as droplets of liquid water. To minimize condensation in the stripping column, the steam flowing to the stripper should contain no liquid water. Therefore, it is passed through a steam drier (SD) where its temperature is raised (above the boiling point), converting all liquid water to vapor and thereby superheating the steam to yield dry steam (section 3.2).

The steam drier is a 6-kW Calrod circulation heater, model JG1522 (General Electric Co., Schenectady, NY). It was installed as a prefabricated unit. The catalog description of the steam drier is included in Appendix A. Electrical power is supplied through a proportional controller in response to the temperature sensed by RTD-22. The voltage to the steam drier is contolled by a high-amperage Powerstat transformer; the maximum voltage drop across the heating element is 208V. During operation, the transformer may have to be adjusted to achieve temperature stability (see 6.2.2). A Wellman thermostat that was supplied with the steam drier was not connected because more sensitive temperature control is possible using RTD-22 and a proportional controller. The operation of temperature sensors and controls is described in sections 5.9 and 6.2.1.

5.4.2.1 Steam drier time switch. Operation of the steam drier is controlled by a Dayton time switch, model 2E026 (Dayton Electric Mfg. Co., Chicago, IL); all other units are controlled by the main time switch, described in section 5.8. The catalog description of the steam drier time switch is included in Appendix A. There are 96 trippers around the face of the 24-hour clock; each one controls the operation of the steam drier during one 15-minute period. Push the tripper in for on, or pull it out for off. There is also a manual override switch immediately below and to the left of the clock face. If the override switch is down, the time switch operates as described; if it is up, the time switch is on. The override therefore can turn the time switch on when it is scheduled to be off, but not vice-versa. If the system is set to turn on in the morning, check that RTD-22 controlling the steam drier is correctly set so the steam drier will indeed turn on as scheduled.

5.4.3 Packed-bed stripping column (PB).

The packed bed stripping column is the heart of the system. This is where the steam and the preheated wastewater are contacted. The stripping column consists of two 8-ft long by 2-in. i.d. lengths of Pyrex beaded glass tubing, rated for 75 psi at 150°C. The two lengths are connected by a Corning Universal beaded coupling (see Appendix A). Above the column is a 2-in. 316 stainless steel cross. The column is connected to this upper cross by a 2-in., 3-convolution PTFE Flexijoint (Ethylene Corp., Murray Hill, NJ) (see Appendix A) and an ANSI flanged-to-beaded-unarmored coupling (Corning Glass Co., Corning, NY) (see Appendix A). The column is packed (packing depth can be varied) with 1/4-in. ceramic Intalox saddles (Norton Co., Irvine, CA).

The saddles are supported by a stainless steel wire mesh located between the cross and the bottom of the column. When loading the packing material, the column is first filled with water before the saddles are introduced; this reduces breakage and promotes random orientation of the saddles.

Steam stripping experiments require close monitoring and control of the temperatures in the stripping column. For this reason the stripping column is more densely instrumented than the rest of the system. The column is insulated with 2-inch fiberglass insulation. Interior and exterior temperatures are sensed by RTDs at the cross above the column and at the bottoms collector at the bottom of the column; only exterior temperatures are sensed by four RTDs along the length of the column. The RTD outputs are logged and displayed by a datalogger (section 5.11). Identification numbers and locations of RTDs on the stripping column are listed in Table 5.1. None of these RTDs exerts any controlling function over the column temperature. Instead, column temperatures are controlled by the temperatures of the incoming streams and by heat tapes. The operator can control the energy input to the heat tapes.

5.4.3.1 Heat tapes. Heat tapes are wrapped around the stripping column and the 2-in. stainless steel pipe cross above the stripping column; there is also a heat tape around the bottoms collector. Their purpose is to reduce heat losses to the environment and maintain temperatures in the column. The heat tapes are Briskeat tapes with fiberglass fabric or silicone rubber covering. Each tape consists of two, three, or four 6-ft lengths in series (Table 5.2). The fiberglass-fabric-covered tapes have a resistance of 3.8 Ohm/ft (nominal 576 W per 6 ft at 115V); silicone-rubber-covered tapes (Briskeat no. BS-61) have resistance of 7.6 Ohm/ft (nominal 288 W per 6 ft at 115V). Eventually all the fiberglass-covered tapes will be replaced by silicone-rubber-covered ones. The voltage drop across the tapes is separately controlled by low amperage transformers (Variac), which are manually adjusted by the operator in response to RTD readings. The maximum voltage drop across the tapes is 120V; they are continuously on during operation.

5.4.3.2 Pressure sensing and control. All vessels are normally connected through open valves during operation. Pressure is monitored in only one vessel, the stripping column. The pressure tap is at the top of the stripping column. This is a 1/2-in. stainless steel tube, which leads to a Bourdon-tube pressure gauge located on the control panel. The pressure at this point is also sensed by a Mercoid switch. When this pressure exceeds a set point, power to all the heaters is shut off and the emergency cooling water bleed opens (section 5.7.3). This cools the system as rapidly as possible.

The pressure drop through the column in monitored by a mercury manometer (Meriam Instrument Co., model 10AA25WM, division of Scott & Fetzer Co., Cleveland OH). The manometer is connected to the top and the bottom of the stripping column by mineral-oil filled Tygon tubing. The mineral oil is isolated from the column gas phase by diaphragms (Vanton Pump and Equipment Co., Hillside, NJ).

The pressure of the superheated steam is sensed by a Bourdon-tube pressure gauge. The gauge is filled with mineral oil and isolated from the steam by a 316L stainless steel diaphragm (Ametek M&G Division). Steam pressure data are used in steam flow calculations (see section 6.10 and Appendix C).

5.4.4 Overheads condenser (OC).

The vapor phase emerging from the top of the packed-bed column consists of steam plus gases that were stripped from the liquid phase. This vapor is condensed and collected in the overheads condenser. The overheads condenser is a stainless steel pipe 13 ft X 8 in. i.d., with bolted flange ends. Cooling water circulates through a coil of 50-ft X 1/2-in. o.d. 316 stainless tubing inside the overheads condenser, providing a cool surface on which the steam condenses.

5.4.4.1 Noncondensable gases. Gases that do not condense with the steam are defined operationally as noncondensable gases. During a run, they accumulate in the headspace of the overheads condenser and can cause operational problems. Some wastewaters contain small concentrations of these noncondensable gases, but certain wastewaters contain large concentrations. Failure of gases to condense in the overheads condenser increases the pressure in the overheads condenser. This increase in downstream pressure reduces the steam flow rate through the system. Eventually the overheads condenser will fill with these noncondensable gases and prevent steam from reaching the cold condensing surface. These factors prevent steady-state operation of the system. Operational symptoms that indicate a buildup of noncondensable gases in the overheads condenser are described in section 6.6. To avoid problems caused by accumulation of noncondensable gases in the overheads condenser, the contents of the overhead condenser are evacuated during a run (see section 6.6, step 8).

5.4.4.2 Cooling water loop. The cooling water moves in a continuous loop, propelled by the condenser pump . The cooling water gains heat as steam condenses on the coil inside the overheads condenser, and gives up heat to the atmosphere through exposed piping. As the cooling water becomes hotter, it loses its ability to remove heat and condense steam. To control the temperature of the cooling water (the parameter which is key to controlling the rate of condensation) some of the cooling water is bled off and replaced with colder water from the city of Richmond water service through valves OC-10 and OC-12.

There are three points in the loop through which cooling water can be bled; these are used for either manual, automatic, or emergency cooling. As water is bled from the cooling loop at any of these points, it is immediately replaced by colder city water through valves OC-10 and OC-12. The **manual** bleed is through valves OC-8 (to control the rate of flow) and OC-9 (to turn it on or off). The **automatic** bleed is controlled (on-off) by a solenoid valve activated by RTD-25 (Asco Red Hat, catalog no. 8211D2, orifice no. 508, 6W, 60 Hz, 120 V, Automatic Switch Co., Florham Park, NJ). The rate of automatic bleed is manually controlled by valve OC-7. When the temperature sensed by RTD-25 exceeds the set point, the solenoid valve opens, bleeding releasing water from the loop at a rate determined by valve OC-7. The **emergency** bleed can be operated manually or set to open automatically when the pressure in the overheads condenser (sensed by a Mercoid switch) exceeds a set point; a solenoid valve opens to rapidly bleed water from the cooling water loop; also all heating power is cut off. Manual or automatic operation is selected by a switch on the control panel labeled "emergency cool". In the "auto" position, the solenoid valve is controlled by the Mercoid switch.

The Mercoid switch (see Appendix A) is set to open this solenoid valve when the pressure exceeds 50 psig. In normal operation, the "emergency cool" switch is left in the "auto" position. The third position of the switch is not used.

The condenser pump is an Eastern model D11, type 105, 1/4 HP centrifugal pump manufactured by LFE Fluid Control Division. Nameplate information and catalog description are included in Appendix A. The condenser pump is controlled by an on-off switch on the control panel; it should always be on during normal operation.

5.4.5 Bottoms collector (BC).

The liquid phase that leaves the bottom of the packed bed (i.e., stripped wastewater) drains into the bottoms collector. The bottoms collector is a stainless steel pipe, 6-ft X 8-in. i.d., with 1-in. fiberglass insulation; it is set at a slight angle from horizontal to ensure complete drainage. The bottoms collector is connected to the cross below the stripping column with a PTFE Flexijoint flexible coupling. A sight glass shows the liquid level in the BC. There is a 1/2-in. o.d. 316 stainless coil inside the bottoms collector. In an emergency, valve OC-11 can be opened to run cold city water through this coil and cool the bottoms collector. Normally this feature is not used. Valves BC-1 and BC-2 drain the bottoms collector for sample collection. Because the bottoms collector is not truly horizontal, the inlet for BC-2 is lower than that for BC-1.

The bottoms collector temperature is sensed by two RTD's: RTD-24 senses the external temperature and is displayed on the control panel, and RTD-16 senses the internal temperature and is output to the data logger.

5.4.5.1 Heat tape. The bottoms collector is wrapped with a heat tape under the insulation. Voltage to the heat tape is contolled by a low-amperage Variac transformer; maximum voltage is 120V. The heat tape is a fiberglass-insulated tape, as described in section 5.4.3.1.

5.4.6 Feed preheater (FP).

During proper operation of the steam stripper, steam leaving the stripping column is condensed in the overheads condenser. No condensation occurs within the stripping column itself. To prevent incoming steam from condensing as soon as it contacts the wastewater, the wastewater is preheated.

The feed preheater consists of a 316L stainless steel pipe with a 316L stainless steel 1/2-in. coil inside. Wastewater feed flows through the coil. The space between the coil and the walls of the feed preheater is filled with hot water. The water is heated by a 6-kW Calrod immersion heater, model MP 4508 (identical to the heater in the steam generator, see Appendix A). A proportional controller operated by RTD-23 supplies 460V electric power. Feed is drawn from a carboy or other container by a pump and passed through the coil; feed leaving the feed preheater goes to the top of the stripping column.

A pressure relief valve (Balley #118, San Francisco, CA) will open to drain the feed preheater if the water pressure exceeds 100 psi. Unless this relief valve opens, there is no need to refill the preheater.

5.5 Raw Wastewater Feed Pump

The raw feed pump is an FMI Lab Pump (model RP-D; see Appendix A). Because it is a reciprocating piston (i.e., positive displacement) pump, the flow rate is independent of the head against which the water is pumped (up to 100 psi). The flow rate is set by a blue pointer which is positioned by a micrometer; this regulates the length of the piston stroke. The approximate pump calibration curve is shown in Figure 5.3. This calibration curve may be used to set a desired feed flow rate, but mass balances should be based on feed flow rate measurements. Feed flow rate measurements are made using a Gilmont F-1400 rotameter. The procedure for calibrating the rotameter is presented in section 6.3.1.

5.6 Flow Measurement and Control

During steady-state operation, steam is generated in the steam generator at the same rate at which it is condensed in the overheads condenser. The most convenient way for the operator to control the rate of steam flow is by using globe valve PB-7 as a throttling valve or by changing the setting on the overheads condenser temperature. The flow rate of wastewater to be treated is controlled by the setting of the feed pump (see section 5.5 and Figure 5.3). The flow rate of cooling water is constant, controlled by the condenser pump (see section 5.4.4.1). Normally there is no need to adjust this.

5.6.1 Raw feed flow-rate measurement.

The feed flow rate is measured with a Gilmont rotameter, model F-1400. Technical details are presented in the manufacturer's literature in Appenix A. The rotameter can be calibrated by pumping water through the rotameter while drawing from a burette; the time required to pump a measured volume gives the flow rate (mL/min). This technique is also used to check the flow rate during operation of the column. A calibration curve for water is presented in Figure 5.3.

5.6.2 Steam flow-rate measurement.

The steam flow rate is measured with a Gilmont rotameter, model F-1500. Technical details are presented in the manufacturer's literature in Appendix A. Because the polypropylene bushings supplied with this instrument cannot withstand the steam temperature, teflon bushings were fabricated and used. The bushings are shown in Figure 5.4.

The rotameter can be calibrated by operating at steady state for a measured period (30 min or more), and condensing and measuring the amount of steam (see section 6.3.2). The procedure for calculating the steam flow rate from the observed temperature, pressure, and rotameter readings is presented in section 6.8. The pressure gauge and protective diaphragm are described in section 5.4.3.2

5.7 Control Panel

The control panel is shown in Figure 5.5. This section describes the functions of each of the controls shown.

5.7.1 Resistance temperature detectors (RTDs).

Of the 18 RTDs in the system, five (RTDs 21 through 25) are displayed on the control panel. The others are displayed on the datalogger (section 5.11). RTDs **sense** the temperature at their respective locations, and put out an electrical signal which can be converted to a readable digital display and can also be used to **control** the temperature. The signals from RTDs 21, 22, 23, and 25 go to proportional controllers. The controllers regulate the amount of energy for heating delivered to the steam generator, steam drier, and feed preheater (in response to signals from RTDs 21, 22, and 23, respectively) and open the automatic cooling water bleed (in response to the signal from RTD 25). It is convenient to think of RTDs 21, 22, 23, and 25 as both sensing and controlling the temperatures, but it should be clear that these functions are actually separated between the RTDs and the controllers. The functioning of the temperature controllers is described in sections 5.9 and 6.2.1. The other RTDs (nos. 4 and 6 through 17) sense temperatures only and are not connected to controllers.

For each RTD displayed on the control panel, there is an on-off switch, two lights, a digital temperature display, and a running time meter. The on-off switches cut power to both the RTDs and their respective controllers. When power is off, the controller will not send power to the respective heating element (steam generator, feed preheater, or steam drier) or open the solenoid valve (overheads condenser cooling water). The red "power" light indicates that power is being supplied to the RTD and that the controller is available for its respective function. The white light indicates that the control function is operating (e.g., the heating element in the steam drier is drawing energy). A red pilot light in the RTD controller display has the same function as the white light. Each running time meter records the cumulative amount of time that energy is being drawn. Note that no function is controlled by RTD-24; therefore the white light is unused. For RTDs 21 through 24, the white light indicates heating; for RTD-25, it indicates that the automatic cooling water bleed is open.

5.7.2 Pressure gauge.

The pressure gauge is connected by a pressure tap to the top of the stripping column. The tap is completely filled with water, and the level of the gauge is below the level of the point at which pressure is sensed; consequently the pressure indicated by the gauge is 7.2 psi higher than the actual pressure.

5.7.3 Emergency cool.

The emergency bleed is a solenoid valve that opens to rapidly bleed warm water from the cooling water loop. It is controlled either manually or automatically, as selected by a switch on the control panel. In the "auto" position, the solenoid valve is controlled by the Mercoid switch. The Mercoid switch is set to open this solenoid valve (and also cut off heating

power) when the pressure exceeds 50 psig. In normal operation, the switch should be left in the "auto" position. Setting the switch to the "manual" position opens the solenoid valve. Do not set this switch to "manual" unless it is actually necessary to cool the system rapidly (see section 5.4.4.2). The third position of the switch is not used. The red "supercool" light indicates that the emergency bleed is open.

5.7.4. Pump switches.

The three pumps (flash evaporator, raw feed, and condenser) are controlled by on-off switches, and their on-off status is indicated by running lights. Normally these are all "on" during operation. Note that the switches actually have three positions; the uppermost one is "on," and the two others are "off."

5.7.5 Master switch.

When set to "off", the master switch overrides all other switches on the control panel except the steam drier. In normal operation it is left "on".

5.8 Main Time Switch

There are two time switches located on the left side of the wooden box behind the control panel. The main time switch controls the entire control panel, except for the steam drier (which is controlled by a separate time switch; see section 5.4.2.1). The main time switch is an Intermatic time switch, model T171 (Intermatic, Inc., Spring Grove, IL). It displays a 24-hour clock with two arrows that indicate the time off and on. There is also a manual override switch immediately below the clock face, which can be used to turn the control panel on when it is scheduled to be off, or vice versa. If the system is left on before the scheduled "on" time, it will continue on until the scheduled "off" time.

5.9 Temperature Sensing and Control

The LBL/SEEHRL steam stripper system was designed to meet two objectives. First, it must simulate, at small semi-pilot scale, the operation of a full-scale steam stripper. Second, it must be sufficiently flexible to operate under a range of experimental conditions, while allowing for the determination of total mass balances. To accomplish these goals, the ability to accurately control and monitor temperatures and pressures in the system is essential.

Such a small pilot-scale system loses more heat to its surroundings than a large one, because it has a much greater surface-to-volume ratio. This makes temperature control much more difficult. Since a major objective is to study the transfer of volatile solutes from the liquid to the gas phase without the complicating factors of evaporation or condensation in the column, it is necessary that temperatures along the stripping column be uniform and that steam entering the bottom of the stripping column be at the same temperature as the column. Steam and water flow rates must also be controllable independently of each other.

To enable the operator to control temperatures in the system, the system is equipped with eighteen resistance temperature detectors (RTDs). These sense and display the temperature at various points in the system. The location and functions of the RTDs are summarized in Table 5.3.

RTDs 21, 22, 23, and 25 both indicate and control temperatures. The other RTDs function as temperature indicators only, and have no automatic controlling functions. The operator, however, can manually adjust conditions (such as voltages to the heat tapes) to control temperatures.

Electrical power is drawn to raise steam, dry the steam, and preheat the wastewater feed. RTD-21, -22, and -23 determine these respective temperatures by controlling the amount of energy drawn for these three uses. In this application, the RTDs control temperatures by regulating the percentage of time "on" for the respective Calrod electric heaters. The method of temperature control and the directions for operation are described in section 5.9.1. RTD-25 operates a solenoid valve (on-off control only) that bleeds warm water from the cooling water loop, thereby making the cooling water colder. The rate of bleeding of cooling water is controlled by globe valve OC-7 (see section5.4.4.2).

5.9.1 RTD temperature controllers.

Four RTD digital controllers (Omega Engineering, model 4201; catalog description in Appendix A) control the temperatures in the steam generator, feed preheater, and steam drier by controlling the amount of energy drawn by these respective functions, and in the overheads condenser by controlling the automatic bleeding of water from the cooling water loop.

The controllers can be set to operate as either on-off or proportional controllers. On-off control is the limiting case of proportional control with a zero bandwidth. On-off control functions like a simple thermostat. When the detected temperature is below the set-point, power to the heater is on; when the temperature sensed is at or above the set point, power is off. Because on-off control can overshoot the set point (because of the nature of resistance heating), the controllers also can be operated as proportional controllers with a variable bandwidth. Normally, RTD controllers are operated as proportional controllers with non-zero bandwidth. For example, assume that the temperature in the steam drier is being controlled, the set point is 100°C, and the bandwidth is 10°C; the temperature control band is therefore 95 to 105°C. If the temperature is 105°C or above, the heater will be on 0% of the time. If the temperature is 95°C or below, the heater will be on 100% of the time. At any temperature between these extremes, the percentage of time on is proportional to the difference between the temperature and the upper end of the temperature control band. For example, at 96°C, the heater would be on 90% of the time. The bandwidth can be varied from zero (on-off control) to 12°C (3% of the full range of the controller).

Figure 5.6 shows the appearance of the RTD controllers. A hinged door covers the bottom row of controls. When power to the RTDs and associated controllers is turned on by the appropriate switch on the control panel, the RTD displays the temperature sensed. To display the set point, push the spring-loaded set-point switch to the right. To change the set point, hold

the set-point switch to the right while adjusting the knob to the right of the switch until the desired reading is displayed. To vary the bandwidth, adjust the appropriate screw as shown in Figure 5.6.

Under some circumstances, the RTD will not be able to stabilize the temperature; for these instances, see section 6.2 on temperature control. In general, the temperature will stabilize somewhere within the control band. When the temperature stabilizes, it may be at a temperature different from the set point. Correct this by adjusting the offset screw (Fig. 5.6). If the temperature oscillates, the bandwidth is too narrow. If the temperature approaches a constant value and then decreases, the bandwidth is too wide.

5.9.2 Heat tapes.

In addition to the temperature control exerted by the proportional controllers, the temperature of the stripping column and of the bottoms collector can be adjusted by heat tapes (see Table 5.2, also sections 5.4.3.1 and 6.2.2). The purpose of these heat tapes is to minimize temperature variation along the column; this can be a particular problem depending on the ambient outside air temperature and wind speed. There are six series of heat tapes around the column; power to each can be independently controlled.

5.9.3 Steam drier transformer.

A high-amperage transformer (Powerstat) controls the voltage to the steam drier. This can be set to minimize overshoot of the temperature set by RTD-22 (also see section 6.2.1.4).

5.10 Pressure Sensors and Controls

During operation, the entire system is isolated from the atmosphere by closed valves. This allows the system to be operated at pressures either above or below atmospheric pressure and permits conditions for determining mass balances. During steady-state operation, the rate of production of steam in the steam generator is balanced by the rate of condensation of steam in the overheads condenser. This creates a pressure gradient causing flow of steam through the system. At any point in the system where two phases are in contact (such as in the steam generator or in the stripping column) the pressure is the same in both phases. Where there is standing water in the system (as in the reservoir of the steam generator or in the overheads condenser or bottoms collector) the pressure on any point beneath the water surface is the sum of the pressure of the steam over the water and the hydrostatic pressure of the water.

If the rate of steam production and condensation are out of balance, there may be a pressure increase in the system. To prevent excessive pressures from being reached in the system, the pressure at the top of the overheads condenser is sensed by a Mercoid switch (see Appendix A and section 5.4.4.1). The Mercoid switch (Type DA 31-55 R5) is a pressure gauge with a liquid mercury contact. The pressure limit can be set by adjusting a pointer, which is visible in the face of the switch. If the pressure should exceed the limit (currently set at 50 psi) it automatically shuts off all electrical heaters in the system and opens the emergency cooling water bleed to cool the system as rapidly as possible. The steam generator and feed

preheater (outside the coil) are also protected by pressure relief valves that are set at 60 psi. The pressure in the overheads condenser is also sensed and displayed on a standard Bourdon tube pressure gauge on the control panel (Type 28 Test Gauge, 0-60 psi, Marsh Instrument Co. Skokie, IL) (see section 5.7.2).

5.11 Datalogger

Temperatures reported by thirteen of the RTDs are automatically recorded by a Digitec Datalogger, model 1101 (Digitec Corp., Dayton OH). There are twenty available data channels (an additional twenty channels can be made available by addition of another interface device), of which thirteen are used. For convenience, the RTD-number and the channel number are the same, but RTDs 21 through 25 are not logged, but rather displayed on the control panel. Table 5.4 lists the contents of the channels. The temperatures are continuously displayed on a rotating basis and are printed at regular intervals (set by the operator) on electrosensitive paper.

CHAPTER 6. OPERATION

6.1 Introduction

This section gives the detailed instructions for startup, control, sampling, and shutdown of the system for a run. Section 6.2 explains the operation of the RTDs and heat tapes, which control temperatures in the system (see also 5.9.1). Section 6.3 gives calibration directions for the raw feed-flow and steam-flow rotameters. Section 6.4 specifies the valve positions during start-up, operation, and shutdown. Sections 6.5 through 6.8 are the detailed step-by-step instructions for operating the system during start-up, run time, shutdown, and cleanup. These can be followed cookbook style, but the operator should also understand the effects of each action and should be prepared to depart from the written instructions when necessary. Section 6.9 gives directions for collecting and analyzing samples. Section 6.10 presents the calculations needed for data reduction, and an example calculation is carried out in section 6.11.

6.2 Control of Operating Temperatures

6.2.1 Resistance temperature detectors (RTDs).

Sections 6.2.1.1 and 6.2.1.2 are the manufacturer's directions for using the RTD temperature controllers to achieve temperature control. Points that must be emphasized, based on experience with this system, are discussed in sections 6.2.1.3 through 6.2.1.7.

6.2.1.1 Bandwidth and set-point setting. The proportional band adjustment widens or narrows the band over which proportional action occurs. A band which is too narrow can cause the temperature to oscillate around the set-point. A band which is too wide can cause discrepancies between the set-point and the actual temperature measured at the sensor.

This setting is properly adjusted when the temperature oscillations just stop. Adjustment of the proportional band control should be done in small increments, allowing time between each adjustment for the process to stabilize. Turning the adjustment clockwise widens the proportional band and should reduce the oscillations to straight-line control in most instances.

6.2.1.2 Manual reset adjustment. After the proportional band is set, the process temperature will stabilize at a point that may deviate slightly from the set-point. This offset is normal with type 4201 controllers and can be corrected by adjusting the manual reset potentiometer. If the digital display indicates a stable temperature lower than the set-point, turn the reset potentiometer clockwise (+ direction), and wait until the process stabilizes. Adjustments should be made in small increments; several minutes may be required for the process to stabilize at the new temperature.

6.2.1.3 Stabilization time. Sufficient time must be allowed for temperatures to stabilize after settings have been changed. The feed preheater is the slowest of all the temperature-controlled units to respond. It should be closely observed for at least 15 min before deciding whether the temperature is rising, falling, oscillating, or stable.

Any operation that can produce a pressure change in the system (e.g., rapidly venting steam, introducing feed water that degasses rapidly, or suddenly reducing the temperature of the water in the cooling loop by rapid bleeding) will affect the temperature readings. Sufficient time must then be allowed to determine whether the temperatures will return to their previous values or whether compensating adjustments of the RTDs will be needed. Changes of 1°C in the steam generator and 2°C in the overheads condenser are common. Very large changes have been observed in the steam drier; the temperature has exceeded 200°C (the upper limit of the RTD temperature display) when the system has been perturbed by a sudden pressure change. When the temperature exceeds 200°C, the display goes blank.

6.2.1.4 Steam drier and overheads condenser. If bandwidth adjustments as prescribed in the manufacturer's instructions do not stabilize temperatures in the steam drier or overheads condenser, the voltage to the steam drier heating element (controlled by the high-amperage transformer, see section 5.4.2) or the cooling water bleed rate (controlled by valve OC-7, see section 5.4.4.2), respectively, must be adjusted. This problem is occasionally encountered because these two units have considerable excess heating and cooling capacity, respectively. Temperature oscillations often cannot be controlled by bandwidth settings alone.

6.2.1.5 Loose connections at RTD lead terminations. Loose connections at the terminations of RTD leads produce symptoms not listed in the manufacturer's troubleshooting guide (see Appendix A). Symptoms of loose connections include sudden large or small changes in the displayed temperatures. Also, the set-point display may change each time the set-point display switch is pressed; the problem is most likely not with the set-point display switch, but with the connection of the RTD lead. Inspect the screw terminals carefully at both ends (the RTD and the proportional controller); the very fine RTD leads may be crushed or broken by the terminal screw, giving the appearance of a tight connection even though adequate contact is not being made.

6.2.1.6 Condensation on probe tips. In a system with saturated vapor, condensation on RTD probe tips may affect temperature readings. This occurs most often with probes that are installed with the tip downward; inaccurate readings are caused when water condenses on the sheath, runs down to the tip, and drops off, blows off, or evaporates. This condition gives a period of steady temperature, followed by a sudden drop and gradual recovery. During the period of recovery, the red "heating" light on the control panel (see section 5.7.1) will be on much longer than during the stable interval. The pattern of temperature variation resulting from condensation can be distinguished from the regular oscillations characteristic of a too-narrow bandwidth setting or of excessive heating or cooling capacity (see section 6.2.1.4).

6.2.1.7 "Cross-talk" among controllers. When the steam stripper system was first operated, problems were experienced with "cross-talk" among the temperature controllers. This is a common problem when high amperage loads are being controlled; voltage transients are developed when one controller turns on or off, sending a false signal to the other controllers and causing them to turn on or off when not needed for temperature control. "Chattering" or frequent switching of controllers is symptomatic of this problem.

The problem was solved by installation of RC (resistance-capacitance) filters across the relay terminals. A 0.1 μf capacitor in series with a 15-ohm, 1-W resistor was installed across all output-controller output terminals. Similar filters, but with two capacitors in series, to give a capacitance of 0.05 μf, were installed across the relay contacts controlling the cumulative timers. This has solved the problem. If similar problems occur in the future, the solution may be to replace the filters, or to adjust their resistance or capacitance.

6.2.1.8 Troubleshooting of proportional controllers. Additional information is contained in the manufacturer's troubleshooting instructions in Appendix A.

6.2.2 Heat tape.

Heat tapes are used to control the temperatures in the stripping column, at the 2-in. stainless-steel pipe cross above the stripping column, and in the bottoms collector (see sections 5.4.3.1 and 5.4.5.1). No automatic controls are used with the heat tapes. Each heat tape is controlled by a separate transformer that should be set to maintain skin temperatures as close as possible to internal temperatures. Insufficient heating results in condensation of steam in the bottoms collector; excessive heating results in evaporation of feed or bottoms. These cause a discrepancy between the cumulative feed volume during a run and the bottoms volume collected.

A change of 3 volts (3 divisions) in the transformer setting produces a change of approximately 1°C in the stripping column temperature within 15 minutes; the cross above the column and the bottoms collector respond much more slowly than the stripping column, because the heat tape is around stainless steel rather than Pyrex glass. Once the proper transformer settings have been established by trial and error, little if any adjustment will be needed to repeat a particular set of operating conditions. Adjustments, if necessary, should be made gradually. To reduce warmup time, heat tapes may be left on the night before a run.

6.3 Rotameter Calibration Procedure

6.3.1 Raw feed rotameter.

The rotameter is calibrated by the "bucket and stopwatch" method. Set the three-way stopcock as shown in Figure 6.1 so that feed is drawn from a 1-L burette rather than from the feed carboy. Use a stopwatch to measure the time needed to pump a precisely known volume. This gives an accurate measurement of the feed flow rate. The rotameter reading should be steady during this procedure; the rotameter reading is taken at the middle of the ball. The burette is filled from a reservoir set at an elevation above the burette. This calibration/flow rate measurement procedure can be performed without interruption of feed to the feed preheater.

The procedure for measuring the feed rate and calibrating the rotameter is as follows. While the system is operating, set the three-way stopcock as shown in Figure 6.1 (position a). Fill the burette. A 100-mL burette is used for low flow-rate calibration and a 500-mL burette is used for high flow-rate calibrations. Change the three-way stopcock to position (b) (Fig. 6.1). The feed pump will continue to deliver water to the feed preheater, but instead of

drawing the water from the reservoir carboy, it will be drawn down from the burette. The time interval needed to pump a known amount of water from the burette into the feed preheater indicates the feed rate. The calculation is shown in section 6.10.1. After making this measurement, return the three-way stopcock to position (a). It is important that the stopcock not be left in any intermediate positions since this will stop the flow.

6.3.2 Steam flow rotameter.

The steam flow rotameter is calibrated by generating steam under steady conditions for one hour or longer. Monitor the rate at which water is drawn from the steam generator by recording the water level in the sight glass. Markings on the sight glass are in intervals of 1 L. At the start of the measured period of time, drain the overheads condenser and the bottoms collector. At the end of the time period, drain these vessels again and weigh the amount of water. The total mass of water in (measured from sight glass readings) should equal the total amount of water out (drained from the overheads condenser and the bottoms collector at the end of the time period). When calculating the mass of water drawn from the steam generator, recall that each liter of water is less than 1 kg, because at elevated temperature the density of water is less than 1.00 g/mL. The steam flow rate calculated from these observations should agree closely with the steam flow rate as calculated by the formulas provided by the manufacturer (see Gilmont catalog p 6-7, in Appendix A, where an example calculation is worked; also see section 6.10.2 and Appendix C).

6.4 Valve Positions during Operation

This section summarizes the settings of valves during normal operation. The following section also gives information on how valves are to be set during start-up.

6.4.1 Steam generator.

During normal operation of the steam generator, valves SG-1, 2, 3, 5, 7, and 8 are closed. Valves SG-4 and SG-6 are open. There is also a pressure relief valve at the top of the steam generator that is set to open when the pressure in the steam generator exceeds 60 psig.

The rate of steam generation depends directly upon the temperature and pressure in the steam generator and the rate of energy input to the steam generator. Pressure in the steam generator is determined by the pressure drop through the system; most of the pressure drop occurs in the packed column and in the throttling valves PB-5 and PB-7 below and above the stripping column, respectively. From the point of view of operational control, the most convenient way to control the rate of steam generation, once the temperature in the steam generator is established, is to control the pressure in the steam generator by using valve PB-5.

6.4.2 Packed-bed stripping column.

Valves PB-1 through PB-3 are normally closed (valve PB-2 drains the packed bed). Valve PB-4 is normally open. Valves PB-5 and PB-7 must be open during a run; they control the rate of steam flow through the column. Normally, PB-7 is

open 1/2 turn during a run, and PB-5 is used for fine control. Valve PB-6 is a ball valve (i.e., it is fully opened or closed). Normally it is opened when warming up the system and closed during a run. Valve PB-8 is normally closed.

6.4.3 Cooling water loop.

There are three points in the loop through which cooling water can be bled; these are used for either manual, automatic, or emergency cooling. As water is bled from the cooling loop at any of these points, it is immediately replaced by colder city water through valves OC-10 and OC-12. The **manual** bleed is through valves OC-8 (to control the rate of flow) and OC-9 (to turn it on or off). The **automatic** bleed is controlled (on-off) by a solenoid valve (activated by RTD-25). The rate of automatic bleed is normally controlled by valve OC-7. When the temperature sensed by RTD-25 exceeds the set point, the temperature controller opens the solenoid valve, releasing water from the loop at a rate determined by valve OC-7. Experience has shown that for minimum temperature fluctuation, it is best to adjust valve OC-7 so that cooling water is automatically bled frequently at a trickle rather than infrequently at a large rate. The **emergency** bleed can be operated manually or set to open automatically when the pressure in the overheads condenser (sensed by a Mercoid switch) exceeds a set point; a solenoid valve opens to rapidly bleed water from the cooling water loop; also all heating power is cut off. Manual or automatic operation is selected by a switch on the control panel labeled "emergency cool". In the "auto" position, the solenoid valve is controlled by the Mercoid switch. The Mercoid switch (see Appendix A) is set to open this solenoid valve when the pressure exceeds 50 psig. In normal operation, the "emergency cool" switch is left in the "auto" position. The third position of the switch is not used.

It is important to note that rapid bleeding of the cooling water will cause a sudden drop in pressure of the overheads condenser. This can cause the packing in the stripping column to be drawn upward into the overheads condenser. Therefore never use the "emergency cool" switch unless it is actually necessary to cool the system rapidly. If packing is ever drawn into the overheads condenser, the bottom of the overheads condenser should be taken off to remove the packing. This is necessary to protect valve OC-5, which would be damaged if it were closed on a piece of packing.

If the operator has neglected to turn on the condenser pump during system start-up and later finds that it must be turned on, valve OC-1 should be opened fully before starting the condenser pump, and the pressure and temperature in the overheads condenser should be allowed to recover somewhat before completely closing the valve. This will prevent dislocation of the packing.

Valves OC-1, -4, -5, and -11 are closed. Valves OC-2, -3, and -6 have been removed from the system. Valves OC-7 and -8 are set to control the rate of automatic cooling and manual cooling water bleed, respectively. Valve OC-9 is normally closed but can be opened as needed for manual bleeding of cooling water. Valves OC-10 and -12 must always be open.

6.4.4 Bottoms collector.

Valves BC-1 and -2 are normally closed during operation. They are opened to vent the system during start-up, to drain the bottoms collector immediately

before a run, and to collect samples during and at the end of a run. Valves BC-3 and BC-4 are normally open during a run.

6.4.5 Feed preheater.

Valve FP-1 is used to fill the feed preheater with water. It is normally closed. Unless the pressure relief valve opens, the feed preheater should not require refilling.

6.5 Start-Up

Because the operator frequently must climb ladders and work in wet areas, safety equipment has been provided and it must be used. Wear a hard hat with a face shield when operating the steam stripper system and use the safety harness when climbing the ladder to the upper deck. Steel toe safety shoes with non-slip soles are recommended.

Steps 1 through 11 of the start-up procedure can be done the day before a run. The steam drier, steam generator, steam feed pump, and cooling water pump can all be set to start automatically before the operator arrives. This saves the time needed to warm up the system.

Note that at the start of a run, the system has achieved stable operation with ASTM Type III water feed and is suddenly switched to raw wastewater feed. For best stability during this change-over, the temperature of the feed should be the same as the ASTM Type III water. To achieve this, the carboy of ASTM Type III water should be refrigerated, or the raw feed should be equilibrated to ambient temperature the night before a run.

1. Select desired operating conditions and record on data sheet (Fig. 6.2). Decide on operating temperatures for all vessels, desired liquid and steam flow rates, and desired scrubbing flow rate (the latter can be zero if significant buildup of noncondensable gases is not anticipated).

2. Prepare acid-washed or -rinsed sample collection bottles. Bottoms and overheads are collected at the end of the run (or at intervals during the run) in plastic 5-gal carboys. Prepare enough carboys to contain the anticipated volume of overheads and bottoms. Normally one carboy will be sufficient for the overheads and two for the bottoms. Aliquots for analysis are collected from the carboys in 1-L glass sample bottles with Teflon-lined caps.

3. Set valves as shown in Table 6.1.

4. Time Switches: If they are scheduled to be off, turn them temporarily on by using the manual override feature (see sections 5.4.2.1 and 5.8). Turn off RTD-22 and master switch at control panel.

5. Check circuit breakers at the stripper circuit-breaker box (behind the control panel) and at the pilot plant circuit-breaker box. The steam stripper operates on circuits 21-22 and 23-24 of the SEEHRL pilot plant circuit breaker box, which is mounted on the back of the primary sedimentation basin of the activated sludge treatment train.

6. Check reading of pressure gauge on control panel. If it is less than 7.2 psi, the pressure tap is not full of water. To fill the pressure tap, close PB-4 (to protect the pressure gauge), connect city water supply to valve PB-1, and fill until the pressure gauge reading does not change. Another way to check this would be to open valve PB-2, BC-1, or BC-2. When the pressure tap is full of water, water will overflow into the top of the packed column and drain out of these valves. Then open PB-4, close PB-1, and disconnect city water supply.

7. Control Panel: set master switch ON, all others OFF.

8. Fill steam generator to desired level with ASTM Type III water. If the water level in the steam generator is visible in the sight glass, then it is probably high enough to prime the flash evaporator pump, and the steam generator can be filled by connecting a reservoir of distilled water to valve SG-8. This will normally be the case. If there is not enough water in the steam generator to prime the steam feed pump, then the steam generator must be filled through valve SG-5 using the raw feed pump, which is self-priming. A low water level in the steam generator may indicate a leak in the seat of the flash evaporator pump.

a. If water is visible in the sight glass, the steam generator can usually be filled using the flash evaporator pump. Verify that the flash evaporator pump is primed, as follows:

Turn the flash evaporator pump on at the control panel. Wait 30 seconds, then watch for water trickling down the sight glass. If none appears, turn the pump off, wait a few seconds, and repeat. Note that the pump prime can be checked by using the pump to recirculate water; it is not necessary to pump water into the steam generator. Water leaking from around the impeller shaft indicates that seals are worn and need replacing.

If the pump is primed, fill the steam generator through valve SG-8, and go to step 8.c. (If not, go to step 8.b.)

b. If the flash evaporator pump is not primed, the steam generator must be filled through valve SG-5, using the raw feed pump (which is self-priming), until there is enough water in the steam generator to prime the flash evaporator pump.

Turn off flash evaporator pump.

Close SG-4. Open SG-5. Place the end of the raw feed intake tube into a container of ASTM Type III water. Set raw feed pump at maximum rate and turn on. Check steam generator sight glass to ensure that water is flowing to the steam generator. After about 5 minutes or when water is visible in the steam generator sight glass, turn the raw water feed pump off and repeat step 8.a to check if the steam feed pump is primed. If the pump is primed, close valve SG-5, open valve SG-4, and go to step 8.c. If it is not, repeat step 8.b.

Alternatively, the reservoir of ASTM Type III water that is used to fill the steam generator can be placed on the second level of the Unistrut support and connected to SG-8. Open SG-8. The elevation of the reservoir will provide adequate head to prime the flash evaporator pump; the steam generator can then be filled through SG-8.

c. Once the flash evaporator pump is primed, the steam generator can be filled. Place the end of the intake tube connected to valve SG-8 into the reservoir (e.g., carboy) of ASTM Type III water. The reservoir should be higher than valve SG-8. Open SG-8. The head of water in the steam generator will cause water to back up into the reservoir, expelling air from the line. As soon as bubbling stops, quickly close SG-6. Turn on the flash evaporator pump and watch for water trickling down the sight glass. If none is seen, repeat step 8.b. (the steam feed pump is not primed).

d. Fill steam generator to desired level. There must be sufficient water in the steam generator to last through the run; operate the pump for about 2 min after the water level reaches the top of the sight glass.

e. Simultaneously close valve SG-8 and open valve SG-6; the steam generator reservoir is now filled.

9. Turn on control panel electronics (master switch is already on). Panel electronics must be on to operate flash evaporator pump, cooling water pump, and steam generator.

a. Flash evaporator pump should already be on (8.a).

b. Turn on RTD-21 (which controls the steam generator temperature) and set the set-point about 10°C higher than the desired operating temperature. (Later the set point will be lowered to the desired operating temperature). Set the bandwidth halfway between zero and maximum.

c. Turn on RTD-23 (which controls the feed preheater temperature) and set the set-point at the desired operating temperature. Set the bandwidth halfway between zero and maximum.

d. Turn on RTD-24 (which indicates the bottoms collector temperature). RTD-24 does not control anything, so the set-point has no effect.

e. Turn on RTD-22 (which controls steam drier temperature) and set the set-point at the desired temperature (185°C is recommended). Optional: if the desired temperature is relatively low (e.g., 140°C), then setting the control temperature higher than the desired operating temperature will allow the system to approach desired operating conditions more quickly.

f. Turn on RTD-25 (which controls the overheads condenser temperature by regulating the automatic bleeding of cooling water)

and set it to a high temperature (e.g., 120°C). Optional: OC-7 may be closed so that when the system starts, there will be no bleeding of cooling water, and the system will warm up more quickly. Be sure to open OC-7 during the run.

g. Adjust high-amperage transformer to regulate voltage to steam drier. A setting of 70 will provide good control for 185°C; lower temperatures will require a lower setting. Do not set the transformer higher than 80, which gives full line voltage. Further adjustments may be necessary later; see section 6.2.1.4.

h. Turn on condenser cooling pump.

i. Set individual timers to zero. These record the cumulative amount of "on" time for each of the temperature controllers. Note that the main run timer on the control panel is not connected.

10. Check the indicated time on the time switches, reset if necessary, and set the time switches to turn on system at the desired time. The main time switch (section 5.8) controls all the equipment except RTD-22 and the steam drier, which are on a separate time switch (section 5.4.2.1). The master switch is in series with the main time switch; both must be on, therefore, to draw power. It is generally convenient to set the timers to turn on the steam drier and steam generator up to 3 hours before the start of the work day; 3 hours is enough time to bring the system up to temperature. Low-amperage transformers controlling the heat tapes (these are not powered through the control panel) can also be turned on the night before. The steam generator should start before the steam drier, so that the steam drier does not simply heat air; it is convenient to set the "on" time to 4:00 a.m. for the steam generator and 7:00 a.m. for the steam drier. The "off" times must be set late enough so that they do not interfere with a run, and yet early enough that the system is off the night before. It may be necessary to change the "off" time during a run to meet both of these conditions. For operation of the timers, see sections 5.8 and 5.4.2.1. For an early start up, steps 1 through 11 can be done the night before a run. Valves should now be set as shown in Table 6.1.

11. The following day, plug in and turn on the transformers that control power to the heat tapes.

12. Set up the wastewater container (usually a drum) and mixer to homogenize the sample. This should be done at least 1 hr before the run begins (step 24).

13. Open valves OC-1, OC-4, and BC-1. All the valves that isolate the overheads condenser and the bottoms collector from the atmosphere are now open.

14. Open SG-5. This will flush out the feed line with steam. Close SG-5 after 10 minutes.

15. Flush entire system with steam.

a. When steam emerges from BC-1 and -2, close them.

b. When steam emerges from OC-5, wait ten minutes to flush the entire system with steam. Then close OC-1, -4, and -5. The system is now isolated from the atmosphere.

16. Change the RTD set points to the desired operating temperatures. Usually, only RTD-21 and RTD-25 have been set above the desired operating temperature (for more rapid heating) and need to be changed. The temperature in the overheads condenser will also be above the desired operating temperature.

17. If OC-7 was closed to ensure rapid heating of the system, open it now. This will permit automatic bleeding of cooling water.

18. Watch temperature displayed by RTD-12. When it reads 1°C above the desired operating temperature, close PB-6 and adjust PB-7 to control the steam flow (PB-7 must be opened approximately 1/4 turn). This will gradually cause the temperature sensed by RTD-12 to rise and that sensed by RTD-25 to drop. Valves should now be set as shown in Table 6.2.

19. Ordinarily, there is no need to adjust the RTD controller settings or the heat tape voltage settings; normally they will have been set correctly from the previous run. If necessary, adjust RTDs and heat tapes to achieve desired operating temperatures throughout the system. First adjust the bandwidths and set-points of the RTDs, then adjust heat tapes to achieve uniform temperature along the column (see sections 6.2.1 and 6.2.2).

20. When the desired operating temperatures are reached, begin the water feed (i.e., place the end of the intake tube in a reservoir of ASTM Type III water and turn the water feed pump on). Normally the steam stripper is started on ASTM Type III water to conserve wastewater because a large amount of water is fed through the system while it is stabilizing. The ASTM Type III water and the feed should be at the same temperature; remove feed from the refrigerator the night before or refrigerate the ASTM Type III water.

21. It is preferable to have the steam-flow rotameter calibrated in advance of a run. However, if it has not been calibrated, the steam flow rate must be measured during start-up. Operate the system with ASTM Type III water. All temperatures, pressures, and the feed rate should be the same as those that will be used during the run. Drain the overheads condenser and then operate the system for 30 minutes. The combined volume of condensed overheads and bottom, minus the volume of feed during 30 minute (calculated as flow rate X time) is the volume of steam produced in 30 minutes.

22. Record operating temperatures at 15-minute intervals on a data sheet (Fig. 6.2). Also record any actions taken. Start the datalogger recording.

23. At this point, ensure that the system is approaching the set point and is operating stably. The temperatures should vary only slightly around the set points. These can be controlled by adjusting the set-point and bandwidth of the RTDs as described in section 6.2.1. For more information on operation of RTDs, see Appendix A. Before a run can begin, temperatures must be stable throughout the system and uniform throughout the column, as indicated by RTDs 6, 7, 8, and 9.

24. Adjust the transformer controls on the heat tapes to get RTDs 6, 7, 8, and 9 reading the same. The feed temperature (RTD-12) should also be the same as the column temperature. This can be adjusted by changing the feed preheater temperature (RTD-23). The temperature at the bottom of the column (RTD-7) can be adjusted by changing the steam drier temperature at the control panel (RTD-22).

6.6 Operation

The actual stripping run should begin only after the system is stabilized. If the temperature in the overheads condenser (indicated by RTD-25) and the bottom of the column (indicated by RTD-24) do not change by more than 0.1°C during a 30-min period, and RTDs 6 through 9 are steady, the system can be considered stable. The temperature in the steam generator and steam drier are not critical; these may vary but should not gradually increase or decrease.

1. At the start of a run, slowly drain the overheads condenser and bottoms collector through valves OC-5 and BC-1 or -2. Do not allow steam to escape, as this will cause a loss of pressure and temperature in the system. Try to maintain a pool of water above the open valve and close it immediately when steam appears. Note that if the overheads condenser temperature is less than 100°C, the overheads condenser will be under a partial vacuum. In this case, the overheads condenser cannot be drained simply by opening a valve; air would enter the overhead condenser rather than any liquid being drained. Prepare a vacuum trap as shown in Figure 6.3. Open valve OC-5. Liquid in the overheads condenser will be drawn into the vacuum trap. When this flow stops, close valve OC-5.

2. Change the feed reservoir from water to wastewater that is at the same temperature. The wastewater should have been homogenized and at the same temperature as the ASTM Type III water.

3. Drain the stripping column through valve PB-2 until the odor of retort water can be detected (5 to 10 minutes). As in step 1, do this slowly to avoid disturbing the system, try to maintain a pool of water above the open valve. Drain overheads condenser and bottoms collector again (see Step 1.).

4. Record the time, and start the stopwatch. Record the displays of all running-time meters.

5. Record all rotameter readings, temperatures, and pressures at 15-minute intervals during the run. Temperature fluctuations should not be greater than 0.2°C at RTD-23, -24, or -25.

6. Sampling. At the start of the run, decide how long the run will be and whether the bottoms collector is large enough to contain the anticipated volume of stripped water. If it is, the overheads condenser will need to be drained only once; this can be either immediately after the run or after cooldown (i.e., the next day). The shutdown procedure varies depending on the sampling procedure which is used.

If the capacity of the bottoms collector is inadequate for the amount of water anticipated to be stripped during a run, the bottoms collector should be drained at intervals (approximately every half-hour). Open valve BC-2, and collect the water in a sampling bottle (e.g., polypropylene; must be able to withstand 120°C) until steam emerges. It is important that the container be filled as full as possible to minimize loss of volatile compounds to the headspace.

7. The condensed overheads should be collected only after the system has cooled down. In the event of crystalline deposit formation in the sight glass, the sight glass can be flushed through valve OC-4 at the end of the run. Collect a sample of the raw feed at the end of the run.

8. Instability of operating conditions during a run may indicate accumulation of noncondensable gases in the overheads condenser. Symptoms which indicate this include:

(1) Water in the cooling loop gets colder because less steam is condensing. Open OC-9 briefly to check this.

(2) Temperature indicated by RTD-24 (bottoms collector) increases.

(3) Temperature indicated by RTD-25 (overheads condenser) remains high and automatic cooling water bleed remains open continuously although the water in the cooling loop is not hot.

(4) Liquid water appears in the steam-flow rotameter.

To correct this problem, evacuate the headspace of the overheads condenser. Connect OC-4 to a vacuum trap as shown in Figure 6.3. Turn on the vacuum pump, and open OC-4. Any water present in the overheads condenser above the bottom of the sight glass will be drawn into the vacuum trap. When the vacuum trap fills with liquid, close OC-4, and transfer the collected liquid into the "overheads" collection bottle. Reassemble the vacuum trap, and open OC-4. Repeat this procedure until all liquid drains into the vacuum trap. Continue the evacuation for two minutes to remove uncondensed gases.

The system can also be operated with constant gas collection as shown in Figure 6.3. Regulate the rate at which gases are evacuated to the series of scrubbing bottles. This minimizes disturbance to the system during the run, and allows better system control.

6.7 Shutdown

The shutdown procedure to be used depends on whether the system will be allowed to cool before the bottoms and overheads are collected. Follow

directions in 6.7.1 or 6.7.2 for shutdown with or without cooling, respectively.

6.7.1 For cool-down before bottoms collection.

1. Turn off master switch and RTD-22 at control panel and close PB-5 and PB-7. These should be done simultaneously. Close PB-4.

3. Proceed from step 5 of section 6.7.2.

6.7.2 Without cool-down before bottoms collection.

1. Turn off raw feed pump and flash evaporator pump.

2. Take final bottoms collector sample and drain overheads from overheads condenser. Collect the liquid in the overheads condenser sight glass through valve OC-4. This flushes out crystalline deposits from the sight glass, which improves the recovery of ammonia. (If overheads condenser is under a vacuum, this collection will have to be done to a vacuum pump; see step 1 of section 6.6).

3. Close PB-5 and PB-7 to isolate the column from the rest of the system (PB-6 was already closed). These should be done as simultaneously as possible.

4. Close SG-4. This prevents additional steam from entering the system and isolates the steam generator from the steam drier.

5. Turn off master switch and RTD-22.

6. Turn off all transformers, but do not disturb the voltage settings. There are five low-amperage and one high-amperage transformers.

7. Record the water level in the steam generator sight glass.

8. **CAREFULLY** vent the steam generator. **CAUTION!!** high-pressure steam will emerge. Crack open SG-3. Steam will emerge until the pressure drops; then air will enter the steam generator.

9. Close PB-4. This will protect the pressure gauge, which is not designed to withstand a vacuum. Valves should now be set as shown in Table 6.3.

10. Close PB-5. This will prevent liquid water from backing up into the steam drier from the bottoms collector.

11. After the system has cooled to ambient temperature, vent the system. This is done stepwise, so that the vacuum is relieved in one vessel at a time (the steam generator was already vented to the atmosphere before cool-down). The steam drier should be vented last, because it is not stainless steel; any rust in the steam drier should not be allowed to enter the other vessels. Depending on whether the noncondensable gases in the overheads condenser are to be collected, the stripping column, bottoms collector, and overheads condenser should be purged with inert gas or vented to the atmosphere.

a. Vent the overheads condenser. If the noncondensable gases are to be collected, open OC-1. (If noncondensable gases are not to be collected, skip this step and proceed to 11-b.)

b. Drain the overheads condenser through valve OC-5. Drain any water in the sight glass through valve OC-4.

c. Vent the stripping column and bottoms collector. Open PB-7. This allows air to enter the stripping column downward, so the packing material will not be disturbed.

d. Open BC-2, and drain the bottoms collector into a sample bottle.

e. Vent the steam drier. (The steam generator was vented before cool-down). Check that SG-3 is open. Open SG-4. When steam drier has been vented, close SG-3.

f. Open PB-5.

6.8 Next-Day Cleanup

1. Connect city water to OC-5.
2. Open OC-5.
3. Close PB-4.
4. Open PB-6 (to reach this valve, go up to the top deck).
5. Open PB-7.
6. Close OC-4.
7. Open BC-1, BC-2, BC-3, BC-4, and BC-5.
8. Fill graduated, small reservoir with ASTM Type III water.
9. Place raw feed pump intake hose in reservoir
10. Run raw feed pump for 10 min, drawing first from small reservoir, then from large.
11. Shut off raw feed pump.
12. Close BC-1, BC-2, BC-3, BC-4, and BC-5.
13. Open BC-3.
14. Reduce flow rate of city water and run 45 min.
15. Shut off city water.
16. Close OC-5.
17. Open OC-4, OC-5, BC-1, BC-2, BC-3, BC-4, and BC-5.
18. Hose down work area.
19. Steam out the entire system. This is done by following the instructions for start-up (Section 6.5) up to step 14. Let steam emerge from BC-1 and BC-2 for one hour, then follow the instructions in 6.7.2 (shutdown without cooling). There is no need to collect any samples.

6.9 Analysis of Samples

Steam stripping is designed to remove dissolved gases from wastewaters. The dissolved gases present in oil shale process waters are principally ammonia, carbon dioxide, and low-molecular-weight organic compounds. Therefore all three streams (influent, bottoms, and condensed overheads) and, if desired, noncondensable gases must be analyzed for these species.

Influent, bottoms, and condensed overheads should be analyzed for dissolved organic carbon (DOC), dissolved inorganic carbon (DIC), and ammonia by the methods developed or validated at LBL and described in analytical protocols (Daughton 1984).

The noncondensable gases can be quantified by displacing the gas (remaining in the system after a run) through a series of two gas-washing bottles, one containing 1N mineral acid and the other containing 1N base. These two solutions are then analyzed by the same methods as the other streams.

6.10 Water and Mass Balance Calculations

This section describes the calculations necessary to interpret the data collected during a run. For accurate evaluation of stripper performance, all material entering and leaving the stripping column must be accounted for after a run. Each stream must be accurately measured and analyzed for the components of interest. Not only must removal efficiencies be calculated, but mass balances must be determined for each analyte (e.g., NH_3, DOC, and DIC). The various streams that must be measured and analyzed are summarized in Table 6.4. The sum of "in" streams should equal the sum of "out" streams for each component and for water. Good mass balances serve to validate the results. Any significant discrepancy must be investigated and, if possible, corrected (see section 4.2).

Before doing the calculations, ensure that all data are in consistent units.

6.10.1 Raw feed calibration.

To verify that the raw feed flow rate is constant during a run, the feed flow rate should be checked at 15-minute intervals. The procedure for feed flow-rate measurement and rotameter calibration is presented in section 6.3.1. The calculation for this measurement is as follows:

$$\frac{([\text{burette reading at start, mL}] - [\text{burette reading at end, mL}])}{(\text{time of pumping, min})} = \text{volume flow rate, mL/min}$$

The results of several calibration runs have been plotted in Figure 5.3 to give a calibration curve for the feed rotameter.

6.10.2 Water balance calculations.

This section describes the step-by-step calculation of the water mass balance. In calculating the water mass balance, it is important to distinguish between mass of water and volume of water, and between mass flow rates and volume flow rates. All streams (steam, feed, bottoms, and overheads) must be measured either as mass or as volume, and converted to mass. Note that the steam flow rate is calculated in g/min, i.e., it is a mass flow rate, while the feed flow rate is calculated in L/min; i.e., it is a volume flow rate, and overheads and bottoms can be measured as either voume or mass.

Water mass balance: It is necessary to know the mass of water entering and leaving the system. The mass of water leaving the system is simply the sum of the masses collected in the overheads condenser and in the bottoms collector,

corrected for holdup in the column if the bottoms were collected after cooldown. These may be determined directly (e.g., by weighing) or by multiplying the measured volumes by the density of water. To compensate for thermal expansion of water, temperature should be recorded when volumes are measured, or volumes should all be measured at ambient temperature. The mass of water entering the system must be calculated from the feed mass flow rate and the steam mass flow rate.

Steam mass flow rate: The steam mass flow rate is calculated from the rotameter reading and the temperature and pressure in the rotameter. Theoretically-based equations relating the steam rotameter reading to the steam volume flow rate are contained in pages 6 and 7 of the Gilmont catalog, Appendix A. A C-BASIC computer program for the Fortune 32:16 which does the same calculations and also calculates the steam mass flow rate is available; it is presented with user instructions in Appendix C. The steam flow calculations are for a Gilmont F-1500 rotameter with a stainless steel float. If the float is changed, the program must also be changed to compensate. Note that at one point in the program there is a choice between calculating the rotameter coefficient (C_R) and reading it from a graph. For certain combinations of values of the Stokes number and R (a geometrical parameter which is related to the scale reading), the graph (on p. 7 of the Gilmont catalog, Appendix A) can be used; otherwise use the formula. It is slightly more accurate to use the graph. Note also that the computer program reports steam flow rates both as volume (mL/min) and as mass (g/min and mol/min); use the mass flow rate in g/min to calculate the water balance.

The steam mass flow rate is the rate of gas entering the stripping column; the rate of gas leaving the column is the mass of condensed overheads divided by the duration of the run. If no evaporation or condensation of water occurs in the stripping column, then these two mass flow rates are equal. If the steam mass flow rate is larger, then condensation of steam in the column occurred during the run; if it is smaller, then flashing (evaporation of the feed) occurred. This should be noted in reporting the data.

Feed volume and mass flow rates: The feed volume flow rate can be calculated either from Figure 5.3 or from the formula $Q = (R - 3.14)/116.72$, where Q is the feed volume flow rate in L/min and R is the rotameter reading. This formula is simply the equation of the line in Figure 5.3. Multiply the feed volume flow rate by the density of water (1.00 kg/L at ambient temperature) to get the feed mass flow rate. Both the Figure and the formula are for a Gilmont F-1400 Flowmeter with a steel float; if either the rotameter or float is changed, then a new calibration curve must be prepared.

The feed mass flow rate is the rate of liquid entering the system; the rate of liquid leaving the system is the mass of bottoms divided by the duration of the run. If no evaporation or condensation of water occurs in the stripping column, then these two mass flow rates are equal. If the feed mass flow rate is smaller, then condensation of steam in the column occurred during the run; if it is larger, then flashing (evaporation of the feed) occurred. This should be noted in reporting the data.

Gas-liquid ratio: The gas-liquid ratio (G/L) is the ratio of the gas mass flow rate to the liquid mass flow rate. Both these flow rates must be in the same units, e.g., g/min. If evaporation or condensation in the column occurred

(see preceding discussion of steam flow rate), then both the gas and the liquid mass flow rates varied throughout the column; the gas-liquid ratio also varied throughout the column. Calculate and report values for both ends of the column.

Water balance: The total mass of water in the "in" streams should equal the total mass of water in the "out" streams. Multiply the steam and feed mass flow rates by the duration of the run to get the mass in. Add the overheads and bottoms to get the mass out. The percentage recovery of water is the mass of water out of the system divided by the mass of water into the system. Note that if the bottoms are collected after the end of the run, then the holdup (i.e., water that was in the column when the run was stopped) is included in the bottoms; for more accurate water balance, the holdup volume should be subtracted from the bottoms volume. The holdup volume can be calculated by the following formula (Leva 1953):

$$h_w = 0.0004\ (L/D_p)^{0.6} \qquad (6\text{-}1)$$

where h_w = volume of liquid holdup, ft^3 water per ft^3 of packing
L = liquid flow rate, $lb/ft^2\text{-}h$
D_p = equivalent packing diameter in inches; for 1/4 in. Intalox saddles, use $D_p = 0.20$

The cross-sectional area of the 2-in. i.d. column is 0.0218 ft^2. The holdup volume calculated by this formula must be subtracted from the measured bottoms volume.

6.10.3. Solute mass balance calculations.

Analyses for the solutes of interest are expressed as mg/L. Therefore to calculate the solute mass balances, all streams must be expressed as volumes of water. To do this, divide the mass of each stream by the density of water at ambient temperature, 1.00 kg/L. The volume for the steam in is the volume of water that was converted to steam. Enter the relevant volumes and analyte data in Tables 6.5, 6.6, and 6.7. Multiply the volumes (L) by the respective concentrations (mg/L) to get the mass (mg) of analyte recovered in each stream (feed, overheads, and bottoms). The mass of each component in the "in" streams should be accounted for in the "out" streams. See section 6.11 for an example calculation.

For each species:

Percent recovery = ([mass of analyte recovered in overheads and bottoms]/[mass of analyte in feed]) x 100. (6-2)

Percent removal = [(mass of analyte in feed) - (mass of analyte in bottoms)] / (mass of analyte in feed) x 100. (6-3)

If the mass balance is close to 100%, the removal as calculated in the following manner should be equivalent:

Percent removal = [(mass of analyte recovered in overheads)/(mass of analyte in feed)] x 100. (6-4)

6.11 Example calculation.

To aid the operator in doing the water and solute mass balance calculations for a run, the following example calculation is provided. The data for this run are as follows:

Feed rotameter reading (average of four readings taken during run)	63.3
Feed volume flow rate (average of four measurements taken by burette and stopwatch), mL/min	549.3
Average temperature during run, °C	
RTD-2	135.7
RTD-3	137.2
Average pressure at steam flow rotameter, psig	17.8
Steam rotameter reading (average of four readings taken during run)	44
Barometric pressure, mm Hg	766
Duration of run, min	30
Volume collected, L	
Overheads	5.38
Bottoms	12.94
Chemical analysis, mg/L	
Feed	
DOC	2845
DIC	994
NH_3	1135
Overheads	
DOC	1996
DIC	673
NH_3	2344
Bottoms	
DOC	111
DIC	22
NH_3	5
Acid solution for scrubbing noncondensable gases	
DOC	47
DIC	0
NH_3	184

Basic solution for scrubbing noncondensable gases	
DOC	0
DIC	2466
NH_3	0

The feed flow rate was measured by both the rotameter and by the burette-and-stopwatch method. From Figure 5.3, the volumetric feed flow rate was (63.3-3.14)/116.72 = 0.515 L/min. At ambient temperature, the density of the feed can be taken as 1.00 kg/L, so the feed flow rate was 0.515 kg/min. The more accurate burette-and-stopwatch method will be used for these calculations; 549 mL/min = 0.549 kg/min. The two methods should be checked against each other. Significant discrepancy means that the rotameter must be recalibrated.

The average rate of overheads condensation is calculated by dividing the overheads volume by the duration of the run: 5.38 L/30 min = 0.179 L/min. Because the overheads volume was measured at ambient temperature, the density of the overheads may be taken as 1.00; therefore the average rate of overheads condensation was 0.179 kg/min. Similarly, the average rate of bottoms collection (the effluent flow rate) was 12.94 L/30 min = 0.431 L/min = 0.431 kg/min.

The cross sectional area of the column (2-in. i.d.) is 0.0218 ft^2. The column is packed 8 ft deep; therefore the total column packing is 0.174 ft^3. Using the feed flow rate from burette and stopwatch measurements, the liquid flow rate was

(0.549 kg/min) (60 min/h) (2.20 lb/kg) (1/0.0218 ft^2) = 3324 lb/ft^2-h

From equation (6-1), the volume of liquid hold-up in the column was

$h_w = 0.0004\ (3324/0.20)^{0.6} = 0.136$ ft^3 of water per ft^3 of packing.

The hold-up volume was (0.136)(0.174) = 0.0237 ft^3 = 0.67 L = 0.67 kg

The steam flow rate was calculated using the program STEAMFLOW (see Appendix C). The output from this calculation follows:

```
RTD-2 TEMPERATURE = 135.7
RTD-3 TEMPERATURE = 137.2
BAROMETRIC PRESSURE = 766
AVERAGE ROTAMETER (PSIG) = 17.8
SP = 1686.5225911813
SCALE READING = 44
R = 12.3248
STOKES NUMBER = 107777.75267215
CR WAS CALCULATED
CR = 1.0362793680177
STEAM FLOW RATE
    68690.953470659  ML/MIN
    82.31455487802 G/MIN
    4.535237183362 MOL/MIN
```

Use the steam mass flow rate, 82.3 g/min, to calculate the water balance and the G/L ratio. For comparison, the average rate of overheads condensation was 179 g/min. The discrepancy indicates that flashing of the feed during the run occurred. When either flashing or condensation occurs in the column, the gas and liquid flow rates (and also the G/L ratio) vary through the column. The gas flow rate at the top of the column in this example was 179 g/min, while at the bottom of the column it was 82.3 g/min. The liquid flow rate at the top of the column was the feed rate, 549.3 g/min, while at the bottom of the column it was 431 g/min. Therefore the G/L ratio varied between 179/549 = 0.326 at the top of the column and 82.3/431 = 0.191 at the bottom of the column. The average G/L ratio was (0.326 + 0.191)/2 = 0.209.

To calculate the water balance:

Water in = feed + steam = (549.3 X 30) + (82.3 X 30) = 18950 g = 18.95 kg

Water out = overheads + bottoms - holdup = 5.38 + 12.94 - 0.67 = 17.65 L = 17.65 kg

Water recovery was 17.65/18.95 = 93%.

To calculate the solute balances for ammonia, DIC, and DOC, the respective data are entered into Tables 6.5, 6.6, and 6.7. Example DOC data from this run (Table 6.8) are used to calculate percent recovery and removal in the following manner. Percent DOC recovery is calculated using the sum of the DOC mass in the overheads and bottoms as the mass of analyte recovered in the overheads and bottoms (25.8 g DOC + 12.6 g DOC = 38.4 g DOC) and the mass of analyte in the feed is the DOC in the feed stream (46.9 g DOC). The percent DOC recovery as calculated from eq. 6-2 is

$$(38.4 \text{ g DOC}/46.9 \text{ g DOC})100 = 82\%.$$

Using the data from Table 6.8, the percent DOC removal calculated from eq. 6-3 is

$$((46.9 \text{ g DOC} - 25.8 \text{ g DOC})/46.9 \text{ g DOC})100 = 45\%$$

where 46.9 g DOC is the mass of analyte in the feed and 25.8 g DOC is the mass of analyte in the bottoms. Alternatively, the percent removal could have been calculated from eq. 6-4 where 12.6 g DOC is the mass of analyte recovered in the overheads and 46.9 g DOC is the mass of analyte in the feed. The resulting equation is

$$(12.6 \text{ g DOC}/46.9 \text{ g DOC})100 = 27\%.$$

The discrepancy between the percentage removal calculations can be attributed to the fact that the DOC recovery (i.e., mass balance) was not perfect (i.e., 100%).

This example of data reduction completes the final chapter of this operating manual. The objectives of these last two chapters were to: (1) familiarize the operator with the equipment, (2) provide a troubleshooting guide, (3) outline the operating protocol, and (4) demonstrate data reporting and reduction techniques. The protocols outlined in these sections should be

used as a guide for the operator and at no time should the operator assume that they are absolute truths. The key to successful operation of the LBL/SEEHRL steam stripper is the operator.

GLOSSARY

activity
Ratio of fugacity measured at the state of interest to the fugacity of a similar solution at standard state. For an isothermal change, activity is the difference in chemical potential measured at the state of interest and the standard state.

activity coefficient
The ratio of activity to a measure of concentration, such as mole fraction.

aerosol
A two-phase system that consists of solid or liquid particles suspended in a gas.

azeotrope
A solution of two or more substances that behaves as a single substance; the vapor and liquid phases have identical compositions.

bottoms
The stripped liquid effluent from a packed stripper.

component
Smallest number of independent chemical constituents with which the composition of every possible phase can be expressed.

critical point
The temperature and pressure beyond which the gas and liquid phases of a compound cannot be distinguished.

degrees of freedom
The number of property variables (e.g., temperature, pressure, and concentration) that need to be fixed to completely define the condition of a system at equilibrium.

driving force
By Fick's first law, the flux of a given solute is in the direction of the negative concentration gradient, i.e., the solute goes from a region of high concentration to a region of low concentration. The negative concentration gradient is referred to as the driving force.

dry steam
Steam that does not contain liquid or aerosol water.

efficiency (separation column)
Degree of band broadening for a given migration distance; expressed as the number of theoretical plates or as HETP.

equilibrium
For chemical reactions see equilibrium constant. Phase equilibrium between a gas and liquid occurs when the rate of condensation equals the rate of vaporization for each compound.

equilibrium constant
For a chemical reaction, this is the ratio of the rate constant of the forward reaction to the rate constant of the reverse reaction.

equilibrium curve
A collection of points that contains all possible pairs of compositions (x,y) in the vapor and liquid phases for a given temperature and pressure.

fixed ammonia
Ammonia that (purportedly) can remain in solution after exhaustive stripping.

flooding
Operating condition at which the conditions inside a packed bed switch from a continuous gas phase/dispersed liquid phase to a continuous liquid phase/dispersed gas phase; also known as inversion.

fugacity
The partial pressure of a component in a mixture of ideal gases. A term that replaces pressure so that the nonideal behavior of a gas is adjusted to correspond to ideal behavior.

gas
A vapor that is heated above its saturation temperature for a given pressure; a superheated vapor.

gas-to-liquid ratio (G/L)
Ratio of quantity of stripping gas used relative to the quantity of liquid stripped; can be calculated on a mass, molar, or volume basis.

height of a transfer unit (HTU)
A combination of flow parameters and mass transfer coefficient that gives one transfer unit of separation. Related to column efficiency of a unit length of packed bed. Small HTU values mean more theoretical plates for a given height and thereby more efficient separation.

Henry's coefficient
Constant of proportionality that relates mole fraction of component A in the gas phase to the mole fraction of A in the liquid phase for dilute solutions.

Henry's Law
For a dilute solution, the solubility of a gas in a liquid phase is proportional to its mole fraction in the gas phase.

ionic strength
A description of the intensity of the electric field in a solution.

loading
The condition that precedes flooding; marked by a tremendous increase in the pressure drop through the packed bed.

molality
In a mixture, the ratio of moles of component (i) to 1000 g of solvent.

molarity
The number of moles of component (i) present in one liter of solution.

mole fraction
In a mixture, the ratio of moles of component (i) to the total number of moles present.

number of transfer unit
The quantity of transfer units required to achieve a desired separation.

overheads
Effluent gas from a stripper.

packed bed
A column or tower filled with randomly oriented inert material that supplies high surface area, while still allowing porosity.

partial pressure
The pressure contributed by a single component in a mixture of gases or vapors.

phase
Physically and chemically uniform part of a system separated from other parts of the system by a definite bounding surface.

plate theory
Description of chromatography as a series of discrete equilibrations between mobile and stationary phases.

Raoult's Law
For a nearly pure solution of component A, the partial pressure of A in the gas phase is the product of its mole fraction in the liquid phase and the pure component vapor pressure.

reflux
That part of a distillation operation where a portion of the effluent gas stream is condensed and returned to the tower or column.

relative volatility (separation factor)
For a binary system, this is the ratio of the volatility of component A to the volatility of component B.

saturated steam
The water vapor directly above the liquid free-surface of boiling water; the vapor phase that coexists with the liquid phase at saturation pressure or saturation temperature.

saturation temperature
Temperature at which two phases of a substance can coexist.

saturation pressure
Pressure at which two phases of a substance can coexist.

steam
The general term implying water vapor. Wet steam contains entrained droplets of liquid water and is at saturation temperature and pressure. Dry steam contains no entrained liquid water at saturation temperature and pressure (i.e., it is pure gaseous water).

steam quality
Determined by the moisture content, dry steam being higher quality than wet steam.

stripping
Transfer of volatile solutes from the liquid to the gas phase by encouraging the contact of the two phases.

superheating
Increasing the temperature of a gas above saturation temperature without increasing the saturation pressure; can only be done in a single-phase system.

theoretical plate
The equivalent of complete equilibration between mobile and stationary phases in chromatographic plate theory. The plate number (N) of a chromatogram is a measure of its efficiency.

transfer unit
The height of a packed bed over which the concentration of a given solute in a phase changes by an amount equal to the average driving force for mass transfer.

vapor
A gas near saturation, where it coexists with liquid at a given temperature and pressure.

vapor pressure
The pressure of a vapor in equilibrium with either its solid or liquid phase at a given temperature.

volatility
The quotient of the gas-phase partial pressure of component A and the liquid-phase mole fraction of A; if component A follows Raoult's Law, the volatility is equivalent to the vapor pressure of pure A at the system temperature.

Table 3.1. Summary of Data Reported for Oil Shale Wastewater Stripping

Wastewater Sample (retort type)	Stripping Gas	Type of Stripper	Column Temperature (°C)	Height of Packed Bed (m)	Gas-to-Liquid Ratio	Ammonia (NH_3-N mg/L) Inf	Ammonia (NH_3-N mg/L) Eff	Dissolved Inorganic Carbon (mg/L) Inf	Dissolved Inorganic Carbon (mg/L) Eff	Dissolved Organic Carbon (mg/L) Inf	Dissolved Organic Carbon (mg/L) Eff	Ref.
Omega-9 (in-situ)	hot, compressed air	countercurrent	82.2	2.07	0.76	3983	1549	8006	4309	840	nd[1]	Hines et al. (1982)
					1.06		1311		4024		680	
					1.44		1310		3803		670	
			93.3	2.07	0.76		57		2394		nd	
					1.06		51		1905		450	
					1.44		0		1808		440	
			104.4	2.07	0.76		0		1759		nd	
					1.06		0		1771		430	
					1.44		0		1686		430	
150-Ton LETC Run-17 (simulated in-situ)	hot, compressed air	countercurrent	82.2	2.07	0.84	3915	1515	8464	1571	2880	2480	Hines et al. (1982)
					1.38		1447		1495		2340	
					1.74		1378		1341		2330	
			93.3	2.07	0.84		1362		616		nd	
					1.38		1345		615		nd	
					1.74		1311		550		nd	
			104.4	2.07	0.84		952		311		2340	
					1.38		946		309		2320	
					1.74		916		291		2320	
Oxy-6 retort water (modified in-situ)	hot, compressed air	countercurrent	82.2	2.07	0.70	1481	55	5457	2894	2500	nd	Hines et al. (1982)
					1.07		45		2785		nd	
			104.4	2.07	0.70		41		1275		1670	
					1.07		10		1187		1550	
Gas condensate (vertical MIS)	steam	countercurrent	94	1.83	0.24	7600	98		nd	822	146	Lewis & Rawlings (1982)
150-Ton LETC retort (Sept 1980) (simulated in-situ)	steam	countercurrent	98.8-102.1	2.44	nd		54%[2]		57%[2]		63%[2]	Habenicht et al. (1980)
Ammonium bicarbonate solution		countercurrent	93.2	2.20	0.38[3]	11000	3.7	47000	220		nd	Murphy et al. (1978)
			82.1	2.20	0.38	11000	330	45000	1000-2000		nd	
Utah in-situ #1	steam	reboiler	nd	0.61	0.08		99.5%		nd		nd	Mercer & Wakamiya (1980)
Utah in-situ #2					0.05		83%		nd		nd	
Utah in-situ #3					0.05		96%		nd		19%	
Utah in-situ #4					0.05		99.5%		nd		17%	
Above ground					0.30		38%		nd		nd	
Simulated in-situ					0.14		98%		nd		nd	
Simulated in-situ					0.11		99.95%		nd		18%	

[1] no data; [2] average percentage removals for an actual on-line operation; [3] calculated assuming steam was used as the stripping gas.

Table 4.1. Association-Dissociation Reactions and Equilibrium Constants

Reactions	$pK_{25°C}$ Exp.[1]	$pK_{25°C}$ Calc.[2]	$pK_{100°C}$ Calc.[2]
$H_2CO_3 = H^+ + HCO_3^-$	6.35	6.36	5.03
$HCO_3^- = H^+ + CO_3^=$	10.33	10.34	9.82
$NH_4OH = NH_4^+ + OH^-$ [3]	nd[4]	4.74	4.61
$NH_4^+ = NH_3 + H^+$	9.24	9.26	7.42
$H_2S = HS^- + H^+$	6.97	6.95	6.16
$HS^- = S^= + H^+$	12.90	12.91	11.13
$H_2O = H^+ + OH^-$	13.99	13.99	12.26
$C_5H_5N = C_5H_5NH^+$ (pyridine)	5.2	nc[5]	nc
$C_6H_6O = C_6H_5O^- + H^+$ (phenol)	9.99	nc	nc

[1] Dean (1979); pyridine value from Katritzky and Lagowski (1968).

[2] Calculated from the van't Hoff equation (Holman 1974).

[3] No evidence exists for a covalent bond between ammonia and water. NH_4OH may actually be a hydrogen-bonded complex that, on the addition of hydrogen ion, results in ammonium ion formation (Butler 1964).

[4] No data available.

[5] Not calculated due to insufficient data.

Table 4.2. Average Errors for Vapor-Liquid Equilibrium Models

Model	Volatile Solute	Temperature Range, °C	Average Error %[1]
Pawlikowski et al. (1982b)	NH_3	80	9.7
Beutier and Renon (1978)	NH_3	80	11.5
API (1975)	NH_3	20-140	36.0
van Krevelen et al. (1949)	NH_3	20-140	72.0
Pawlikowski et al. (1982b)	H_2S	80	6.7
Beutier and Renon (1978)	H_2S	80	15.1
API (1975)	H_2S	20-185	18.0
van Krevelen et al. (1949)	H_2S	20-185	24.0
API (1975)	CO_2	20-120	17.0
van Krevelen et al. (1949)	CO_2	20-120	35.0

[1] Calculated as
$|(\text{reported experimental data})/(\text{value obtained from model})| - 1.0 \times 100$

Table 4.3. Height of Transfer Units Calculated from Empirical Correlations

	HTU (ft)	
20% flooding	S = 1.25	S = 2.00
HTU_G [1]	0.432 [2]	0.502
HTU_G	0.0515 [3]	0.0541
HTU_L [4]	0.0263 [5]	0.0224
HTU_L	0.0429 [6]	0.0387
HTU_{OG} [7]	0.465 [8]	0.547
HTU_{OG}	0.486 [9]	0.559
HTU_{OG}	0.0844 [10]	0.0989
HTU_{OG}	0.105 [11]	0.132
50% flooding		
HTU_G	0.424 [2]	0.493
HTU_G	0.0678 [3]	0.0712
HTU_L	0.0419 [5]	0.0358
HTU_L	0.0582 [6]	0.0525
HTU_{OG}	0.476 [8]	0.565
HTU_{OG}	0.497 [9]	0.598
HTU_{OG}	0.120 [10]	0.143
HTU_{OG}	0.141 [11]	0.176

[1] Height of a transfer unit for the gas phase only; [2] Sherwood and Holloway (1940); [3] Onda, Takeuchi, and Okumoto (1968); [4] Height of a transfer unit for the liquid phase only; [5] Onda, Sada, and Murase (1959); [6] Onda et al. (1968); [7] Overall Height of a transfer unit for both gas and liquid phases combined; based on gas phase concentrations and calculated from the expression: $HTU_{OG} = HTU_G + S(HTU_L)$; [8] HTU_G from Sherwood and Holloway (1940) and HTU_L from Onda et al. (1959); [9] HTU_G from Sherwood and Holloway (1940) and HTU_L from Onda et al. (1968); [10] HTU_G from Onda et al. (1968) and HTU_L from Onda et al. (1959); [11] HTU_G from Onda et al. (1968) and HTU_L from Onda et al. (1968).

Table 4.4. Values of Physical Constants Used in the Design Example

Physical Constant	Value
temperature	110°C (383°K)
system pressure	21.40 psia (1.46 atm)
gravitational constant	4.17×10^8 ft/h^2
Henry's Law constant	18.3 atm
liquid viscosity	0.231 cp (0.559 lb/ft·h)
liquid density	59.35 lb/ft^3
liquid diffusivity (ammonia in water)	5.57×10^{-4} ft^2/h (1.44×10^{-4} cm^2/h)
water surface tension	61.80 dynes/cm (4.235×10^{-3} lb/ft)
gas viscosity	0.0125 cp (3.0239×10^{-2} lb/ft·h)
gas density	0.0516 lb/ft^3
gas diffusivity (ammonia in water)	0.3451 cm^2/s (1.337 ft^2/h)
universal gas constant	0.08206 L·atm/mol·K (0.00290 ft^3/mol·K)
packing size	1/4-in. Intalox Saddles
packing diameter	0.0167 ft
packing surface area	300 ft^2/ft^3
packing factor (C_1)	2.00
packing surface tension	61 dynes/cm
packing factor (c_f)	600

Table 4.5. Calculation of Henry's Law Constant for Oil Shale Wastewaters

Method of Calculation	Oil Shale Wastewater	H, atm	T, °C
API (1978)	Paraho	18.92	110
API (1978)	150-Ton (Run 13)	18.78	110
API (1978)	Oxy-6 gas condensate	18.72	110
API (1978)	Geokinetics	18.53	110
API (1978)	composite	18.51	110
API (1978)	Omega-9	18.47	110
API (1978)	Tosco HSP	18.33	110
API (1978)	Oxy-6 retort water	18.32	110
API (1978)	S-55	18.29	110
API (1978)	Rio Blanco sour	18.20	110
Edwards et al. (1978)		17.76	110
		0.906	25
Edwards et al (1975)		0.913	25

Table 4.6. Number of Transfer Units Required to Achieve 99% Ammonia Removal[1]

Wastewater	NTU_{OG}
Oxy-6 retort water	17.24
Rio Blanco sour	17.24
150-Ton (run 13)	17.24
S-55	15.14
composite	14.68
Paraho	14.64
Oxy-6 gas condensate	14.16
Tosco HSP	14.06
Geokinetics	13.64
Omega-9	13.50

[1] Equation of Colburn taken from Bennett and Myers (1974); based on overall gas-phase mass-transfer coefficient (S = 1.25).

Table 4.7. Height of a Packed Bed Required to Achieve 99% Removal of Ammonia from Oil Shale Wastewaters

Wastewater	Height of Bed, m	
	Calculation A [1]	Calculation B [2]
Oxy-6 retort water	2.04	0.58
Rio Blanco sour water	2.04	0.58
150-Ton (run 13)	2.04	0.58
Oxy-6 gas condensate	1.89	0.52
Paraho	1.89	0.52
S-55	1.89	0.55
composite [3]	1.86	0.52
TOSCO HSP	1.80	0.52
Geokinetics-9	1.77	0.49
Omega-9	1.77	0.49

[1] Values for calculation A were derived using the H_G calculation from Sherwood and Holloway (1940) and the H_L correlation of Onda, Takeuchi, and Okumoto (1968).

[2] Values for calculation B were derived using the empirical correlation of Onda, Takeuchi, and Okumoto (1968) to calculate the H_G and H_L values.

[3] Equal volumes of each of the nine waters.

Table 4.8. Heats of Stripping for Ammonia and Carbon Dioxide at 25°C

Reaction	n [1]	H (kcal per mole of solute) [2]
NH_3 (aq) $\rightleftharpoons$ NH_3 (g) + H_2O (l)		
	1	6.99 [3]
	10	8.05 [3]
	55.55	8.17 [3]
	100	8.14 [3]
	200	8.25 [4]
	infinite	7.29 [5]
CO_2 (aq) $\rightleftharpoons$ CO_2 (g) + H_2O (l)		
	55.55	4.85 [3]

[1] n = moles of H_2O per mole of solute.

[2] Calculated from heats of formation (H_f^o): H_f^o (products) - H_f^o (reactants); when H > 0, energy is required (endothermic).

[3] Dean (1979).

[4] Weast (1978).

[5] Perry and Chilton (1973).

Table 5.1. Location of RTDs on the Packed-Bed Stripping Column

RTD no.[a]	Output to datalogger channel[a]	Location, ft[b]
RTD-11	11	0.54 (cross external)
RTD-12	12	(interior of cross above column)
RTD-6	6	3.5
RTD-9	9	8.5
RTD-8	8	11.66
RTD-7	7	15.75
RTD-16	16	(interior of BC)
RTD-5	5	(exterior of BC)

[a] RTD numbers correspond to datalogger channels for RTDs 1-16.

[b] Distances are measured downward from the bottom of the cross at the top of the column.

Table 5.2. Location of Heat Tapes on the Packed-Bed Stripping Column

Tape Series	Tape Number	Length of Column Covered, ft[a]	Cumulative Length of Column, ft[a]
A (silicone)	1	0.75	0.75
	2	0.83	1.58
	3	0.79	2.37
	4	0.83	3.15
B (silicone)	5	0.83	3.98
	6	0.92	5.0
	7	0.83	5.8
	8	0.92	6.7
C (fiberglass)	9	0.75	7.5
	10	0.83	8.3
	11	0.92	9.3
D (fiberglass)	12	0.92	10.2
	13	1.17	11.4
	14	1.00	12.4
E (fiberglass)	15	1.04	13.4
	16	1.00	14.4
	17	0.38	14.8
F (fiberglass)	18	0.38	15.2
	19	1.08	16.3

[a] Distances are measured downward from the bottom of the cross at the top of the column.

Table 5.3. Location and Function of RTDs[a]

RTDs 0 through 16 are displayed and recorded by the datalogger. The datalogger channel numbers are the same as the RTD- numbers. They are not displayed at the control panel.
RTDs 0 through 16 have no controlling functions, but the operator can adjust voltage to heat tapes to control the temperatures.

Device	Location	Controlling Function	Comment
RTD-0			(number not assigned)
RTD-1			(number not assigned)
RTD-2	steam rotameter in		datalogger channel 2
RTD-3	steam rotameter out		datalogger channel 3
RTD-4	BC (column end)		datalogger channel 4
RTD-5	PB bottom (external)		datalogger channel 5
RTD-6	PB external		datalogger channel 6
RTD-7	PB external		datalogger channel 7
RTD-8	PB external		datalogger channel 8
RTD-9	PB external		datalogger channel 9
RTD-10			(number not assigned)
RTD-11	exterior of cross at top of PB		datalogger channel 11
RTD-12	interior of cross at top of PB		datalogger channel 12
RTD-13	lower overheads condenser		datalogger channel 13
RTD-14	interior of feed line above PB		datalogger channel 14
RTD-15			(number not assigned)
RTD-16	interior of BC		datalogger channel 16

RTDs 21 through 25 are displayed on the control panel. Their outputs are not automatically recorded.
RTDs 21, 22, 23, and 25 have controlling functions.

RTD-21	top of SG	Controls energy input (percentage of time on) to heating element in SG	
RTD-22	steam exit	Controls energy input (percentage of time on) to heating element in SD	Voltage to SD is separately controlled by Powerstat
RTD-23	top of FP	Controls energy input (percentage of time on) to heating element in FP	Detects temperature of water outside of coil. Must not be set higher than RTD-25.
RTD-24	bottom of PB	Has no controlling function	
RTD-25	top of PB	Controls flow of cooling water	

[a] All RTDs are Omega Engineeering (model 4201). Temperature is displayed to the nearest 0.1°C.

Table 5.4. Contents of Datalogger Channels.

Channel	RTD	Signal
0		(channel not used)
1		(channel not used)
2	RTD-2	steam rotameter in
3	RTD-3	steam rotameter out
4	RTD-4	bottoms collector
5	RTD-5	column bottom (external)
6	RTD-6	external column
7	RTD-7	external column
8	RTD-8	external column
9	RTD-9	external column
10		(channel not used)
11	RTD-11	cross external
12	RTD-12	cross internal
13	RTD-13	lower overheads condenser
14	RTD-14	feed preheater
15		(channel not used)
16	RTD-16	bottoms collector internal
17		(channel not used)
18		(channel not used)
19		(channel not used)

Table 6.1. Valve Settings for Start-Up of Steam Stripper and after Step 11.

SG-1	FP-1	OC-1	BC-1	PB-1
SG-2		OC-2[a]	BC-2 open[b]	PB-2
SG-3		OC-3[a]	BC-3 open	PB-3[a]
SG-4 open		OC-4	BC-4 open	PB-4 open
SG-5		OC-5 open[b]		PB-5 open
SG-6 open		OC-6[a]		PB-6 open
SG-7		OC-7[c]		PB-7 open
SG-8		OC-8		
SG-9[a]		OC-9		
		OC-10 open		
		OC-11		
		OC-12 open		

All other valves are closed.

[a] These valves have been removed from the system.

[b] These valves are open to provide steam circulation to the extremities of the system and to provide a vent.

[c] This valve may be open or closed; see step 9f.

Table 6.2. Valve Settings after Step 19.

SG-1	FP-1	OC-1	BC-1	PB-1
SG-2		OC-2[a]	BC-2	PB-2
SG-3		OC-3[a]	BC-3 open	PB-3[a]
SG-4 open		OC-4	BC-4 open	PB-4 open
SG-5		OC-5		PB-5 open
SG-6 open		OC-6[a]		PB-6
SG-7		OC-7 open		PB-7 open[b]
SG-8		OC-8		PB-8
SG-9[a]		OC-9		
		OC-10 open		
		OC-11		
		OC-12 open		

All other valves are closed unless otherwise noted.

[a] These valves have been removed from the system.

[b] Must be adjusted to control steam flow through stripping column.

Table 6.3. Valve Settings after Shutdown.

SG-1	FP-1	OC-1	BC-1	PB-1
SG-2		OC-2[a]	BC-2	PB-2
SG-3 open[b]		OC-3[a]	BC-3 open	PB-3[a]
SG-4		OC-4	BC-4 open	PB-4
SG-5		OC-5		PB-5
SG-6 open		OC-6[a]		PB-6
SG-7		OC-7 open		PB-7
SG-8		OC-8		PB-8
SG-9[a]		OC-9		
		OC-10 open		
		OC-11		
		OC-12 open		

All other valves are closed unless noted otherwise.

[a] These valves have been removed from the system.

[b] Crack open carefully, see step 8 of 6.7.2.

Table 6.4. Measurements Needed to Complete Mass Balances

Stream	Direction	Method for measuring total volume after a run	Chemical species to be quantified for mass balance
steam	in	Multiply length of run by average steam mass flow rate during the run. This value should be checked against (overheads) + (bottoms).	This stream is ASTM Type III water; no chemical analyses are needed.
feed	in	Multiply length of run by average feed flow rate during and at end of run.	NH_3, DIC, DOC
overheads	out	Record total volume drained from OC during and at end of run.	NH_3, DIC, DOC
bottoms	out	Record total volume drained from BC during and after run.	NH_3, DIC, DOC
uncondensed gases	out	It is not necessary to measure the volume of gas; rather, record volumes of the acid and basic solutions through which the gas was bubbled.	NH_3, DIC, DOC
scrubbing water	in	If water was sprayed into the overheads condenser to dissolve uncondensable gases, multiply the flow (from rotameter reading) by the length of run.	This stream is either ASTM Type I or a prepared acid or base solution; no analyses are needed.

Table 6.5. Ammonia Balance Calculation Worksheet

Stream	Direction	Total volume during run, L	NH_3-N, mg/L	NH_3-N, mg
Steam[a]	in	____	____	____
Feed	in	____	____	____
Overheads	out	____	____	____
Bottoms	out	____	____	____
Acid solution through which uncondensed gases are scrubbed	out	____	____	____
Basic solution through which uncondensed gases are scrubbed	out	____	____	____

[a] Volume of water that was converted to steam.

Table 6.6. Dissolved Organic Carbon (DOC) Balance Calculation Worksheet

Stream	Direction	Total volume during run, L	DOC, mg/L	DOC, mg
Steam[a]	in	____	____	____
Feed	in	____	____	____
Overheads	out	____	____	____
Bottoms	out	____	____	____
Acid solution through which uncondensed gases are scrubbed	out	____	____	____
Basic solution through which uncondensed gases are scrubbed	out	____	____	____

[a] Volume of water that was converted to steam.

Table 6.7. Dissolved Inorganic Carbon (DIC) Balance Calculation Worksheet

Stream	Direction	Total volume during run, L	DIC, mg/L	DIC, mg
Steam[a]	in	____	____	____
Feed	in	____	____	____
Overheads	out	____	____	____
Bottoms	out	____	____	____
Acid solution through which uncondensed gases are scrubbed	out	____	____	____
Basic solution through which uncondensed gases are scrubbed	out	____	____	____

[a] Volume of water that was converted to steam.

Table 6.8. Example Dissolved Organic Carbon (DOC) Balance Calculation.

Stream	Direction	Total volume during run, L	DOC, mg/L	DOC, g
Steam[a]	in	2.47	0	0
Feed	in	16.48	2845	46.9
Bottoms	out	12.94	1996	25.8
Overheads	out	5.38	2338	12.6
Acid solution through which uncondensed gases are scrubbed	out	1.00	47	0.047
Basic solution through which uncondensed gases are scrubbed	out	1.00	0	0

[a] Volume of water that was converted to steam.

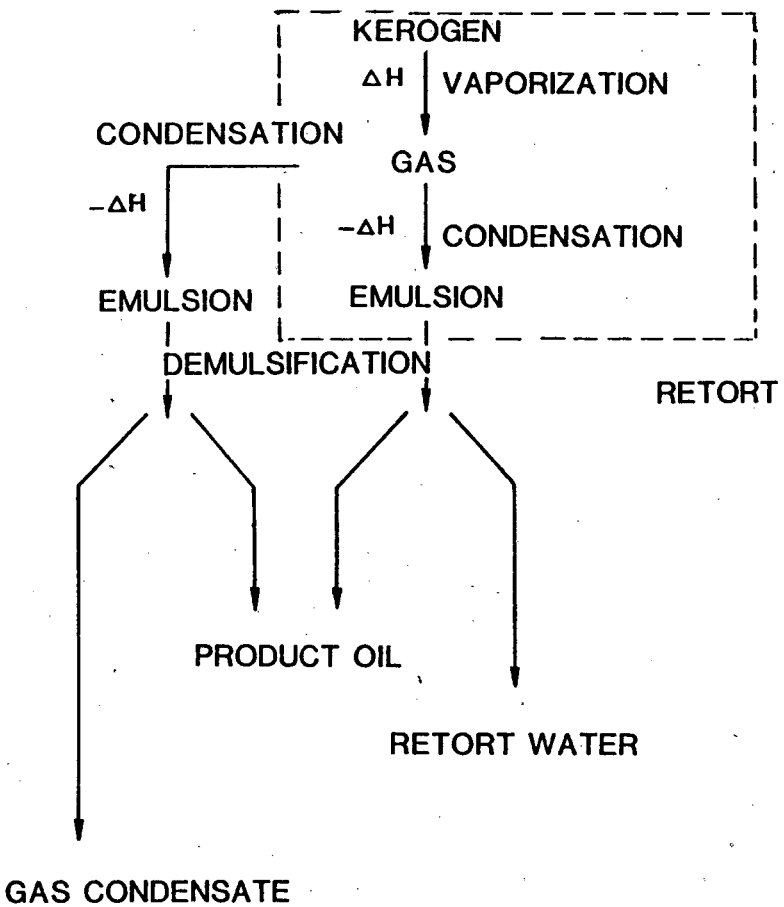

MODIFIED AND TRUE IN-SITU RETORTING

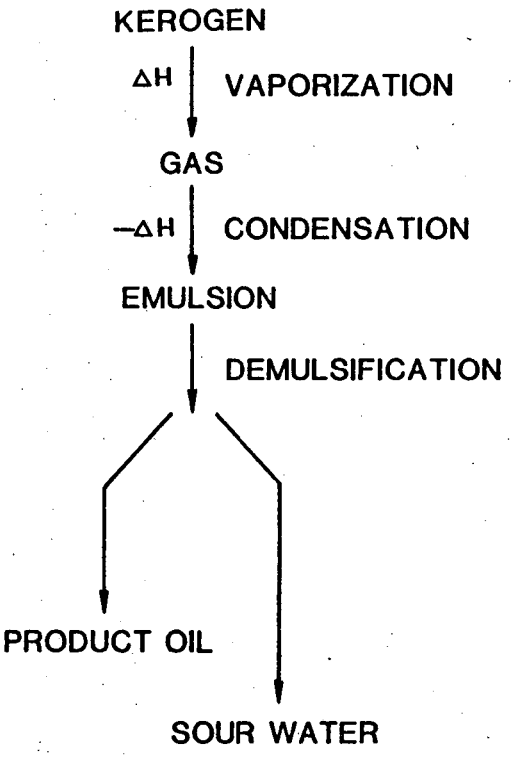

SURFACE RETORTING

Figure 1.1 Origins of Oil Shale Wastewaters.

XBL 849-3796

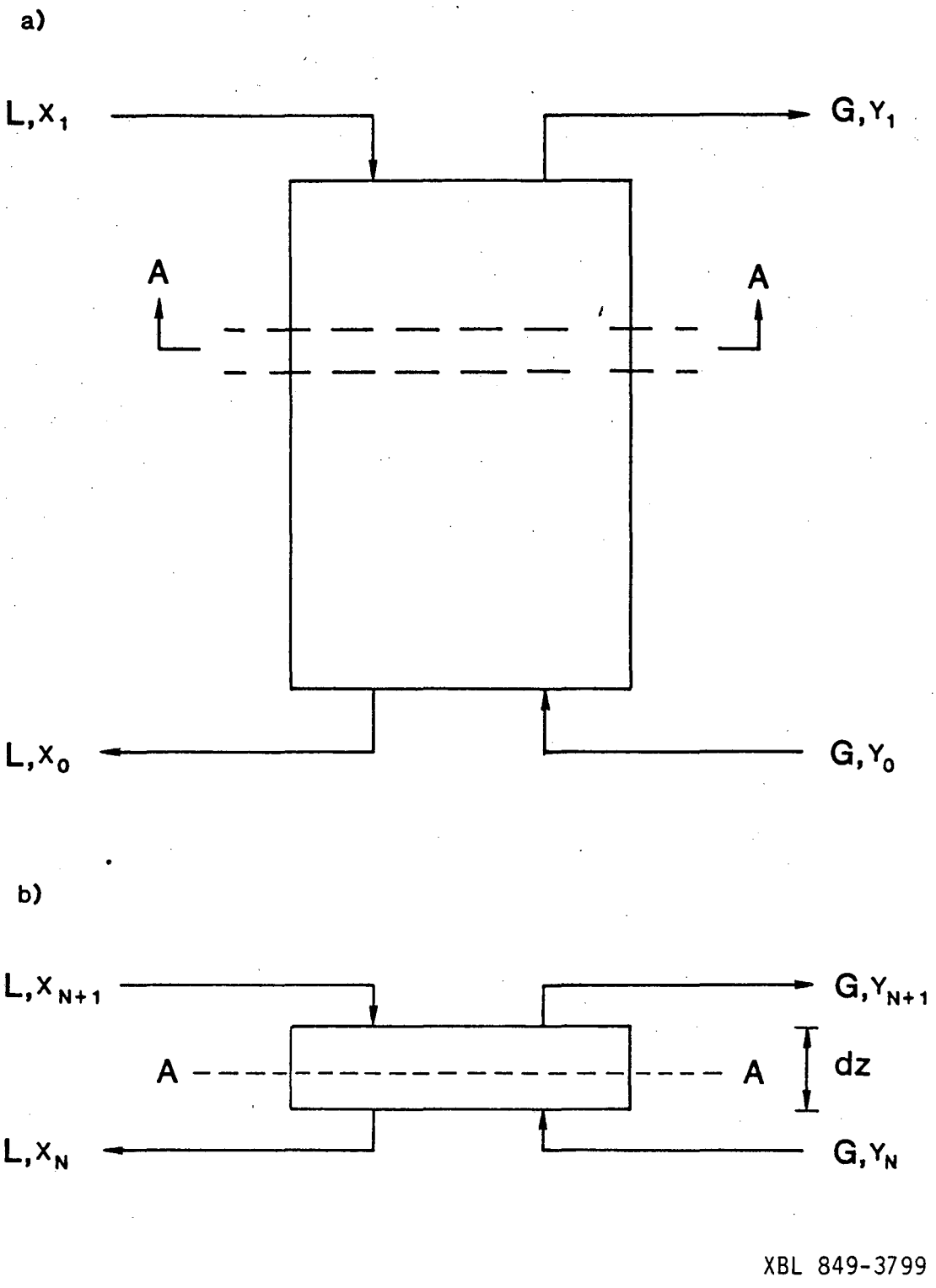

Figure 4.1 Idealized Schematic of a Steam Stripper.

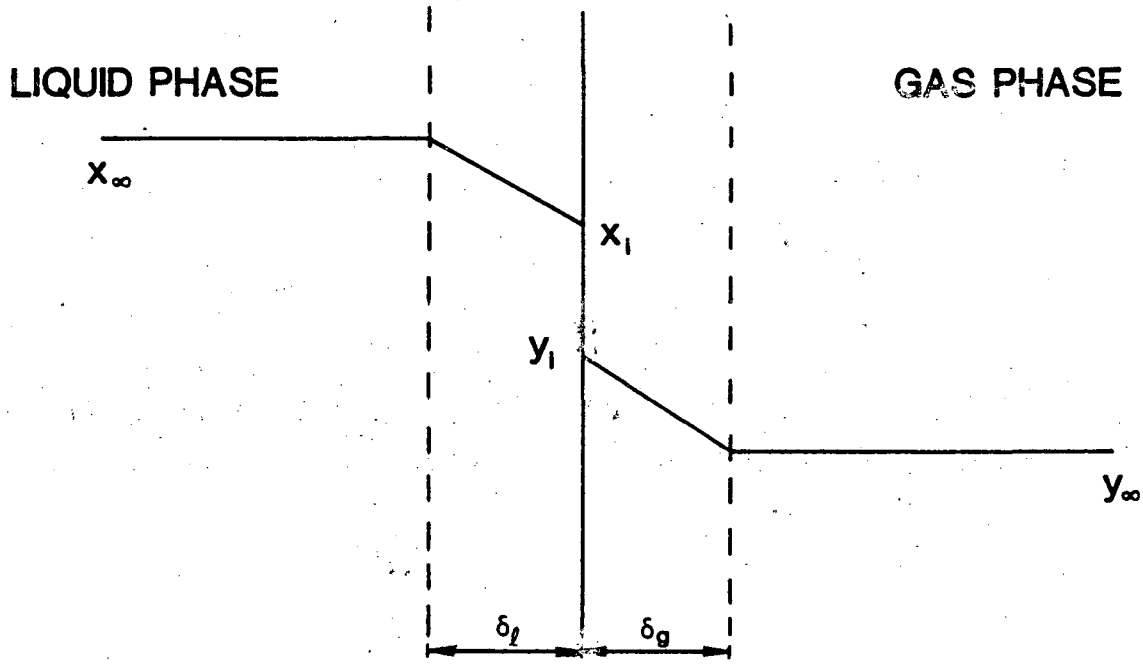

x_i Liquid-phase mole fraction at interface

y_i Gas-phase mole fraction at interface

x_∞ Liquid-phase mole fraction in bulk solution

y_∞ Gas-phase mole fraction in bulk solution

δ_ℓ Liquid-phase boundary layer

δ_g Gas-phase boundary layer

XBL 849-3798

Figure 4.2 Mass Transfer at a Phase Boundary.

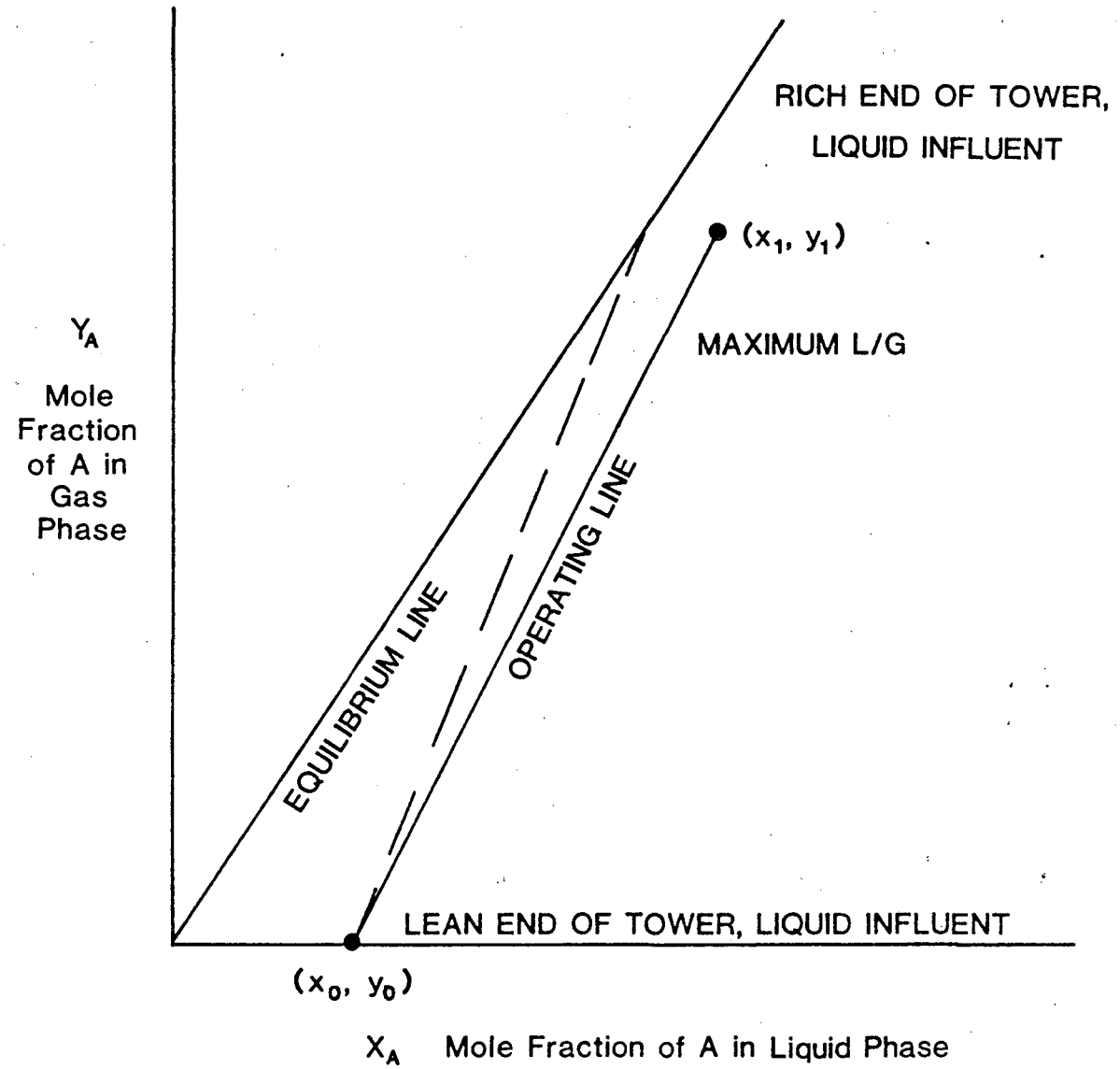

Figure 4.3 Use of Equilibrium and Operating Lines in Packed Tower Design.

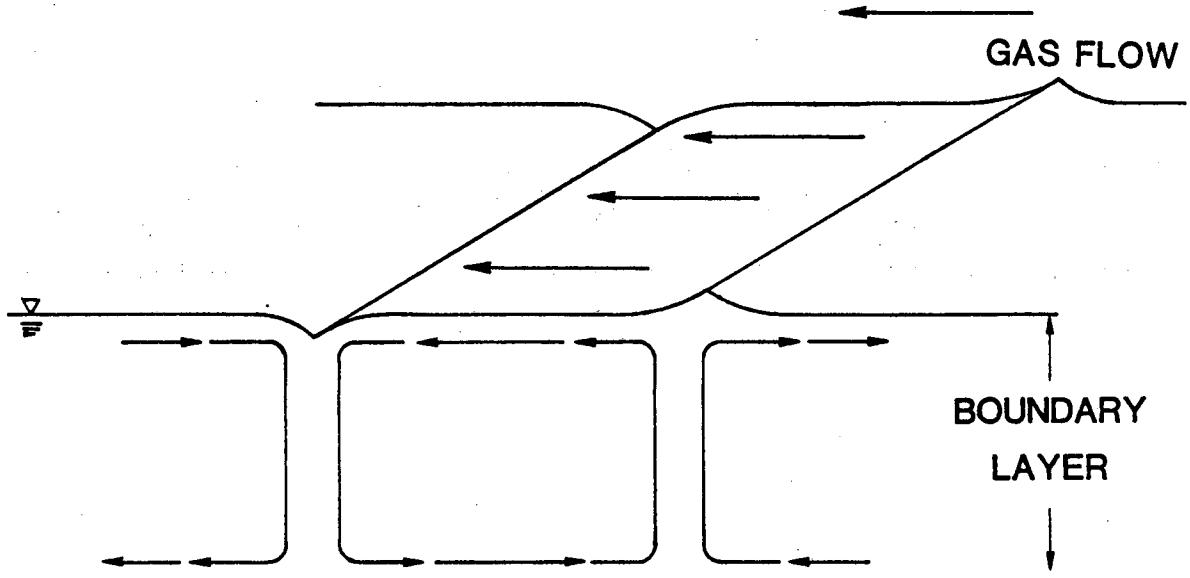

Figure 4.4 Internal Circulation Patterns Leading to the Formation of Roll Cells.

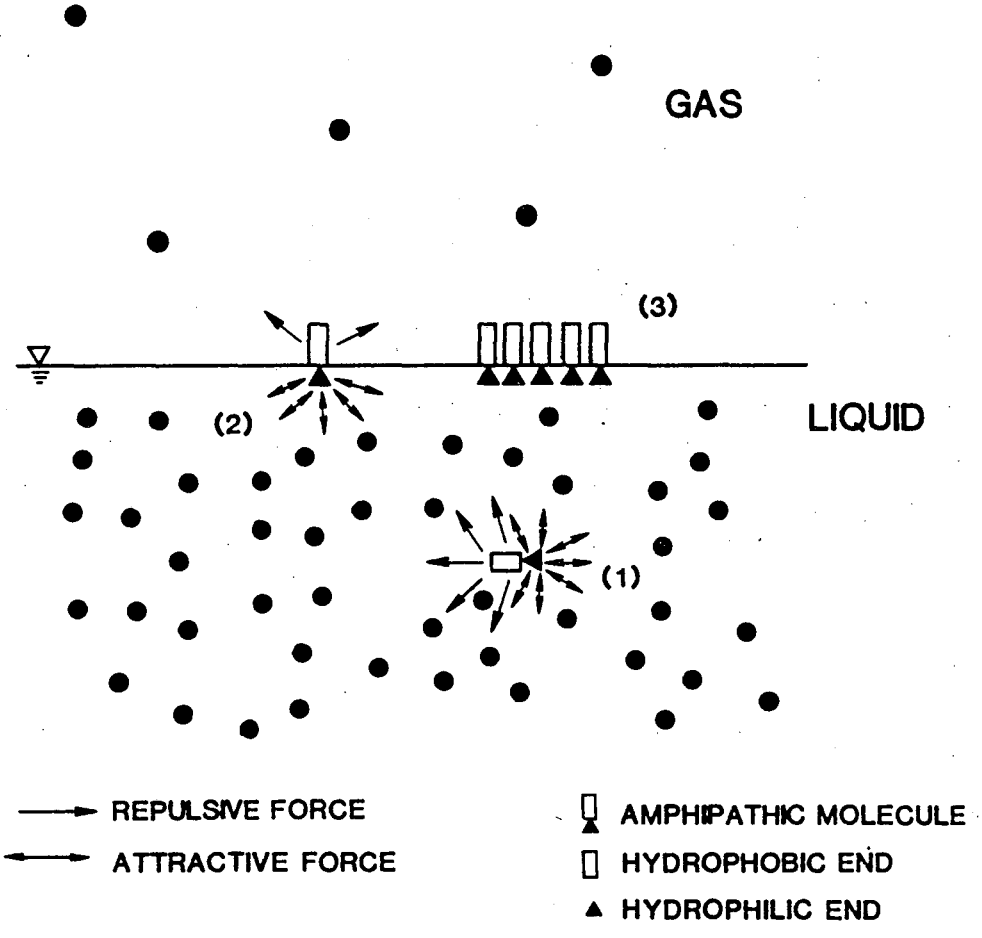

(1) POSITION OF HIGH FREE ENERGY, HIGH REPULSIVE FORCE ON HYDROPHOBIC END

(2) POSITION OF MINIMUM FREE ENERGY, LOW REPULSIVE FORCE ON HYDROPHOBIC END

(3) MONOLAYER OF SURFACTANT MOLECULES

XBL 849-3795

Figure 4.5 Surfactant Model.

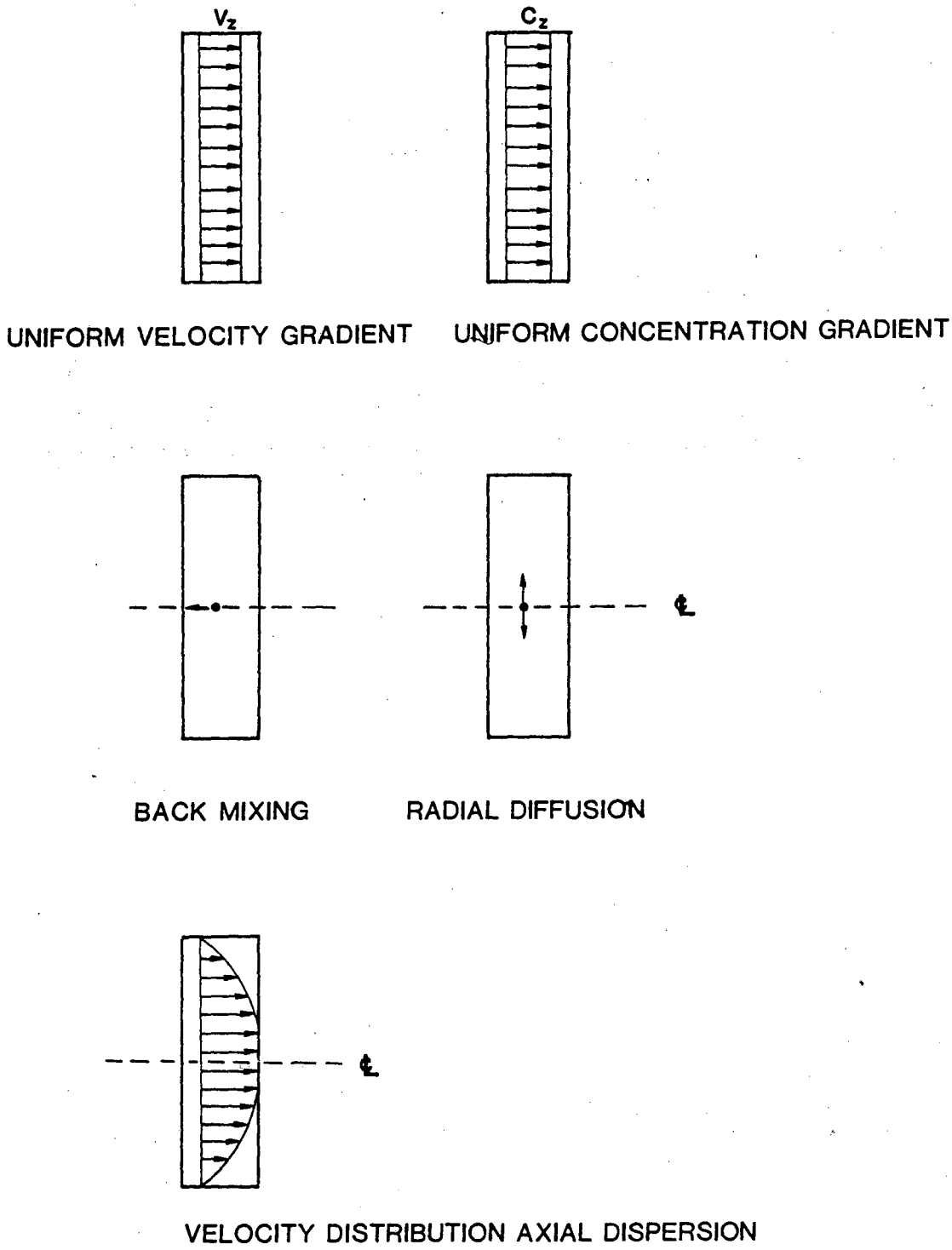

Figure 4.6 Velocity and Concentration Gradient Profiles for Laminar Flow.

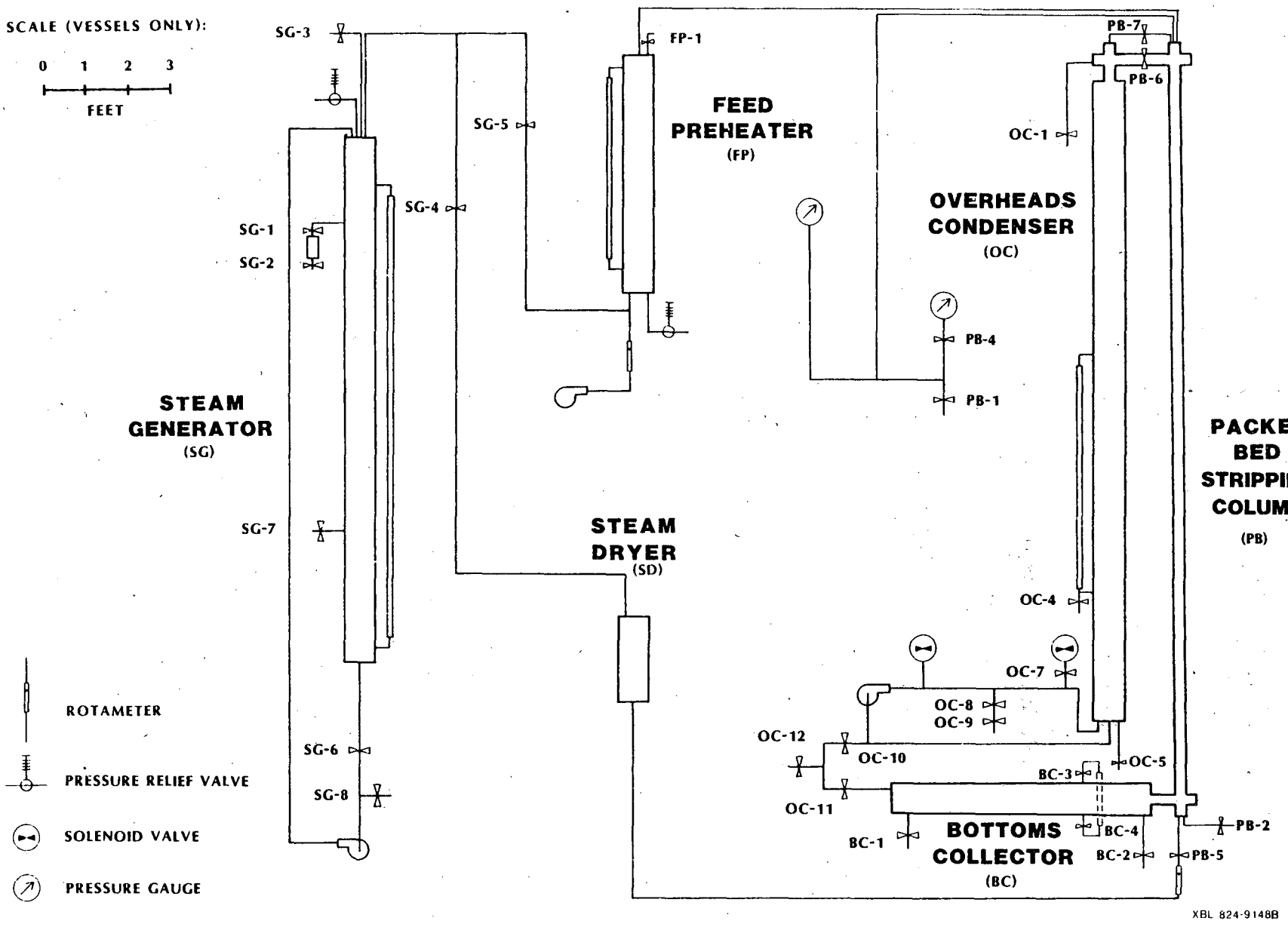

Figure 5.1 Schematic Diagram of the LBL/SEEHRL Steam Stripper System.

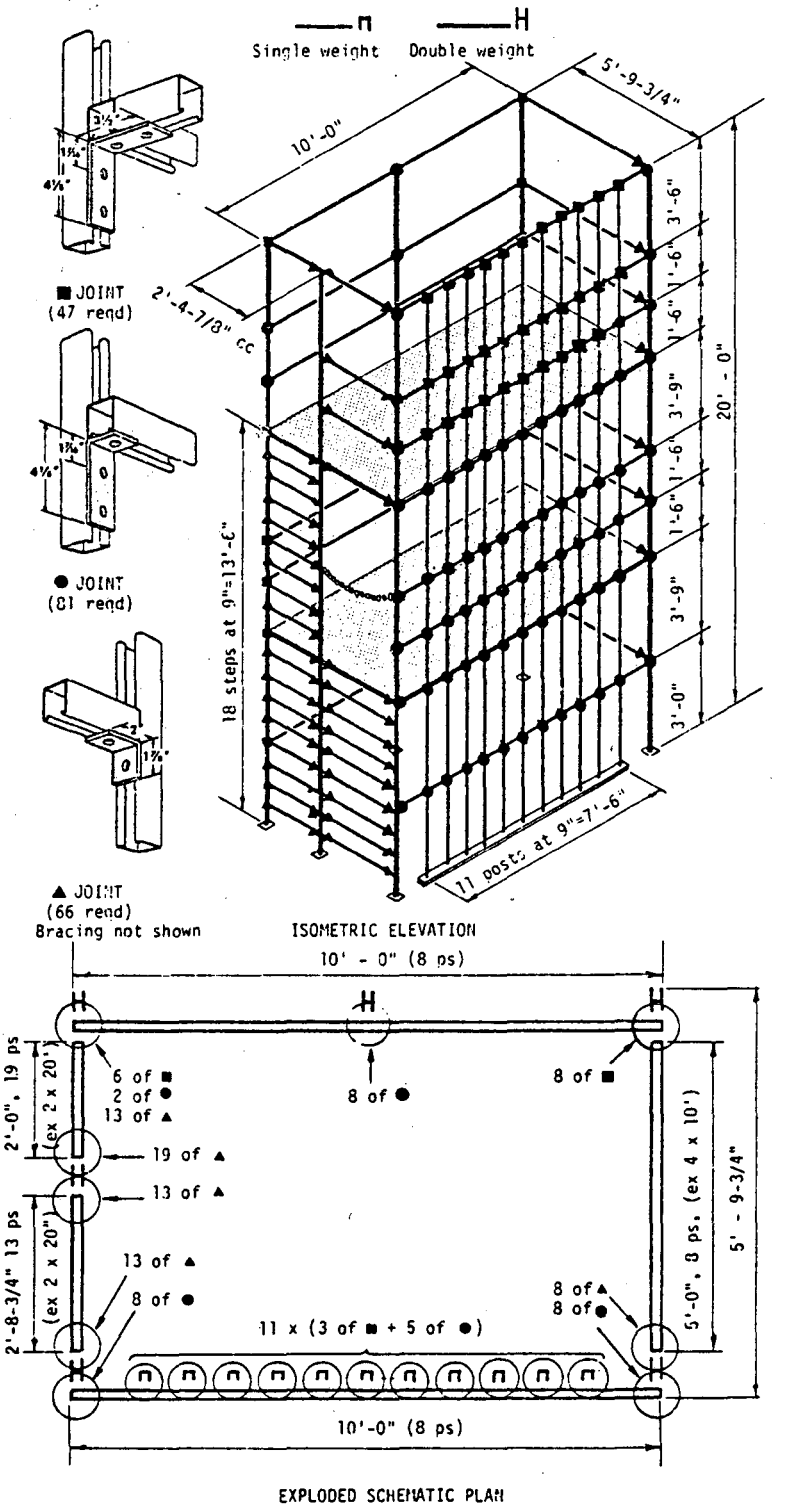

XBL 849-3806

Figure 5.2 Structural Support.

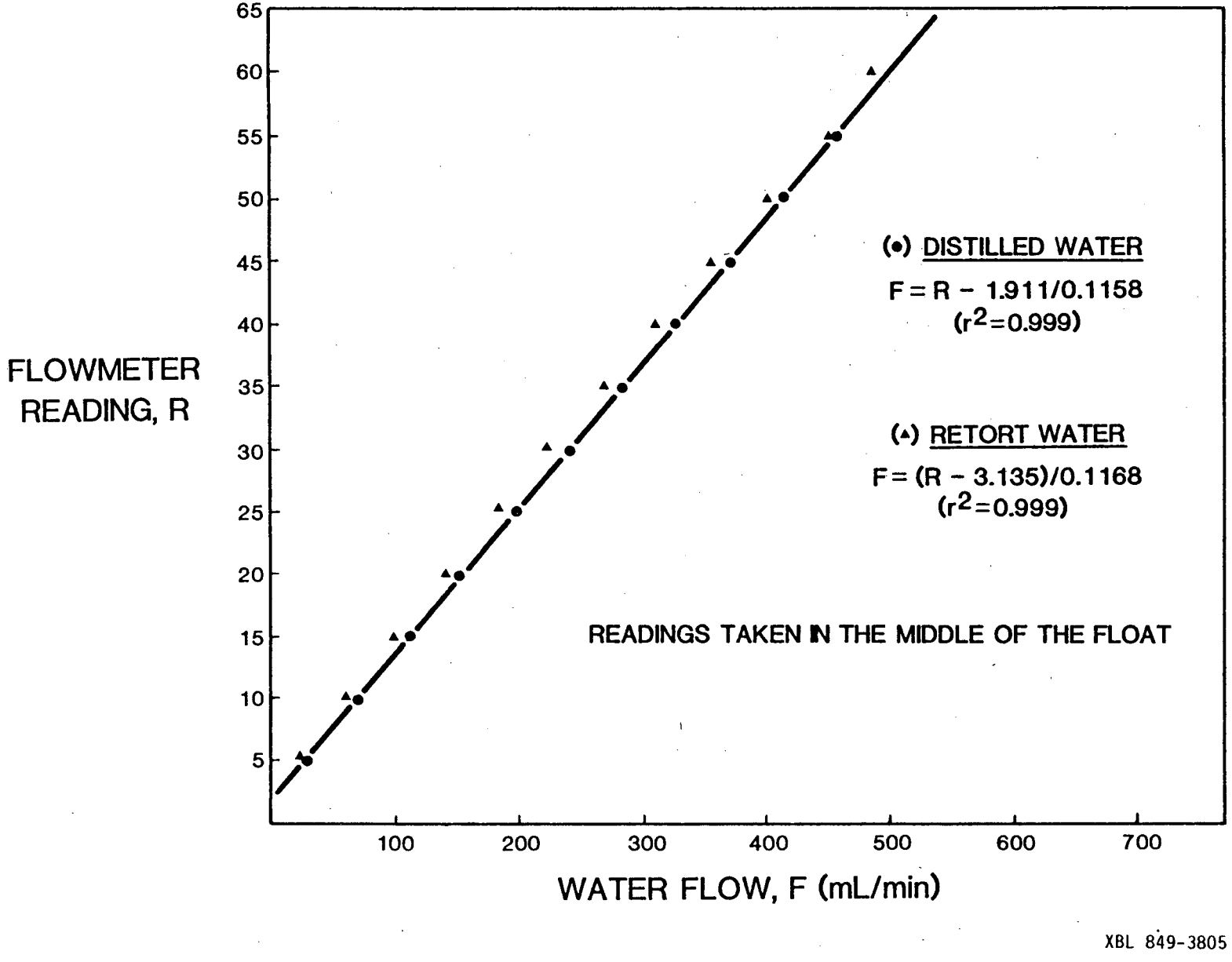

Figure 5.3 Calibration Curve for Raw Feed Rotameter.

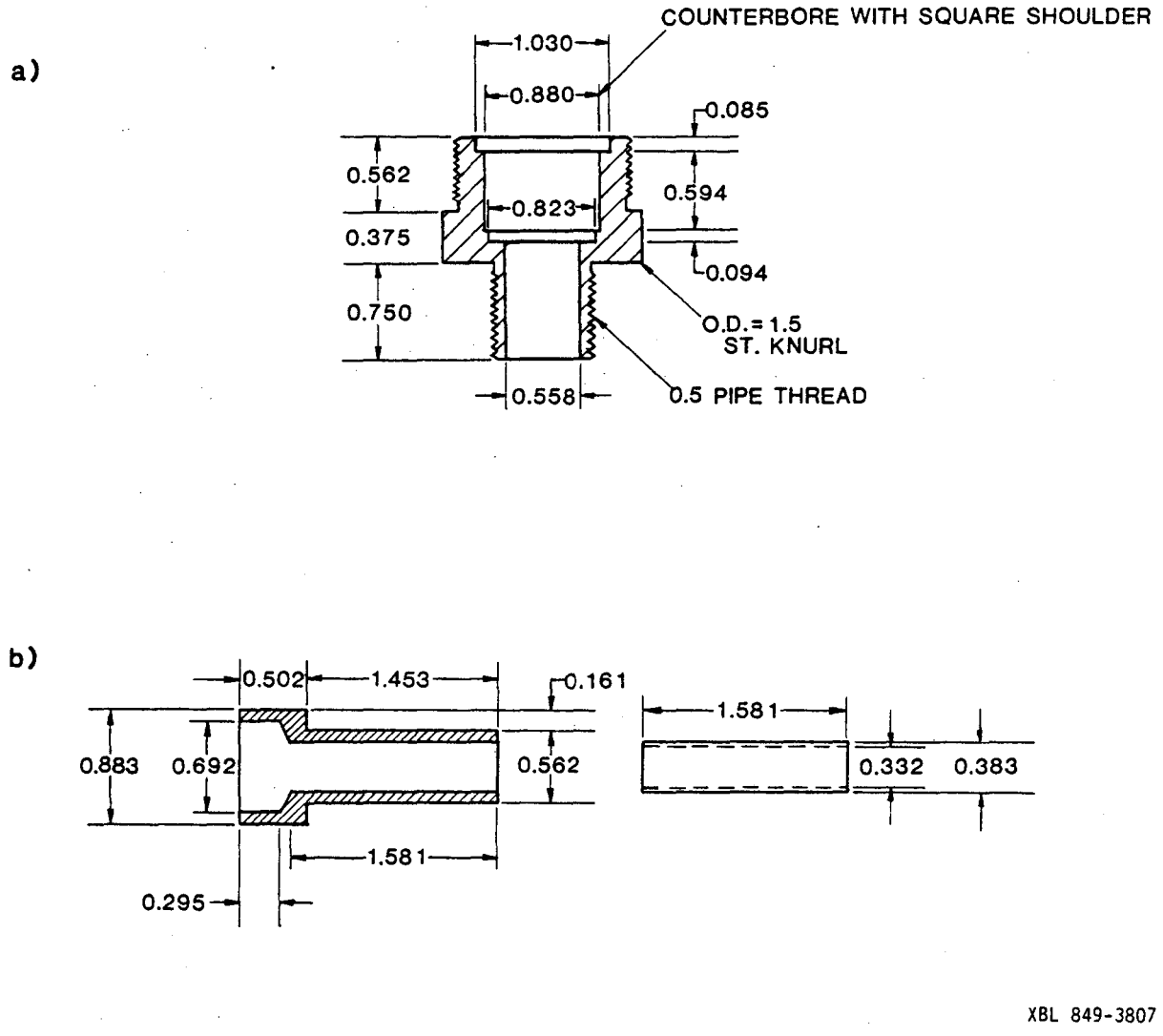

Figure 5.4 Bushing for Steam-Flow Rotameter (All Dimensions in Inches).
a) Teflon Bushing.
b) Insert for Bushing.

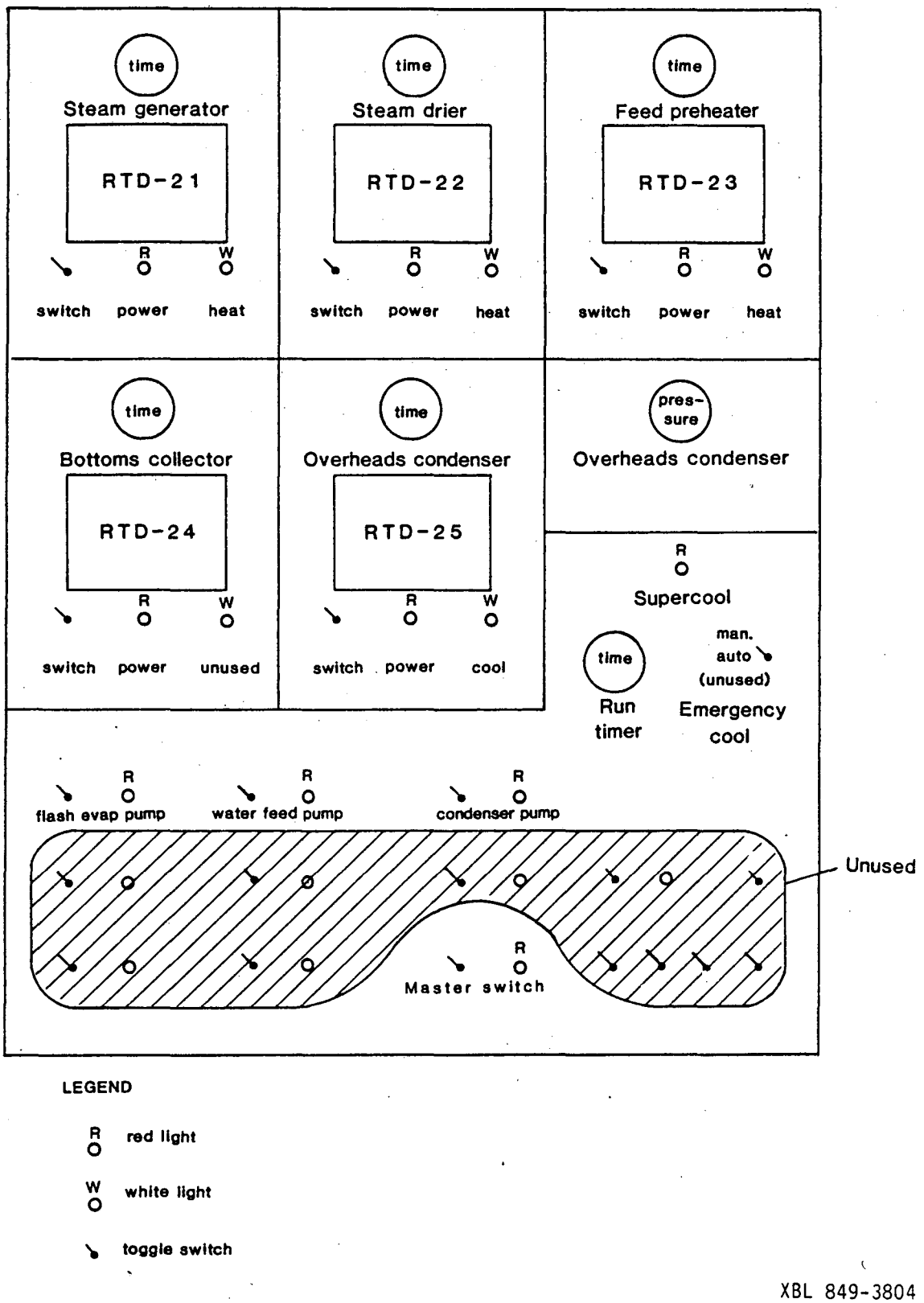

Figure 5.5 Control Panel.

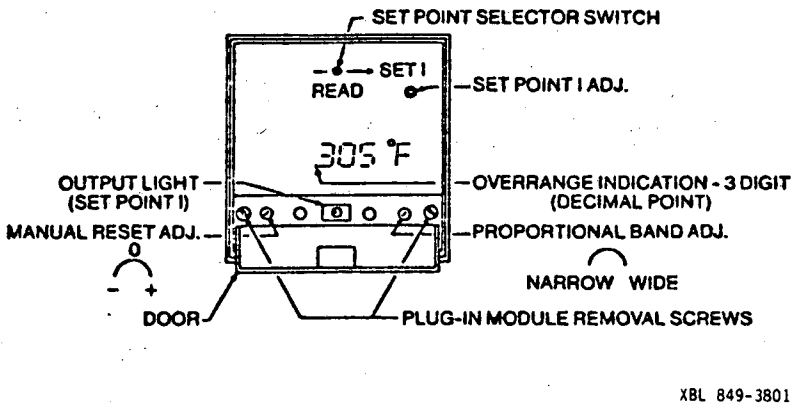

Figure 5.6 Omega RTD Controller. Courtesy of OMEGA ENGINEERING, INC., An OMEGA GROUP Company.

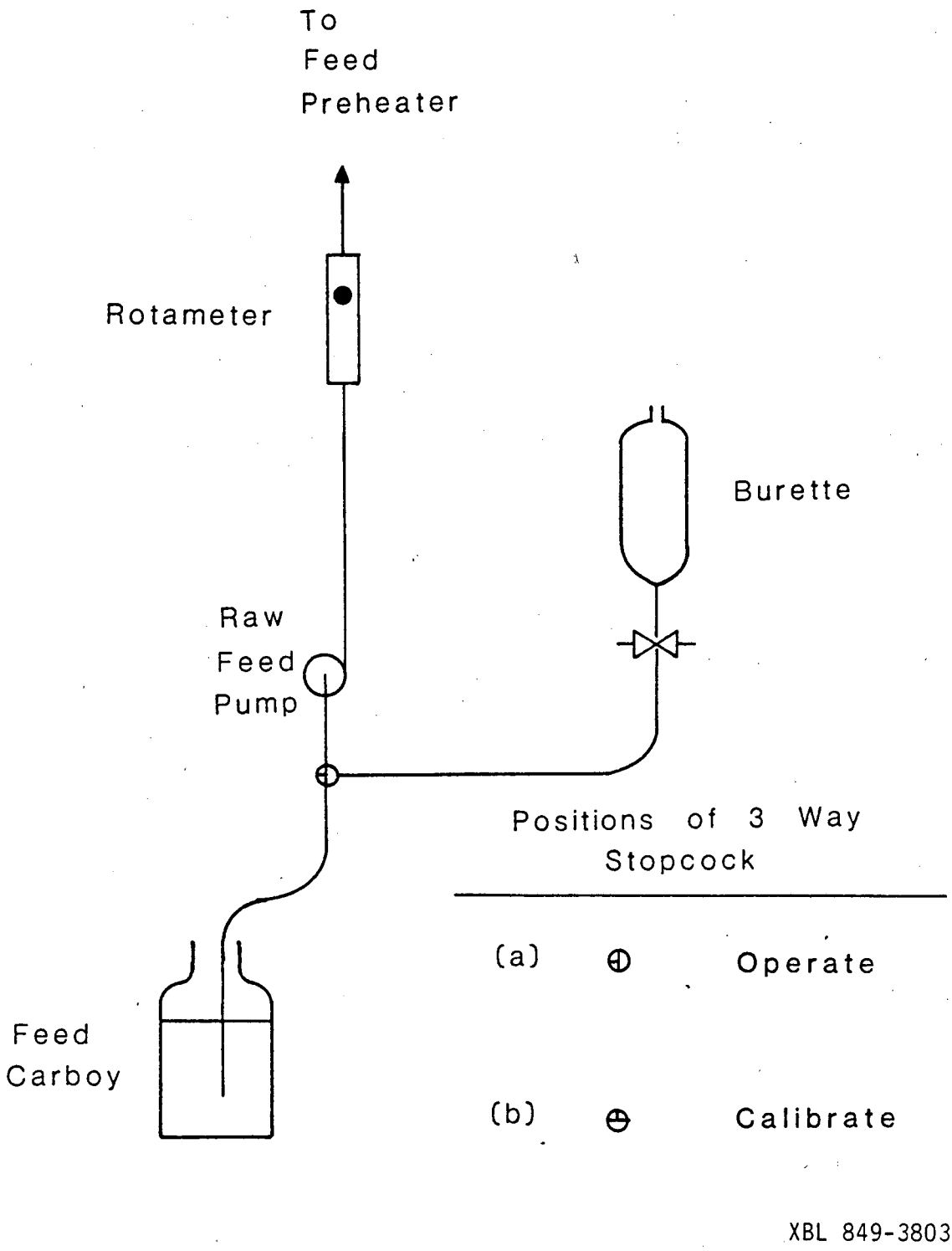

Figure 6.1 Direct Measurement of Raw Feed Flow Rate and Calibration of Raw Feed Rotameter.

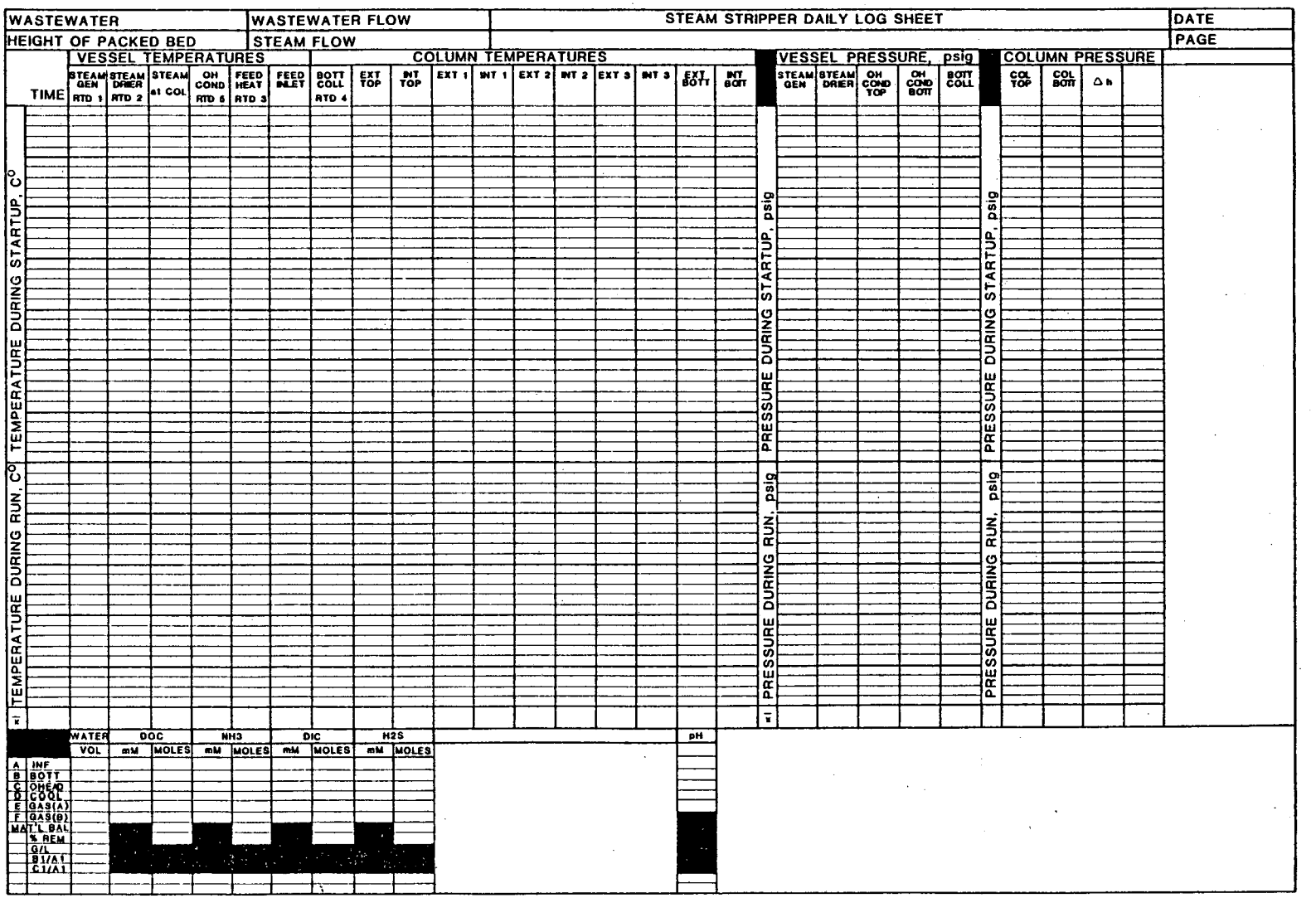

XBL 849-3793

Figure 6.2 Data Sheet.

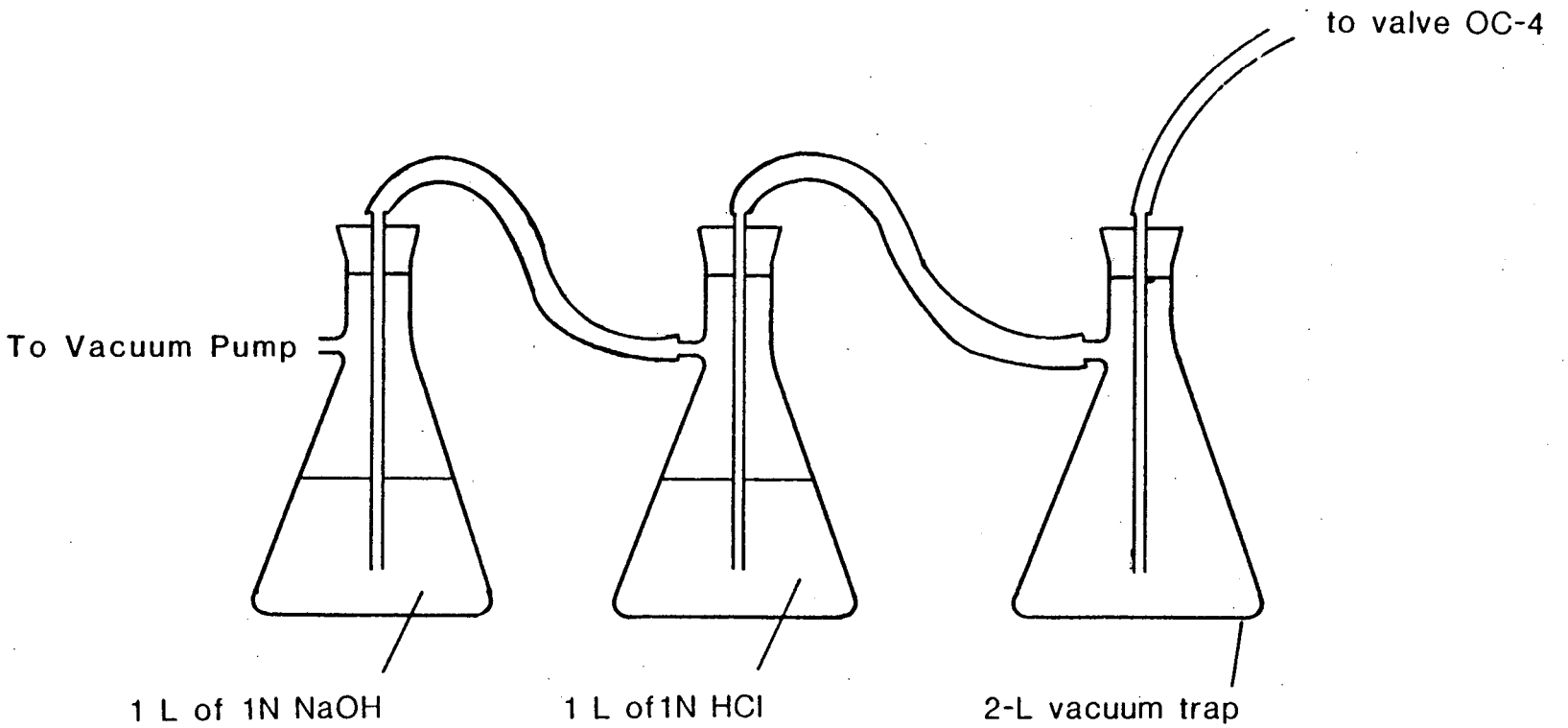

Figure 6.3 Arrangement of Vacuum Traps for Collecting Noncondensable Gases.

REFERENCES

American Petroleum Institute
"Sour Water Stripping Project Committee on Refinery Environmental Control," American Petroleum Institute, Refining Department, 1975, API Publication 946.

American Petroleum Institute
"A New Correlation of NH_3, CO_2, and H_2S Volatility Data from Aqueous Sour Water Systems," American Petroleum Institute, Refining Department, 1978, API Publication 955, 119 pp.

APHA
Standard Methods for the Examination of Water and Wastewater, 15th ed.; American Public Health Association: Washington, D.C., 1981.

Babcock & Wilcox
Steam/Its Generation and Use, Babcock & Wilcox: New York, NY, 1972; Chapter 2.

Bailey, J.E.; Ollis, D.F.
Biochemical Engineering Fundamentals, McGraw-Hill Book Co.: New York, N.Y., 1977.

Bennett, C.O.; Myers, J.E.
Momentum, Heat, and Mass Transfer, 2nd ed.; McGraw-Hill Book Co.: New York, NY, 1974.

Beutier, D.; Renon, H.
"Representation of NH_3-H_2S-H_2O, NH_3-CO_2-H_2O and NH_3-SO_2-H_2O Vapor-Liquid Equilibria," Ind. Eng. Chem. Process Des. Dev., 1978, 17, 220-30.

Beychok, M.R.
Aqueous Wastes from Petroleum and Petrochemical Plants, John Wiley and Sons: New York, NY, 1967.

Bird, R.B.; Stewart, W.E.; Lightfoot, E.N.
Transport Phenomena, John Wiley and Sons, Inc.: New York, NY, 1960.

Bomberger, D.C.; Smith, J.H.
"Use Caustic to Remove Fixed Ammonia," Hydrocarbon Process., 1977, 56(7), 157-62.

Brian, P.L.T.; Vivian, J.E.; Mayr, S.T.
"Cellular Convection in Desorbing Surface Tension-Lowering Solutes from Water," Ind. Eng. Chem. Fundam., 1971, 10(1), 75-83.

Butler, J.N.
Ionic Equilibrium. A Mathematical Approach, Addison-Wesley Publishing Co., Inc.: Reading, MA, 1964.

Colburn, A.P.
"The Simplified Calculation of Diffusional Processes. General Consideration of Two-Film Resistances," Trans. Am. Inst. Chem. Eng., 1939, 35, 211-36.

Danckwerts, P.V.
Gas-Liquid Reactions, McGraw-Hill Book Co.: New York, NY, 1970.

Daughton, C.G. (Ed.)
"A Manual of Analytical Methods for Wastewaters," 2nd ed.; Lawrence Berkeley Laboratory: Berkeley, CA, 1984, LBL-17421.

Daughton, C.G.; Sakaji, R.H.
"Separation of Ammonia from Organic Nitrogen Using Tubular Microporous Polytetrafluoroethene Membranes: Nonosmotic Dissolved-Gas Dialysis," Lawrence Berkeley Laboratory: Berkeley, CA, 6 July 1984, LBID-948.

Daughton, C.G.; Sakaji, R.H.
"Oxy-6 Retort Water: Preparation of Composite Sample," Report to D. Sheesley and R.E. Poulson, Laramie Energy Technology Center, 9 July 1980.

Dean, J.A. (Ed.)
Lange's Handbook of Chemistry, 12th ed., McGraw-Hill Book Co.: New York, NY, 1979.

Edwards, T.J.; Maurer, G.; Newman, J.; Prausnitz, J.M.
"Vapor-Liquid Equilibria in Multicomponent Aqueous Solutions of Volatile Weak Electrolytes," AIChE J, 1978, 24(6), 966-76.

Edwards, T.J.; Newman, J.; Prausnitz, J.M.
"Thermodynamics of Aqueous Solutions Containing Volatile Weak Electrolytes," AIChE J, 1975, 21, 248-58.

Farrier, D.S.; Poulson, R.E.; Skinner, Q.D.; Adams, J.C.; Bower, J.
"Acquisition, Processing and Storage for Environmental Research of Aqueous Effluents Derived from In Situ Oil Shale Processing," the Second Pacific Chemical Engineering Congress (PAChEC 1977) Vol II, pp. 1031-35.

Gunn, D.J.
"Mixing in Packed and Fluidised Beds," Chem. Eng. (London), 1968, issue no. 219, CE 153-72.

Habenicht, C.H.; Jovanovich, A.; Shaffron, M.; Wallace, J.; Hicks, E.; Liang, L.
"Steam Stripping and Reverse Osmosis for the Treatment of Oil Shale Wastewaters: Report of a Field Test," Water Purification Associates, Cambridge, MA, November 1980, Project 5-31343, 94 pp.

Healy, J.B., Jr.; Jones, B.M.; Langlois, G.W.; Daughton, C.G.
"Biotreatment of Oil Shale Wastewaters," in Proceedings of the 16th Oil Shale Symposium, Gary, J.M., Ed., 1983, Colorado School of Mines Press: Golden, CO., p. 498-511.

Hines, A.L.; Pedram, E.O.; Punnoose, S.; Poulson, R.E.
"Hot Gas Stripping of Oil Shale Retort Waters," in Proceedings of the 15th Oil Shale Symposium, Gary, J.H., Ed., 1982, Colorado School of Mines Press: Golden, CO, p. 468-78.

Holman, J.P.
Thermodynamics, McGraw-Hill Book Co.: New York, NY, 1974.

Jones, B.M.; Sakaji, R.H.; Thomas, J.F.; Daughton, C.G.
"Microbial Aspects of Oil Shale Wastewater Treatment," in Energy and Environment Division 1981 Annual Report, Lawrence Berkeley Laboratory: Berkeley, CA, 1982, LBL-13500, Chapter 4, p. 51-57.

Katritzky, A.R.; Lagowski, J.M.
The Principles of Heterocyclic Chemistry, Academic Press: New York, NY, 1968.

King, C.J.
"The Additivity of Individual Phase Resistances in Mass Transfer Operations," AIChE J, 1964, 10, 671-7.

King, C.J.
Separation Processes, 2nd ed., McGraw-Hill Book Co.: New York, NY, 1980.

Leenheer, J.A.; Noyes, T.I.; Stuber, H.A.
"Determination of Polar Organic Solutes in Oil-Shale Retort Water," Eviron. Sci. Technol. 1982, 16, 714-723.

Leva, M.
Tower Packings and Packed Tower Design, 2nd ed., The United States Stoneware Co.: Akron, Ohio, 1953.

Levenspiel, O.; Bischoff, K.B.
"Patterns of Flow in Chemical Process Vessels," in Advances in Chemical Engineering, Vol. 4, T.B. Drew; J.W. Hoopes, Jr.; T. Vermeulen (Eds.), Academic Press: New York, NY, 1963, 95-198.

Levenspiel, O.; Weinstein, N.J.; Li, J.C.R.
"A Numerical Solution to Dimensional Analysis," Ind. Eng. Chem., 1956, 48(2), 324-6.

Lewis, R.C.; Rawlings, G.D.
"Laboratory Treatability Testing of Selected Oil Shale Process Wastewaters," in Proceedings of the 36th Industrial Waste Conference, Purdue University, Ann Arbor Science: Ann Arbor, MI, 1982, p. 341-49.

Mecklenburgh, J.C.; Hartland, S.
The Theory of Back Mixing, John Wiley & Sons, New York, NY, 1975.

Mercer, B.W.; Wakamiya, W.
"Analysis, Screening, and Evaluation of Control Technology for Wastewater Generated in Shale Oil Development," in Pacific Northwest Laboratory Annual Report for 1979, Bair, W.J., Ed., February 1980, part 5, PNL-3300, pp. 35-8.

Metcalf & Eddy, Inc.
Wastewater Engineering: Treatment Disposal Reuse, 2nd ed., revised by G. Tchobanoglous, McGraw-Hill Book Co.: New York, NY, 1979.

Murphy, C.L.; Hines, A.L.; Poulson, R.E.
"Hot Gas Stripping of Simulated InSitu Oil Shale Retort Water," Prepr. Pap. Am. Chem. Soc., Div. Fuel Chem., 1978, 23(2).

Onda, K; Sada, E.; Murase, Y.
"Liquid-Side Mass Transfer Coefficients in Packed Towers," AIChE J., 1959, 5(2), 235-9.

Onda, K.; Takeuchi, H.; Okumoto, Y.
"Mass Transfer Coefficients Between Gas and Liquid Phases in Packed Columns," J. Chem. Eng. (Jpn), 1968, 1, 56-62.

Pawlikowski, E.M.; Newman, J.; Prausnitz, J.M.
"Phase Equilibria for Aqueous Solutions of Ammonia and Carbon Dioxide," Ind. Eng. Chem. Process Des. Dev., 1982, 21(4), 764-70.

Pawlikowski, E.M.; Newman, J.; Prausnitz, J.M.
"Vapor-Liquid Equilibrium Calculations for Aqueous Mixtures of Volatile, Weak Electrolytes and Other Gases for Coal-Gasification Processes," in Chemical Engineering Thermodynamics, Newman, S.A., Ed., Ann Arbor Science: Ann Arbor, MI, 1983, p. 323-37.

Pearson, F.; Diyamandoglu, V.; Nurdogan, Y.; Wong, S.; Selleck, R.
"Steam Stripping of Shale Oil Wastewater-Phase I," Sanitary Engineering Research Laboratory Report, Draft, December 1980, UCB-SERL 80-8, 76 pp.

Perry, R.H.; Chilton, C.H.
Chemical Engineer's Handbook, 5th ed., McGraw-Hill Book Co.: New York, N.Y., 1973.

Perry, R.H.; Chilton, C.H.; Kirkpatrick, S.D.
Chemical Engineer's Handbook, 4th ed., McGraw-Hill Book Co.: New York, N.Y., 1963.

Persoff, P; Hunter, L.; Daughton, C.G.
"Atmospheric Emissions From Codisposed Oil Shale Wastes: A Preliminary Assessment," Lawrence Berkeley Laboratory, March 1984, LBID-890, 36 pp.

Pitzer, K.S.
"Thermodynamics of Electrolytes. I. Theoretical Basis and General Equations," J. Phys. Chem., 1973, 77, (2), 268-77.

Pitzer, K.S.; Kim, J.J.
"Thermodynamics of Electrolytes. IV. Activity and Osmotic Coefficients for Mixed Electrolytes," J. Am. Chem. Soc., 1974, 96(18), 5701-7.

Prausnitz, J.M.
Molecular Thermodynamics of Fluid-Phase Equilibria, Prentice-Hall, Inc.: Englewood Cliffs, NJ, 1969.

Probstein, R.F.; Hicks, R.E.
Synthetic Fuels, McGraw-Hill Book Co.: New York, NY, 1982.

Raphaelian, L.A.; Harrison, W.
"Organic Constituents in Process Water from the In-Situ Retorting of Oil from Oil-Shale Kerogen," Argonne National Laboratory Report, February 1981, ANL/PAG-5, 33 pp.

Schmidt-Collérus, J.J.; Prien, C.H.
"Investigations of the Hydrocarbon Structure of Kerogen from Oil Shale of the Green River Formation," in Science and Technology of Oil Shale, Yen, T.F., Ed., Ann Arbor Science Publ.: Ann Arbor, MI., 1976, p. 183-92.

Scriven, L.E.
"Flow and Transfer at Fluid Interfaces. Part I. Lessons from Research," Chem. Eng. Educ., 1968, 2, 150-5.

Scriven, L.E.
"Flow and Transfer at Fluid Interfaces. Part II. Models," Chem. Eng. Educ., 1969a, 3, 26-9.

Scriven, L.E.
"Flow and Transfer at Fluid Interfaces. Part III. Convective Diffusion," Chem. Eng. Educ., 1969b, 3, 94-8.

Sternling, C.V.; Scriven, L.E.
"Interfacial Turbulence: Hydrodynamic Instability and the Marangoni Effect," AIChE J, 1959, 5(4), 514-25.

Sherwood, T.K.; Holloway, F.A.L.
"Performance of Packed Towers--Experimental Studies of Absorption and Desorption," Trans. Am. Inst. Chem. Eng., 1940, 36, 21-37.

Sherwood, T.K.; Pigford, R.L.; Wilke, C.R.
Mass Transfer, McGraw-Hill Book Co.: New York, NY, 1975.

Shulman, H.L.; Ullrich, C.F.; Proulx, A.Z.; Zimmerman, J.O.
"II. Wetted and Effective-Interfacial Areas, Gas - and Liquid-Phase Mass Transfer Rates," AIChE J, 1955, 1(2), 253-8.

Stumm, W.; Morgan, J.J.
Aquatic Chemistry, Wiley-Interscience: New York, NY, 1970.

Thibodeaux, L.J.
Chemodynamics, John Wiley and Sons: New York, NY, 1979.

Treybal, R.E.
Mass-Transfer Operations, 3rd ed., McGraw-Hill Book Co.: New York, N.Y., 1980.

van Aken, A.B.; Drexhage, J.J.; de Swaan Arons, J.
"Prediction of Azeotropes in the Systems NH_3-H_2O and SO_2-H_2O," Ind. Eng. Chem. Fundam., **1975**, 14(3), 154-7.

van Krevelen, D.W.; Hoftijzer, P.J.
"Kinetics of Simultaneous Absorption and Chemical Reaction," Chem. Eng. Prog., **1948**, 44, 529-36.

van Krevelen, D.W.; Hoftijzer, P.J.; Huntjens, F.J.
"Composition and Vapour Pressures of Aqueous Solutions of Ammmonia, Carbon Dioxide, and Hydrogen Sulphide," Recueil, **1949**, 68, 191-216.

Wallace, J.R.; Culbertson, W.J.; Habenicht, C.H.; Shaffron, M.
"A Transportable Steam Stripper for the Pilot Scale Treatment of Oil Shale Wastewaters: Design, Field Testing, and Chemical Analysis," in Proceedings of the 14th Oil Shale Symposium, Gary, J.H. (Ed.), Colorado School of Mines Press: Golden, CO., **1981**, p. 330-6.

Weast, R.C. (Ed.)
CRC Handbook of Chemistry and Physics, 59th ed.; CRC Press, Inc.: West Palm Beach, FL, **1978**.

Yen, T.F.
"Structural Investigations on Green River Oil Shale Kerogen," in Science and Technology of Oil Shale, Yen, T.F. (Ed.), Ann Arbor Science Publ.: Ann Arbor, MI, 1976, p. 193-203.

APPENDIX A Manufacturer's Literature

Copies of Appendix A can be obtained, at cost, from the Sanitary Engineering and Environmental Health Research Laboratory (University of California Richmond Field Station, 1301 So. 46th St., Bldg. 112, Richmond, CA 94804). Requestors should ask for Appendix A to SEEHRL Report 84-3.

This Appendix contains manufacturer's literature on items of equipment that have been installed in the LBL/SEEHRL steam stripper system. These items have been arranged in the following order for reference:

1. Mercoid Pressure Controls
2. Eastern D-Series Pumps
3. FMI Lab Pumps
4. Calrod Circulation Heaters
6. Omega series 4200 RTD controllers
7. Gilmont Instruments Flowmeters (Rotameters)
8 PTFE Flexijoint Coupling
9. Corning Beaded Pyrex Tubing

For general information on RTDs, refer to: Practical Temperature Measurements, Hewlett Packard applications note 290, Hewlett Packard Corp., Palo Alto, CA 1980. For general information on rotameters, refer to Buyer's Guide for Rotameters, Fischer & Porter catalog 10A-1000-81, Fischer & Porter, Warminster, PA 1980.

The original work orders that were written for fabrication of the LBL/SEEHRL steam stripper system are available for reference at SEEHRL, Bldg. 112, University of California Richmond Field Station, 1301 S. 46 St., Richmond, CA 94804.

APPENDIX B Photographs for Identification of Valves and Transformers.

All valves in the steam stripper system can be identified by referring either to Figure 5.1 or to the photographs in this Appendix. Use them together for positive identification. To find a particular valve, use Table B-1 to determine in which Figure it can be found. Figure B-12 identifies the low-voltage transformers (variacs) which control power to the heat tapes on the stripping column (see Table 5-2).

Table B-1. Figures in Appendix B for identification of valves.

SG-1	B-7	FP-1	B-9	OC-1	B-11	BC-1	B-2	PB-1	B-6
SG-2	B-7			OC-2[a]		BC-2	B-1	PB-2	B-1
SG-3	B-8			OC-3[a]		BC-3	B-1	PB-3[a]	
SG-4	B-8			OC-4	B-1	BC-4	B-1	PB-4	B-6
SG-5	B-8			OC-5	B-1			PB-5	B-1
SG-6	B-2			OC-6[a]				PB-6	B-10
SG-7	B-7			OC-7	B-5			PB-7	B-10
SG-8	B-2			OC-8	B-5				
				OC-9	B-5				
				OC-10	B-3				
				OC-11	B-4				
				OC-12	B-4				

[a] These valves have been removed from the system.

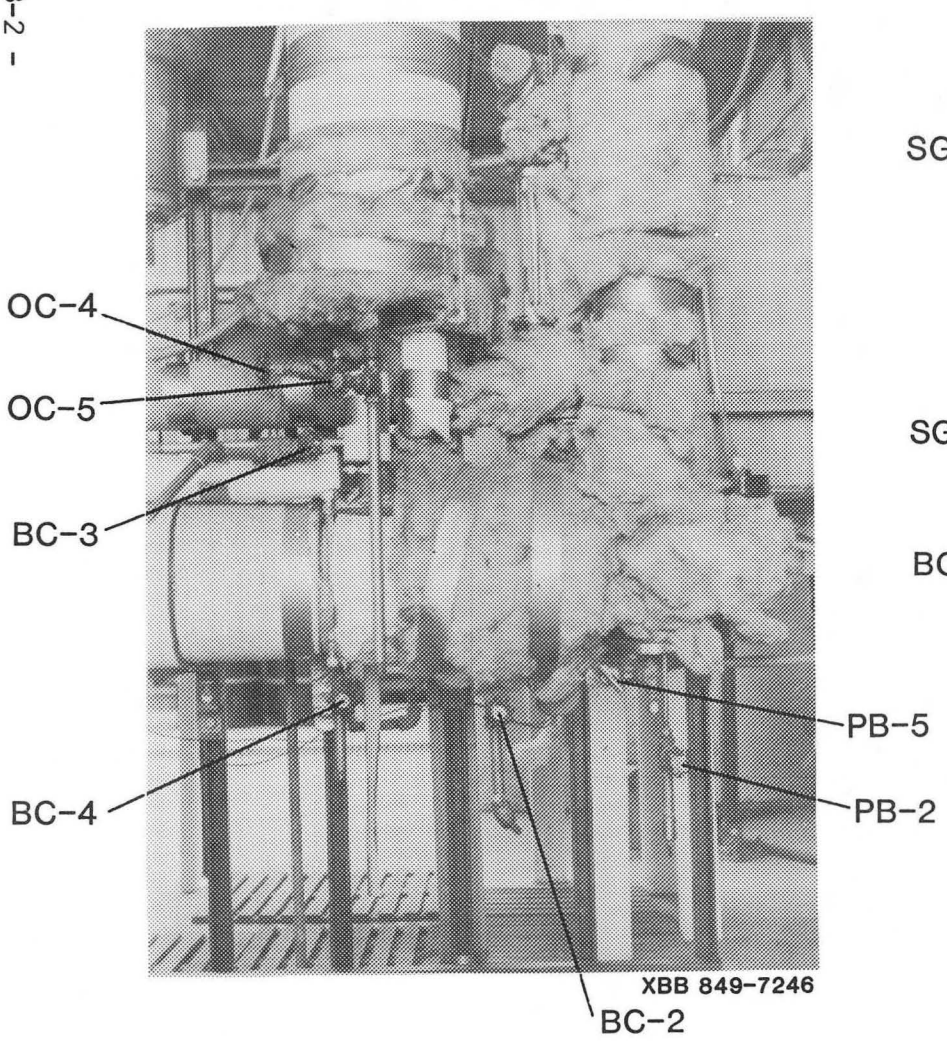

Figure B-1. Lower ends of overheads condenser and stripping column, and right end of bottoms collector. Photograph taken at ground level, showing valves BC-2, -3, and -4; PB-2 and -5; and OC-4 and -5.

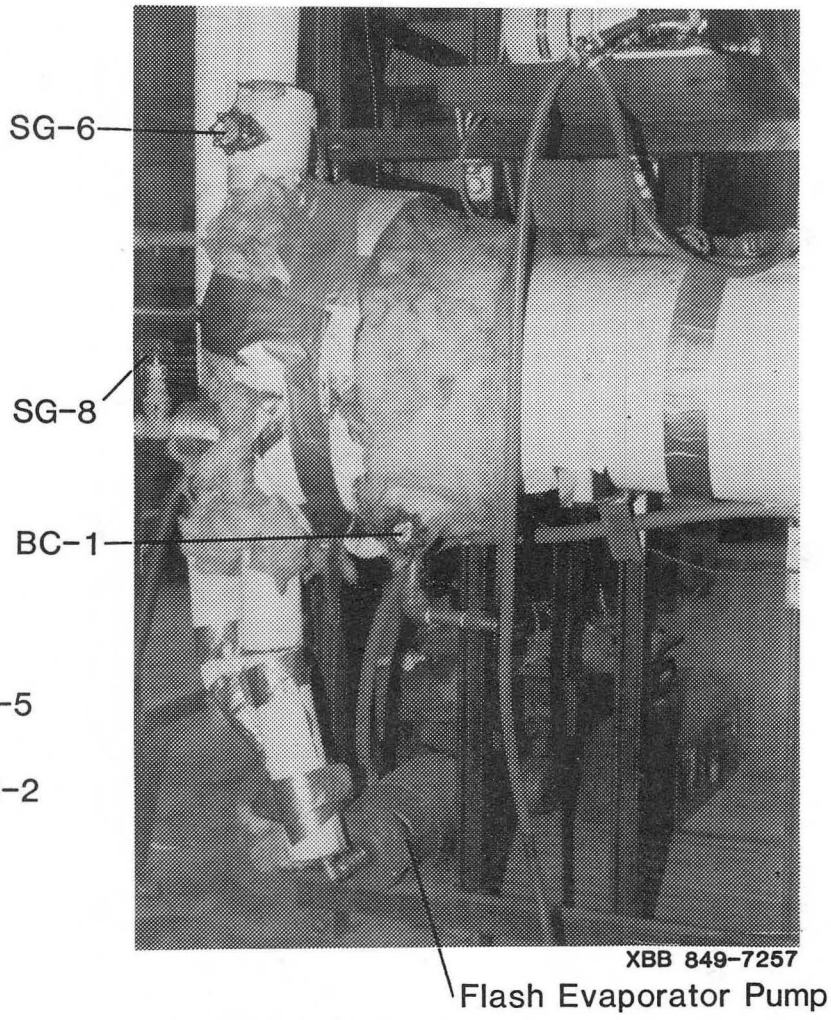

Figure B-2. Left end of bottoms collector. Photograph taken at ground level, showing flash evaporator pump and valves SG-6 and -8, and BC-1.

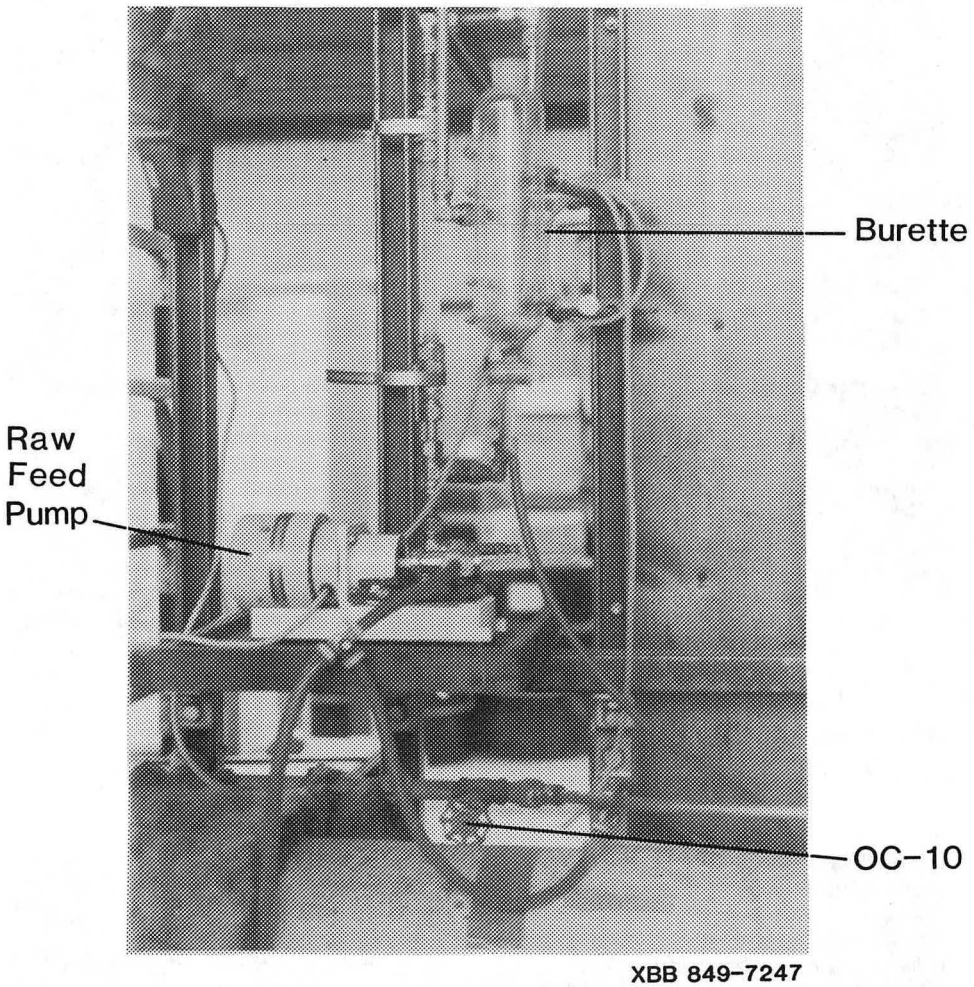

Figure B-3. Raw feed pump and burette used for calibration. Photograph taken at ground level, showing valve OC-10.

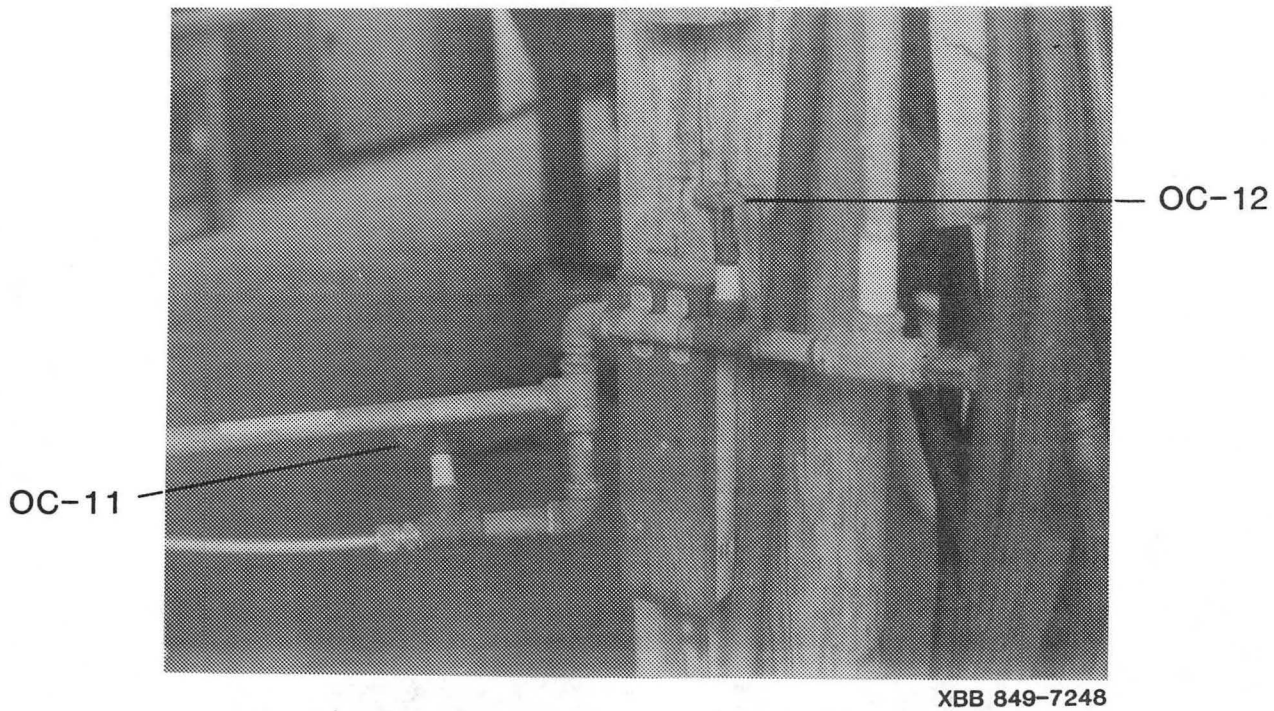

Figure B-4. Cooling water supply line. Photograph taken at ground level, showing valves OC-11 and 12.

Figure B-5. Valves controlling bleed rate of cooling water. Photograph taken at ground level inside operator's area, showing valves OC-7, -8, and -9.

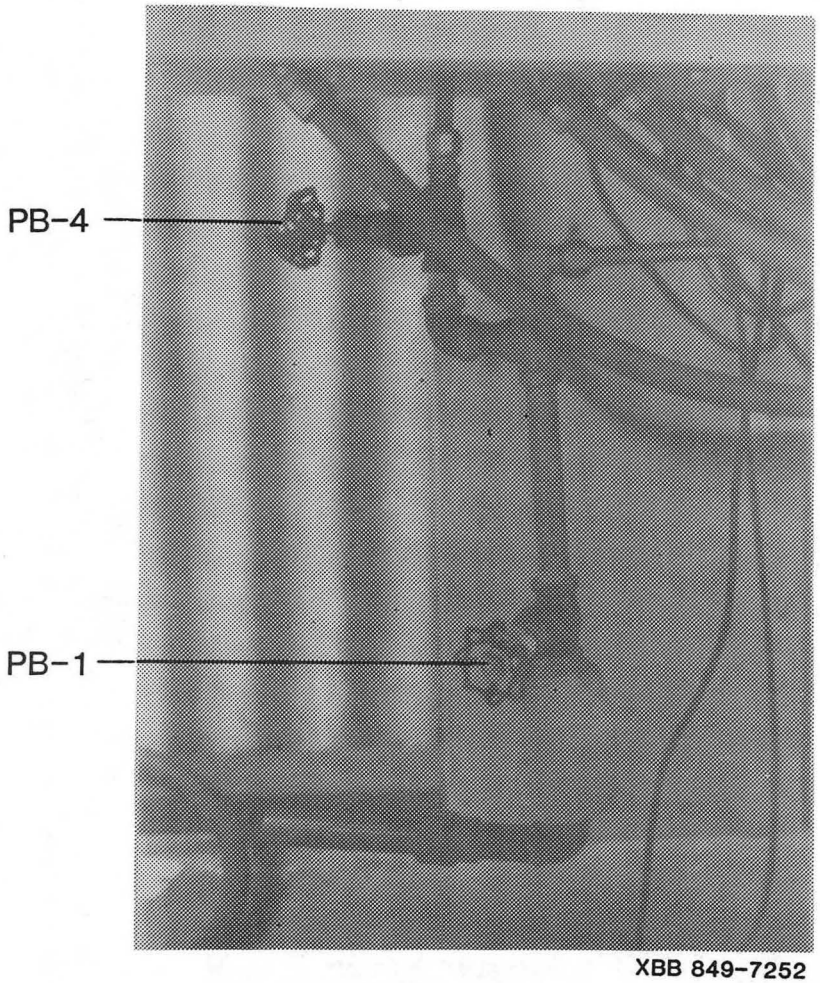

Figure B-6. Photograph taken behind and beneath control panel, showing valves PB-1 and -4.

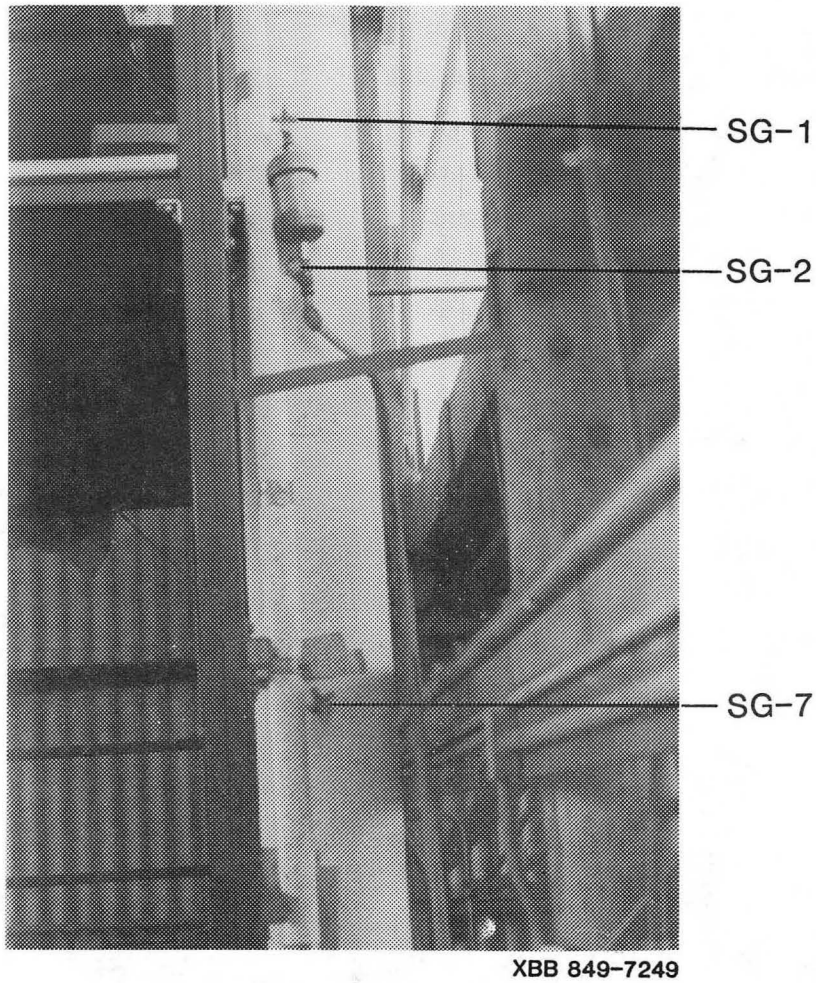

Figure B-7. Side view of steam generator, showing valves SG-1, -2, and -7. Note that valve SG-1 is at the level of the top deck.

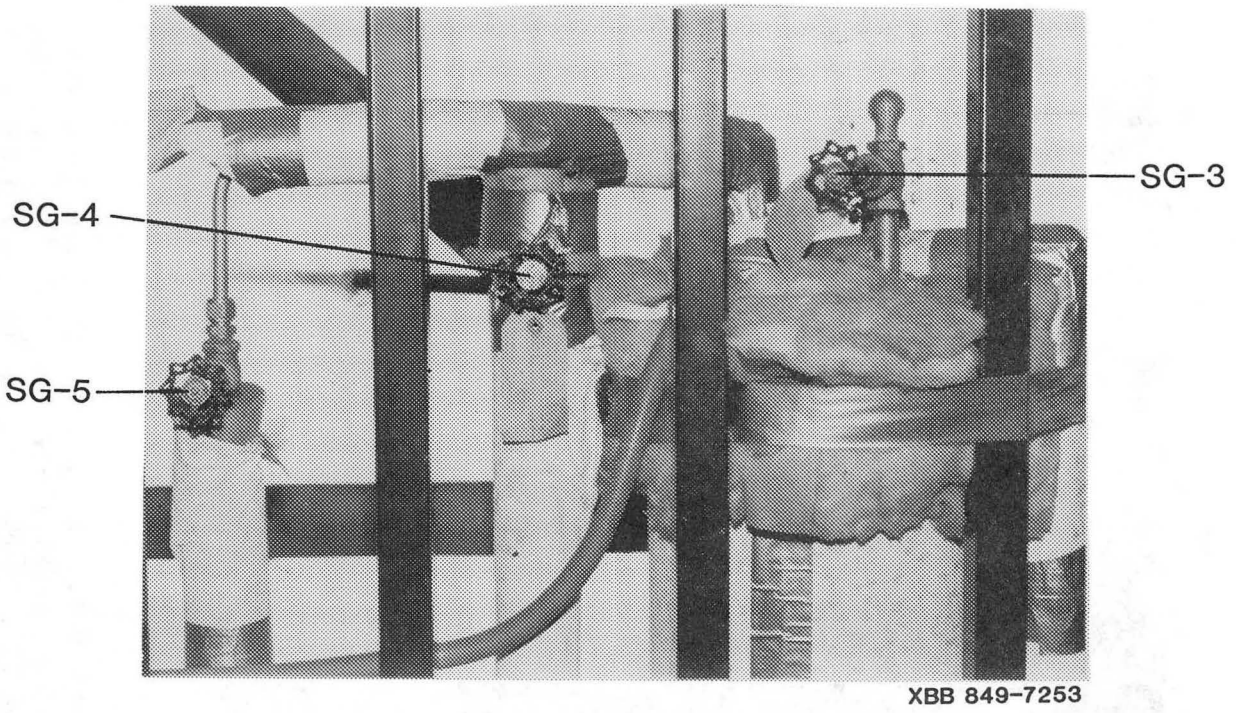

Figure B-8. Top of steam generator. Photograph taken on top deck, showing valves SG-3, -4, and -5.

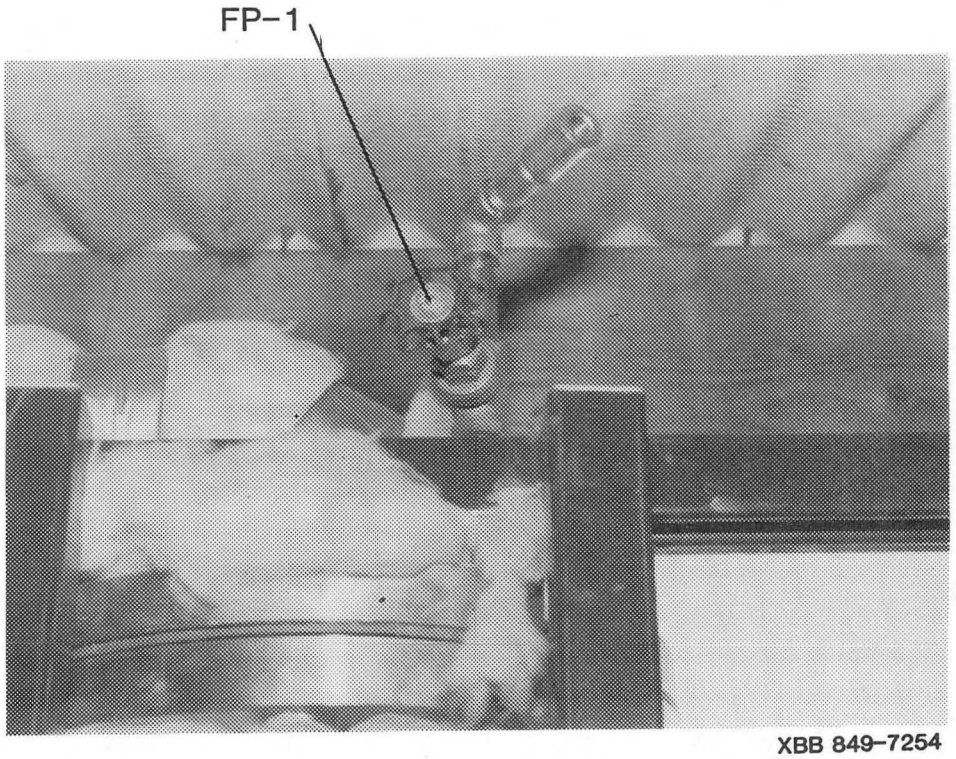

Figure B-9. Top of feed preheater. Photograph taken on top deck, showing valve FP-1.

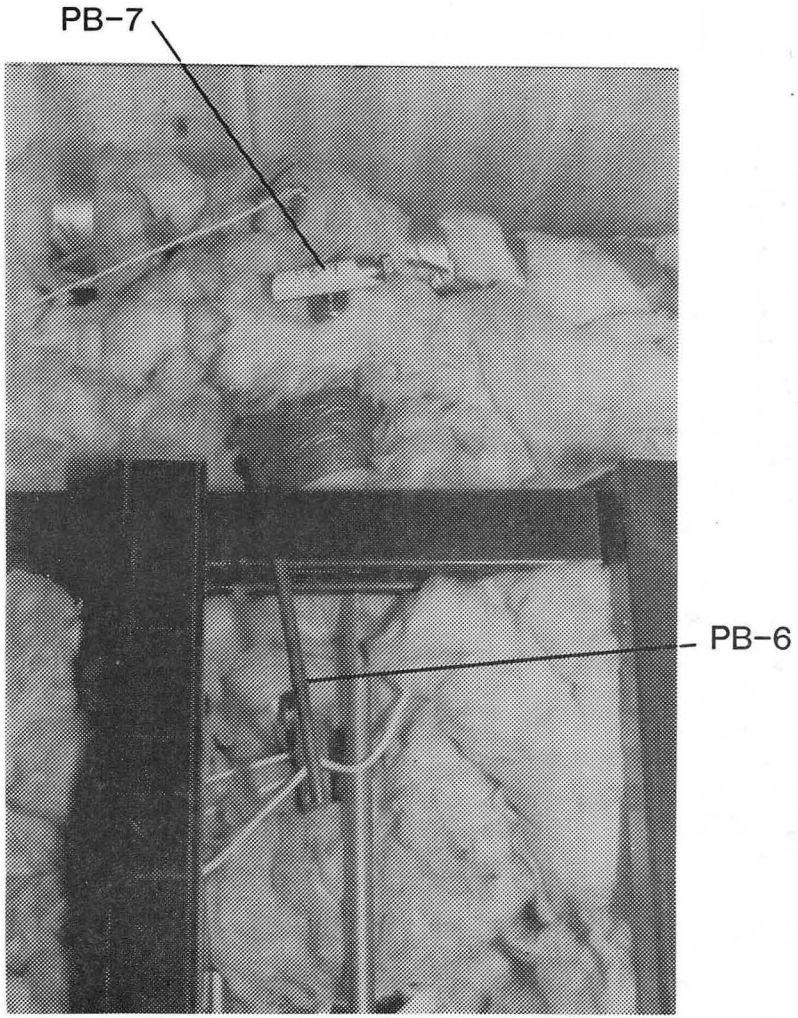

Figure B-10. Top of stripping column. Photograph taken on top deck, showing valves PB-6 and -7.

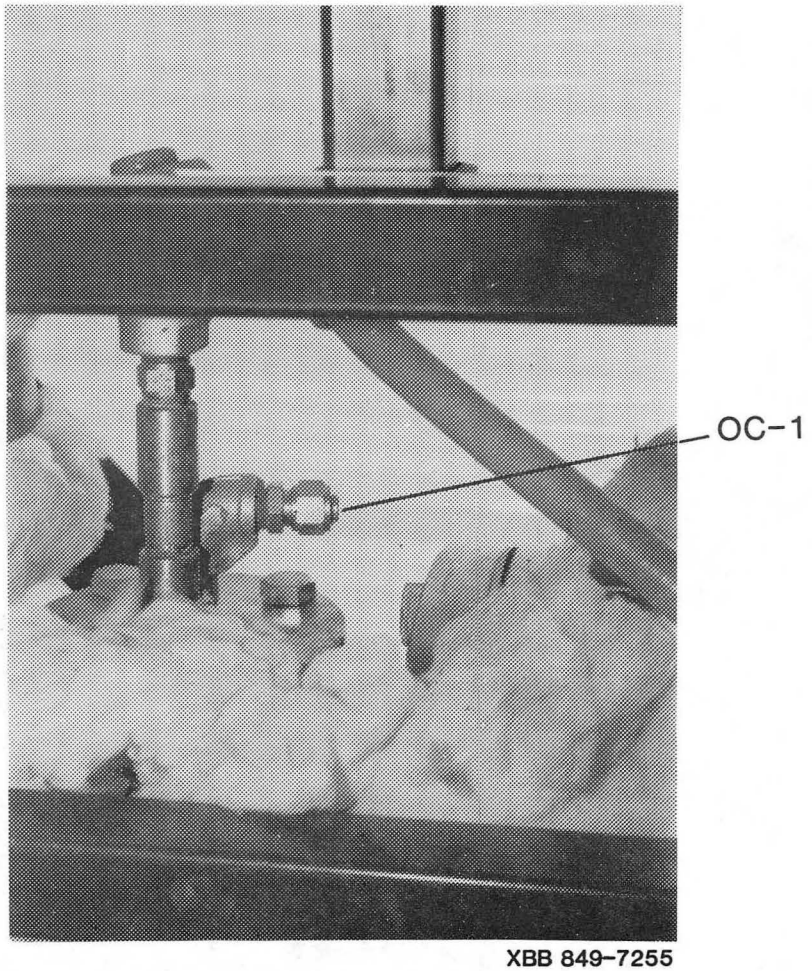

Figure B-11. Swagelok plug replacing valve OC-1. Photograph taken on top deck.

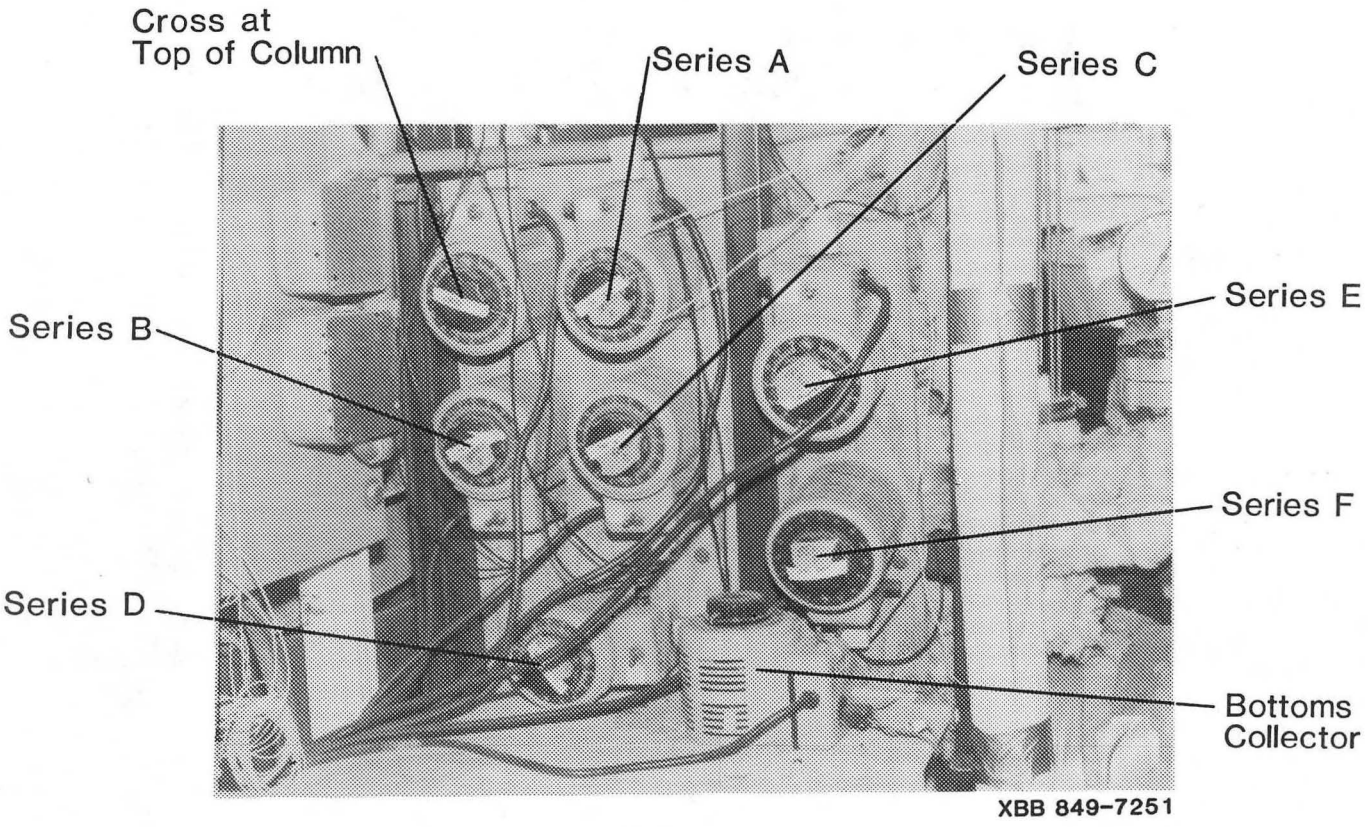

Figure B-12. Low-voltage transformers (variacs) for controlling heat tapes (see Table 5-2). Photograph taken at ground level inside operator's area.

APPENDIX C Steam Flow Program STEAMFLOW

This program calculates the steam flow rate from the temperatures, pressures, and rotameter reading recorded by the operator during a run. It is written in C-BASIC to run on the Fortune Systems 32:16 computer. When the program is run according to these instructions, the computer finds the program in the directory "reports" under the file name "steamflow.b." Then it compiles the program into a machine-language program "steamflow.i." When steamflow.i is run, the computer requests input data from the operator and produces an output file "steamflow.p" The operator can read this output file on the screen and can also have it printed. An example output is presented, with input data, in section 6.11.

In these instructions, (return), (execute), (cancel), and (space) refer to three special keys on the keyboard and the space bar.

1. Log in.

2. Key !(execute)
   This will put you into UNIX. The computer will respond with a $ prompt when it is ready for the next step.

3. Key cd(space)/u/reports(return)

4. Key ls(space)-las(space)steam*

5. Key cbas(space)steamflow.b(return)

6. Key rbas(space)steamflow.i(return)

7. The screen will ask you for input data. Enter each datum as it is requested, and end each entry with (return). Be sure to enter data in the correct units (as requested by the message on the computer screen).

8. When no more input data are required, the computer will respond with the $ prompt, and create a file called "steamflow.p." If there is an existing file by this name, it will be overwritten.

9. To view the output:
   Key screen(space)steamflow.p(return)

10. Key e

11. Key q

12. To print output: turn on the IDS 560 dot matrix printer and set it to "on-line."
    Key lpr(space)-hp(space)2(space)steamflow.p

13. To re-run the program, go to step 6.

14. Log out:
    Key ctrl-d (hit control and d simultaneously)
    This will get you out of UNIX.

15. Key (cancel) twice. Log-in screen will reappear.

The following is a complete listing of the program. Note that lines 300, 370, and 420 refer to a steel float in the rotameter. If the float is changed, these lines must be changed in the program. If the rotameter is changed to a different model, line 340 must be changed.

```
100 REM STEAMFLOW CREATED ON APPLE 2+ BY PETER PERSOFF
110 REM TRANSLATED TO CBASIC BY BONNIE JONES
115 LPRINTER
120 INPUT "ENTER AVERAGE TEMPERATURE RECORDED BY RTD-2 (DEG C)";T2
125 PRINT "RTD-2 TEMPERATURE =";T2
130 INPUT "ENTER AVERAGE TEMPERATURE RECORDED BY RTD-3 (DEG C)";T3
135 PRINT "RTD-3 TEMPERATURE =";T3
140 INPUT "ENTER BAROMETRIC PRESSURE (MM HG)";BP
145 PRINT "BAROMETRIC PRESSURE =";BP
150 INPUT "ENTER AVERAGE PRESSURE RECORDED AT THE ROTAMETER (PSIG)";OP
155 PRINT "AVERAGE ROTAMETER (PSIG) =";OP
160 REM OP IS OVERPRESSURE RECORDED AT THE ROTAMETER
170 LET OP = (OP / 14.696) * 760
180 REM SP IS STEAM PRESSURE
190 LET SP = OP + BP
200 PRINT "SP =";SP
210 REM ST IS STEAM TEMPERATURE (DEG K)
220 LET ST = ((T2 + T3) / 2) + 273.15
230 REM SD IS STEAM DENSITY (G/CM3)
240 REM MOLECULAR WEIGHT OF STEAM IS 18.15
250 LET SD = ((18.15 / 22414) * (273.15 / ST) * (SP / 760))
260 REM LINE 280 CALCULATES VISCOSITY OF STEAM AS A FUNCTION OF TEMPERATURE,
NOT VALID AT HIGH PRESSURE (E.G., 10 ATM OR MORE)
270 REM SV IS STEAM VISCOSITY (CP)
280 LET SV = 0.00004 * (ST - 273.15) + 0.0082
290 REM FD IS FLOAT DENSITY (E.G., 8.02 FOR STAINLESS STEEL)
300 LET FD = 8.02
310 INPUT "ENTER SCALE READING 0 TO 100";SR
315 PRINT "SCALE READING =";SR
320 REM CALCULATE R FROM SCALE READING
330 REM THE RELATIONSHIP IN LINE 340 IS FOR AN F-1500 FLOWMETER; SEE
CALIBRATION CURVES FOR OTHER FLOWMETERS
340 LET R = 0.8716 + 0.2603 * SR
350 PRINT "R =";R
360 REM WF IS THE MASS OF THE FLOAT IN GRAMS
370 LET WF = 8.60169
380 REM CALCULATE THE STOKES NUMBER
390 LET SN = ((1.042 * WF * (FD - SD) * SD * (R ^ 3)) / ((SV ^ 2) * FD))
400 PRINT "STOKES NUMBER =";SN
410 REM DI IS THE FLOAT DIAMETER IN INCHES
```

```
420 LET DI = 0.5
430 INPUT "CALCULATE CR OR READ FROM GRAPH ON PAGE 7 OF GILMONT CATALOG.  IF
CALCULATE, ENTER 1, IF READ ENTER 0";Z1
432 IF Z1 = 1 THEN 435
433 IF Z1 = 0 THEN 437
435 PRINT "CR WAS CALCULATED"
436 GOTO 440
437 PRINT "CR FROM GILMONT CATALOG"
438 GOTO 440
440 IF Z1 = 0 THEN 520
450 REM SEE GILMONT CATALOG PAGE 7
460 LET LR = LOG (R) / 2.303
470 LET A = (3.08 * LR) - 1.25
480 LET B = 3.83 - (1.17 * LR)
490 LET C = ((LOG (SN) / 2.3025851) - (0.111 * LR))
500 LET CR = ((((B ^ 2) + (4 * A * C)) ^ 0.5) - B) / (2 * A)
510 GOTO 530
520 INPUT "ENTER CR FROM GRAPH";CR
530 PRINT "CR =";CR
540 REM CALCULATE VOLUMETRIC FLOW RATE
550 LET QA = R * ((R / 100) + 2)
560 LET QB = (((WF * (FD - SD)) / (FD * SD)) ^ 0.5)
570 LET QC = 59.8 * DI * CR
580 REM Q IS THE VOLUMETRIC FLOW RATE (ML/MIN)
590 LET Q = QA * QB * QC
600 REM QM IS MASS FLOW RATE (G/MIN)
610 LET QM = Q * SD
620 REM QN IS THE MOLAR FLOW RATE (MOL/MIN)
630 QN = QM / 18.15
640 PRINT "STEAM FLOW RATE"
650 PRINT Q;" ML/MIN"
660 PRINT QM;" G/MIN"
670 PRINT QN;" MOL/MIN"
680 END
```

TECHNICAL INFORMATION DEPARTMENT
LAWRENCE BERKELEY LABORATORY
UNIVERSITY OF CALIFORNIA
BERKELEY, CALIFORNIA 94720